MANUFACTURING, ANALYSIS AND

EXPERIMENTAL TESTING OF MULTI-BLADED

PROPELLERS FOR SUAS

By

BEN BETTINGER

Bachelor of Science in Mechanical & Aerospace

Engineering

Oklahoma State University

Stillwater, OK

2010

Submitted to the Faculty of the
Graduate College of the
Oklahoma State University
in partial fulfillment of
the requirements for
the Degree of
MASTER OF SCIENCE
May, 2012

MANUFACTURING, ANALYSIS AND

EXPERIMENTAL TESTING OF MULTI-BLADED

PROPELLERS FOR SUAS

Thesis Approved:

Dr. Jamey Jacob

Thesis Adviser

Dr. Andrew Arena

Dr. Joseph Conner

Dr. Sheryl A. Tucker

Dean of the Graduate College

TABLE OF CONTENTS

LIST OF TABLES

Table   Page

LIST OF FIGURES

Figure   Page

CHAPTER I

INTRODUCTION

Over the last few decades, Small Unmanned Aircraft Systems (SUAS) have

become a critical tool for tactical use. They play a key role alongside our soldiers serving

abroad to help locate and eliminate potential threats to American lives. SUAS have also

emerged as a driving force in the agricultural industry of the world by providing up-to-

date crop monitoring and harvest optimization information. The applications for SUAS

are nearly endless, ranging from pipeline inspection to endangered species monitoring.

They also expect to find significant use in first responder applications, including police,

fire fighting, immigration and homeland security. However, SUAS have one major

limiting factor that is crucial to several of the applications that they are used for, viz. their

acoustic signature, i.e. noise of the propulsion system.

The emergence of SUAS with its many potential applications has increased the

demand for improved small aircraft components. For custom built SUAS, optimized

propellers are rarely available off the shelf. This lack of availability leads to the demand

for a method that produces highly reliable custom propellers that are particularly easy to

manufacture within a reasonable time frame. This paper presents a unique method for

creating multi-bladed composite propellers that have been optimized to a vehicle's thrust

and noise requirements.

Drawing from previous work in this area the manufacturing method for creating these propellers will focus on providing a simple, yet effective process. The manufacturing process combines wet lay-up techniques with precision hand carving to produce solid carbon fiber composite propellers. The composite propellers are then experimentally tested to verify their performance parameters and their reliability. The method produces high quality propellers that are comparable to commercially available ones with the advantage of being tailored to performance requirements for a specific SUAS.

Thesis Goal and Objectives

The motivation behind this thesis is the desire to be able to build custom propellers that are optimized to a specific vehicle's performance parameters. The critical performance parameter that is being optimized is low noise by reducing the operational RPM at cruise of the propeller. There are few manufacturers in industry that are willing to produce in low production numbers custom propellers without carrying a hefty cost and extensive lead time. Building custom propellers that have been optimized to desired characteristics is a feasible option to overcoming the industry costs and lead time.

The overarching goal of this thesis is to develop, implement and quantify a unique and innovative manufacturing process for constructing multi-bladed SUAS propellers.

Objectives:
- Construct multi-bladed propellers using current propeller manufacturing techniques:
  - Use available technology to manufacture rapid proto-typed blades.

       ▲ Use CNC milling machine to produce wooden laminate blades.

       ▲ Apply wet lay-up techniques to produce composite propellers.

  − Develop a new technique for propeller construction from lessons learned:

       ▲ Use wet lay-up techniques to build a composite propeller with solid core.

       ▲ Use wet lay-up techniques to build a hollow composite propeller.

  − Test and Analyze custom propellers:

       ▲ Measure the deflection induced by a known load at various locations.

       ▲ Use load versus deflection data to predict the load at a known deflection.

       ▲ Verify load versus deflection data by using advanced beam analysis for predicting structural properties and deflections.

The process overview can be seen in Figure 1, showing the path followed highlighted in orange. There are two main branches to building propellers that need to be evaluated simultaneously, blade optimization and blade manufacturing, in order to produce an operational propeller. Blade manufacturing techniques will be the starting point for this paper.

Figure 1 – Propeller design and construction process

CHAPTER II

LITERATURE REVIEW

The first patented use of a propeller for moving an object through a fluid dates back to the early 1800s. In 1836, Francis Pettit Smith patented the first screw propeller that would eventually power the British steamship, the SS Archimedes, in 1839 (Macfarlane 1851:109). However, without a technique for manufacturing, Francis Smith's screw propeller patent was just a bunch of pretty pictures. In order to take these designs and produce tangible results, a manufacturing process had to be developed. Several techniques for creating propellers are hand carving of wooden propeller blades, machining of metal blades and the most current technique of using a resin transfer molding process to create composite blades. Each of these methods has advantages and disadvantages based on the conditions in which they operate. The detailed manufacturing processes for creating each of these blades is described in the following sections.

Origins of Propeller Manufacturing – Wooden Propellers

The earliest manufacturing of aircraft propellers can be traced back to the beginning of the 20th century. At that time, propellers were constructed by hand and craftsmen only utilized carefully selected hardwood. Craftsman would glue thin layers of wood together and then trim the layers within a certain percentage of the final geometry.

The specific propeller geometry was carved by hand using airfoil shaped templates along the length of each blade. This may seem straightforward compared to complex contemporary methods, but this is a lengthy process requiring countless man-hours to create these works of art.
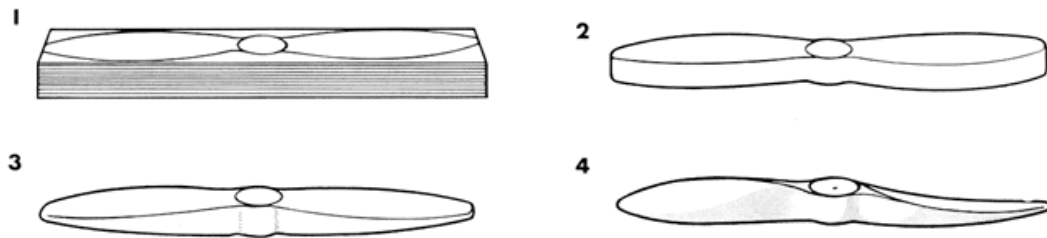
Figure 2 – Wooden propeller manufacturing process

There are two main processes for building a wooden propeller by hand: preparing the wood and hand-carving the wood. There are three steps to prepare the wood for manufacturing: selection of good hardwood, drying the wood, and bonding the wood. This is followed by two different techniques for carving the propeller by hand. The first method requires the layers of wood be glued before any hand carving is done. The second method requires the layers be individually pre-cut then glued. Each of these steps and methods is further discussed in the subsequent paragraphs.

The first and most important step involved in constructing a wooden propeller is the selection of good hardwood. Broadly defined, good hardwood is hardwood that has a higher Young's modulus than shear modulus and has the ability to stand up to the elements. More specifically, selection of the wood consists of optimizing several material properties such as strength, weight, density, shrinkage, and grain orientation. Hardwoods are typically chosen to use for their strength to weight ratio, their predilection to maintain radial dimensions and their strength in the direction of their annual rings

(United States Army Air Corps 1921:60). The most common type of cut for propeller manufacturers is the quarter sawn cut due to its shrinkage characteristics. Vertical sawn wood will shrink in thickness of the cut and flat sawn wood will shrink in width of the cut. For these reasons a quarter sawn cut is chosen to try to equalize the shrinkage in both directions. Figure 3 shows the various wood cuts along the annual rings of an oak log.
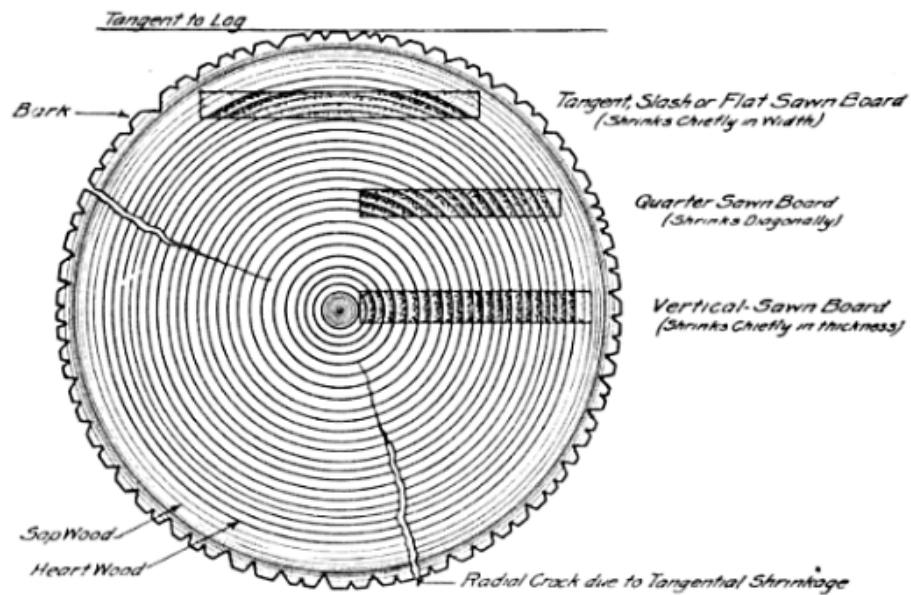
Figure 3 – Various wood cuts and shrinkage (United States Army Air Corps 1921:60)

The hardwoods that are typically used during the manufacturing of wooden propellers are white oak, birch, mahogany, spruce and walnut; however, various others types are used depending on geographical location. Mahogany and walnut do not shrink as much as other hardwoods, making them desirable in that aspect, but they are not as durable as oak and birch.

The second step is drying the freshest piece of wood that can be found. A fresh piece of wood is defined as one that is recently cut and has not been exposed to the elements for more than a day. The combined exposure to the sun and air causes the outer

portion of the wood to dry first resulting in an overall uneven drying. This drying-out effect can cause the wood to develop cracks making it undesirable for propeller manufacturing. Kiln-drying of the lumber is the preferred way to evenly dry the wood without inducing cracking by drying too quickly (United States Army Air Corps 1921:86). The kiln must have the ability to control the relative humidity, air circulation and the temperature in order to dry the lumber evenly without defects. Once the lumber has dried to the desired moisture content it is ready to be cut down to pieces roughly 1/4" to 3/4" thick depending on the propeller size and then milled for straightness. Since the density of the wood varies along the length of each piece, groups of laminates must be carefully selected to have a reasonably uniform distribution. Grain orientation is important for torsional stiffness and the centrifugal force experienced by the blade during use.

The third step is bonding the hardwood. This stage emphasizes safety and ensures that the wooden propeller does not fly apart during actual use. Although various types of glue can be used to hold the laminates together, the most commonly used adhesive is resorcinol. Resorcinol is very resistant to high temperatures and can withstand almost all service conditions. One bonding method is to place the laminates in a hot box to allow the wood to heat to a temperature of roughly 100° F and then apply the glue (United States Army Air Corps 1921:88). The higher temperature expands the wooden pores and allows the glue to be easily absorbed into the wood. If the temperature is not high enough, the wooden pores remain small and the glue cannot be as easily absorbed. Combinations of wooden clamps and/or presses are then applied for support for the

duration of time required for the glue to dry. A final clamped set of laminates is shown in Figure 4.
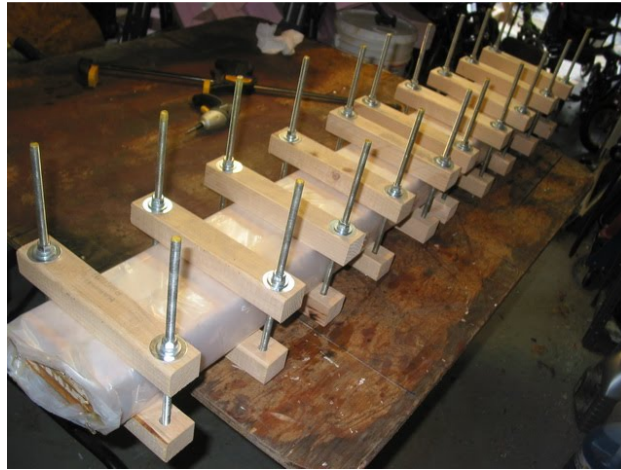
Figure 4 – Gluing laminates together (Kearns 2009)

After the propeller wood has been selected, trimmed and glued to the desired thickness required, the method for carving out the final propeller shape varies based on the manufacturer of the propeller. Initially, the basic methodology is the same: use templates to carve out the desired shape. However, the final steps to achieve the desired end product are different.

The first method to create wooden propellers requires that all the wooden layers are epoxied together to form one larger rectangular block that encompasses the entire outer dimensions of the final propeller. An outline of the propeller is placed on the top surface of the rectangular block, representing the front face of the propeller, then traced and cut out. The next step is to use another outline along the length of the side of the propeller, trace and cut out. The final shaping of the propeller is left to be carefully carved out by hand tools using airfoil templates along the length of each blade.

The second method to create wooden propellers is very similar to the first with a slight change in the order of processes. The first process in this method is to use

templates to cut out rough outlines of the stacked pieces based on their vertical position within the wooden laminate. The individual pieces must be placed in the precise order and epoxied together to form a rough looking propeller as in Figure 5. The wooden laminate is now carved down by hand using files or chisels. Once again, airfoil templates are used along the length of the propeller to create the desired final shape of the propeller.

Figure 5 – Wooden laminate with pre-cut layers (Bahnson 2011)

Now that the final geometry of the wooden propeller has taken shape, it is time to apply a finishing coat to the wood for durability and protection against the elements. A simply polyurethane finish could be applied to the wooden propeller for minimum protection; however after the field testing of many wooden propellers, it became customary to additionally attach a metal sheath around the leading edge and some type of treatment to the tips for durability. Tip treatments have ranged from copper tips to pigskin tips to fabric covered tips; it all depends on the preference of the manufacturer's customers.

Fred Weick, chief engineer of the Engineering and Research Corporation, describes a method known as the Schwarz process for manufacturing reinforced wooden

propellers in his paper, "Composite Wood and Plastic Propeller Blades" (Weick 1939). The Schwarz Co. in Germany originally developed this method for producing wooden blades. The core of the blades is composed of laminated spruce and compreg joined together by a scarf joint. Compreg is laminated hardwood that has been built up from 1/8" thick hardwood veneer impregnated with phenol-formaldehyde resin and heat pressed together under massive force (Weick 1939). Combined by a scarf joint, the compreg and spruce layers are stacked to the desired thickness of the blade. The Engineering and Research Corp. has found that typical modulus of elasticity for compreg is between $3x10^6$- $4x10^6$psi. This is roughly half the modulus of elasticity of duralumin, an aluminum alloy used in metal blades (Daniels 1922).

The Schwarz process follows the same steps as described previously for shaping the blade geometry. A leading edge protective strip is attached by soldering wire mesh to both lips and tacking the wire mesh to the wooden core. The wooden core of the blade is then coated with cellulose-acetate plastic and placed under pressure to allow the plastic to seep into the pores of the wood. The cellulose-acetate plastic smooth's the offset created by the metal leading edge protective strip and helps to bond the wire mesh to the wooden core. This process for creating propellers blades was adopted from the Schwarz Co. in Germany by Airscrews, Ltd. in England and the Engineering and Research Corp. in Washington, D.C. circa 1930.

Developments of composite wooden propellers with higher elastic moduli started the transition from wooden blades to blades that had higher material strengths such as aluminum and steel. The only problem would be manufacturing of a metal blade that

could be as light as a wooden blade. This process for creating relatively light metal blades is described in a later section.

With the advancement of technology comes a better manufacturing process to become more productive, more precise, and more efficient. The labor intensive method for making wooden propellers has evolved over the last hundred years into a computer controlled process that allows the manufacture to more efficiently produce wooden propellers with better accuracy.

Computer Numerical Control (CNC)

As computers began to become more powerful in processing power, integration of computers into everyday manufacturing processes became a standard for better efficiency and precision. The early days of numerical control required punch cards to be used to drive mills, while current methods only require G-code to be written and loaded onto a computer controlling the mill. CNC's provide the user with the ability to accurately mill out complex 3-dimensional parts from almost any material. The accuracy obtained from using CNC's is unrivaled by hand cutting of the equivalent part. The basic modern CNC consists of a tool spindle attached to several direct-drive stepper motors that move in the x, y, and z directions along the length of a milling table. The motors and spindle are controlled by a computer that reads in the G-code line by line to control the precise position that the tool will be located at along each line of G-code. Current CNCs vary in the number of axes that they can machine a part in from a simple 2-axis CNC to a more complex 6-axis CNC. The main axes are in the x, y and z direction along a stationary part with the option to increase the degrees of freedom by rotating along any one of the three axes.

The CNC revolutionized manufacturing across the world making complex parts easier to create and mass produce. Not only did CNCs improve manufacturing processes of simple parts, it also changed the way wooden propellers were produced. The next step in the evolution of wooden propeller manufacturing came from the ability to accurately machine the complex curves that make up the blade geometry.

CNC milling of Wooden Propellers

The advancement in wooden propeller manufacturing has taken giants leaps since the first wooden propeller was carved out by hand tools using airfoil shaped templates. This labor intensive process changed from relying on the craftsmanship of an individual to the processing power and precision provided by a computer. The vast majority of wooden propeller manufacturers currently benefit from the use of a CNC milling machine that allows them to follow the same method described previously with the added benefit of minimizing labor intensive man-hours carving out the blade geometry and increasing the precision, accuracy, and repeatability of the design.

This method for manufacturing of wooden propellers follows the same steps as the earlier method described up to right after the laminates are glued together and allowed to dry. There are several methods that can now be followed that are completely dependent on the type of CNC milling machine that will be used. The first method will be for a 3-axis CNC and is the most basic in concept. The wooden laminates are aligned on the 3-axis CNC in order to allow the front surface of the propeller geometry to be machined out. The layers of laminate must be securely tightened to the milling table and the milling tool must be zeroed according to the G-code origin point. After loading the pre-coded G-code for the front surface into the CNC milling computer, the machining of

12

the front surface can begin. Figure 6 and 7, from Sensenich Wood Propeller Company, displays modern propeller construction techniques for wooden propellers.
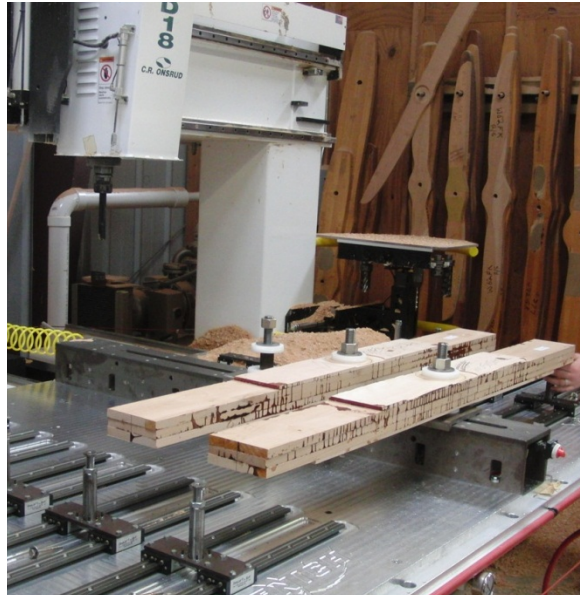
Figure 6 – Sensenich Wooden Propeller CNC milling

After milling of the front surface of the propeller is complete, the part is flipped over and must be re-aligned perfectly with the original position in order to ensure that the two milled sides form consistent leading and trailing edges (Gospodnetić and Gospodnetić 1993). This step is where higher axis CNC milling machines can be utilized to reduce any error induced by rotating the wooden propeller.

Figure 7 – Sensenich Wooden Propeller after front surface milled

13

The precision of the milled surfaces is only as good as the milling bit and incremental step size, leading to a small amount of hand finishing required at the end of the CNC milling process. Finishing of the wooden propeller is the same as described earlier with a coat of polyurethane varnish, some type of metal leading edge and fabric wrapped around the tip for increased protection. These types of wooden propellers were typical for aircraft engines up until World War II. World War II saw the advancement of aircraft engine horsepower and torque, thus creating the demand for higher strength propeller blades. The demand for better propellers led to the use of stronger materials such as aluminum and steel with only one logical way to manufacture them.

The Next Generation – Steel and Aluminum Propellers

With higher powered engines becoming more readily available for improved aircraft performance, there was an increased demand for propellers that could withstand the higher centrifugal and torsional forces exerted by these engines. The next generation propeller would have to be stronger and lighter than its predecessor, the wooden propeller. Strength could be achieved by heat treating materials such as aluminum and steel, but the weight issue had to be resolved by decreasing the quantity of material required for each blade. The solution to this problem was a hollow steel propeller blade with an internal steel rib structure.

In order for a hollow steel propeller to be created, the front and back surfaces of the propeller needed to be individually machined out and joined along the leading and trailing edge of the blade. This required two sheets of steel to be milled out to the exact dimensions on the inner and outer surfaces. Aeroprop, one of the leading manufacturers of steel propellers during World War II, used a multiple planer with tracer attachment to

get the inner and outer surfaces milled to specifications (General Motors Corporation 1944:24). Figure 8 shows an Aeroprop employee using a multiple planer with tracer to machine the exact geometry of the outer surface of the steel blade (Moltrecht 1981:5).

Figure 8 – Aeroprop worker using multiple planer on steel blade (General Motors Corporation 1944:25)

The front and back surfaces are combined in a brazing process, a metal-joining process in which a filler metal is heated above its melting temperature and evenly disturbed between two surfaces. The Pittsburgh Screw & Bolt Corp. uses a different technique known as the atomic hydrogen method to weld the two surfaces together (Foley 1933). The steel blade is then tempered until it becomes white-hot for a time period of seven minutes (General Motors Corporation 1944:26). The process by which the Pittsburgh Screw & Bolt Corp. heat treated their steel blade was to heat the blades in an electric furnace until the temperature of the steel reached 1650°F then quench the steel in oil. Directly after quenching, the steel received a second heat treatment for 3 hours at a temperature range of 1000-1100°F. This heat treatment process yielded ultimate strengths of 1.38×10^5 - 1.45×10^5 psi and a reduction of area between 57% and 62%.

Figure 9 – Aeroprop worker heat treating steel blade (General Motors Corporation 1944:26)

Once the steel blade has gone through its heat treating process, the blade is ready to be hand polished to smooth out any imperfections. The finished blade must be smoothed to within ten thousands of the initial blade geometry (General Motors Corporation 1944:27). These tight tolerances help to ensure that minimal blade balancing will have to be done before the final inspection of the blades. Unlike the wooden laminate layers used for the wooden propellers, the steel sheets used for the front and back surfaces of the steel propeller blade will have a better density distribution along the length of the blade. The method for manufacturing of hollow steel propeller blades also applies to aluminum and aluminum alloy propeller blades. Many of the current maritime propellers are constructed in a similar method, however without the need for a hollow core to reduce weight.

With aluminum as the primary material for construction, maritime propellers are manufactured in a similar way to steel and aluminum aircraft propellers. Selection of the material is based on the environmental conditions that the propeller will be exposed to, the extent of forces exerted on the propeller blades, repair capability, cost and the

manufacturability of the material (Gangler 1997). Composition of an alloy is generally

geared towards the overall strength and corrosion resistance of an alloy depending on the

environmental conditions it will be operating in. Aluminum and aluminum alloys have

been the primary choice of metal propeller blade manufacturers due to the weight savings

and the ease of machinability compared to steel. With better technologies becoming

more readily available, other manufacturing processes were attempted to create stronger,

lighter and cheaper propeller blades.

Investment Casting of Propellers

With CNC milling machine's precision on the rise, propeller manufacturing

methods to produce cheaper and better blade surface finishes without the need for hand

finishing were attempted using several casting processes. High precision CNC milling

machines allow for master molds or a propeller pattern to be created depending on the

casting method used. Two common casting techniques are die-casting and investment

casting. Die-casting uses a cast iron reusable mold while investment casting uses an

expendable break away mold method that will be further discussed for propellers.

Casting of metal propellers seemed to be an economical solution that allowed a variety of

metals to be used, quicker manufacturing times, and better surface finishes on the

propeller blades.

Investment casting makes use of an expendable wax, plastic or frozen mercury

pattern that can easily be melted away to form the cavity for the propeller casting. The

pattern is then coated in a ceramic material that is usually a refractory slurry mainly

containing zinc peroxide (ZnO_2). The pattern is then repeatedly dipped in the slurry until

a sufficient coating of ceramic encompasses the pattern. This method is known as the

shell method of investment casting which typical creates a ¼" shell of ceramic around the pattern (Bralla 2007:29). Figure 10 shows a maritime propeller pattern being coated in the ceramic slurry.

Figure 10 – Maritime propeller pattern with ceramic coating

Additional stucco material may be coated on top of the ceramic to increase the hardness of the mold. The entire mold is then heated to a temperature hot enough to melt away the pattern material from within the mold. The mold is then baked to allow the ceramic material to fully solidify. Once cooled, the ceramic mold is now ready for the selected propeller metal to be poured into the cavity and allowed to harden. The final step in this method is to break away the ceramic mold from the hardened metal propeller while disposing of the ceramic pieces from the mold. Figure 11 shows an example of a metal propeller that has just been removed from the ceramic mold.

Figure 11 – Maritime metal propeller

The required amount of surface finishing for a metal propeller made using the investment casting method is significantly less than that of a metal propeller that is directly CNC milled out due to tooling marks left by the CNC machine. However, both methods produce quality propellers with their differences coming in manufacturing time. Variations of the basic investment casting process have been undertaken to try to improve the surface finish precision even more.

Up until the invention of the computer-aided multi-axis milling machine circa 1980, Navy metal propellers were created using a casting and hand grinding process (Gangler 1997). The aluminum propellers were cast then hand finished to tolerances outlined in ISO 484. Aluminum was used over steel and titanium due to the ease of casting and lower machining costs (Gangler 1997). The concept of reusable molds is a way to cut manufacturing costs which then leads to another technique for manufacturing propeller blades.

Injection Molded Propellers

Building on the concept of propeller casting leads to another manufacturing technique that is extremely similar but for non-metal materials with lower melting temperatures. Injection molding of propellers is similar to investment casting of metal propellers with the added benefit of reusing the propeller molds many times. Special plastics that are infused with glass or carbon fibers can easily be used to provide manufacturers with a relatively inexpensive product that maintains the structural integrity of a desired propeller blade. These inexpensive and rigid materials have led to massive amounts of injection molded propellers to become readily available to the radio controlled (RC) aircraft community at low costs.

One of the first steps in any manufacturing process is to create a master mold from which numerous parts will be fashioned out of. Typical injection molds are created from blocks of aluminum or steel using a CNC milling machine. Depending on the precision of the CNC machine, the metal mold halves will be hand finished to eliminate any tooling marks that are not consistent with the propeller geometry. Once the final metal molds are in finished form, the composition of the material needs to be analyzed. Most injection molded propellers are composed of material that is tailored to the specific structural forces that will be exerted on the blades by different engine types. Many of the available propellers on the market today that have been manufactured by injection molding methods are made up of long glass or carbon fibers and resin. This is commonly seen in propellers manufactured by companies such as Advanced Precision Composites (APC), Windsor Propeller Company, Inc., Graupner, and Aero-naut. After the material composition has been selected the injection molding process can begin.

Injection molding machines can be very complex in design; however they can be broken down into simple processes that take place in order to complete a part. The mold halves for the propeller must be securely fastened to the clamping mechanism in the machine. Depending on the size of the part, clamping mechanisms have to apply pressure that can exceed several tons of pressure to the molds. Once the mold halves are clamped together under pressure, the raw material for the propeller needs to be loaded into a hopper or bin to be heated to the materials melting temperature. A screw mechanism then drives or injects the molten raw material into the mold until filled. The part is cooled usually using water cooling to allow for even cooling across the part. After cooling to the specified temperature for the material, the part is ejected from the mold

halves and any additional material is removed. Figure 12 shows a simple injection molding process that could be used to produce propellers.
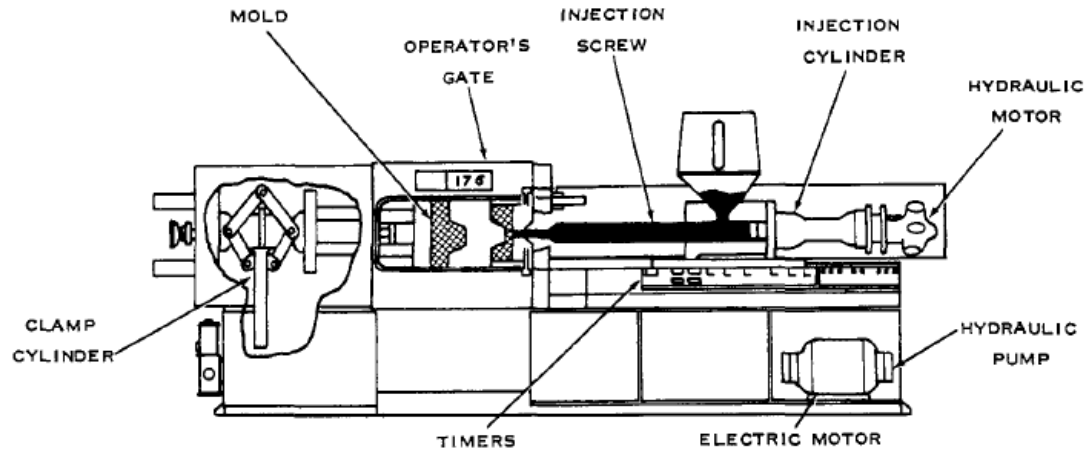
Figure 12 – Injection molding process (Rosato et al 2000: 7)

A study by the Mechanical Engineering Department of Lunghwa University of Science and Technology in Taoyuan, Taiwan developed a cost effective manufacturing process that incorporates rapid prototyping, rapid tooling, and high speed CNC machining to produce high precision metal and plastic propellers (Hsu et al 2007). The process involves rapid prototyping two male mold plugs, one for each side of the propeller blade with an injection hole at the hub of the front surface. The rapid prototyped molds are then coated in a refractory slurry to resist the high temperature of the molten metal that is about to be poured on them. Molten aluminum alloy is poured onto the rapid prototyped molds and allowed to solidify. The rapid prototyped molds are then removed and disposed of, leaving the hardened aluminum alloy female molds which are surface finished by precision CNC machining. With the two finished aluminum alloy female propeller molds, two paths can now be taken to produce propellers using either the investment casting method or the injection molding method. If the investment casting

method is followed, then a wax propeller pattern is created from the molds to use in the process described previously. If the injection molding process is to be used then the two molds halves that were created out of aluminum are used in an injection molding machine as described earlier with the desired material. Figure 13 shows the process for creating the aluminum mold halves using the described method of rapid prototyping, rapid tooling and high precision CNC machining.

| Rapid Prototyped Master Mold Halves | Mold Coated in a Refractory Slurry | Pouring Molten Aluminum in Cavity |
| Removing Rapid Prototyped half | CNC finishing of aluminum mold | Injection Mold Halves |
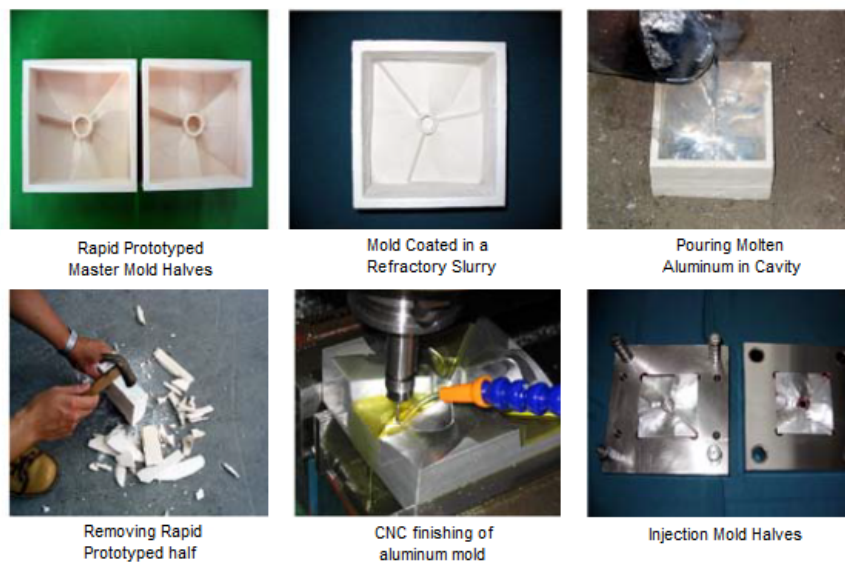
Figure 13 – Injection mold creation process (Hsu et al 2007)

Although the actual part produced by injection molding methods is relative inexpensive, the machinery required for this process is very expensive. This requires large scale manufacturing of propellers to be required in order for this process to be justified. Building on the concept of propeller molds leads into the next manufacturing process to create these geometrically complex parts, only the material that is used is changed.

Composite Propellers using Wet Lay-up

The process for combining dry fiber with resin to form a hardener material that far exceeds the material strengths of the individual materials is known as a hand lay-up or wet lay-up. Wet lay-up is commonly referred to as open molding, whose aerospace origins can be traced back to the beginning of the 20th century (Potter 1999). This method is the oldest form of creating polymer-matrix composites (Miracle and Donaldson 2001: 450). The method of creating propeller blades by wet lay-up techniques is a process that is heavily dependent on time and craftsmanship. Although resin transfer molding (RTM) processes are predominantly used in industry, this method is still considered when production quantities are relatively low. Like many of the other methods for manufacturing propellers, the resin transfer molding process is simply one variation of the open molding method for composites.

The first step to any propeller manufacturing technique is to have a good mold from which the propeller can be produced. Molds can be made from a variety of materials such as aluminum, steel, medium density fiberboard, tooling gel coat, or a combination of these materials. A cheap, yet effective way to create molds for wet lay-ups is to use layered medium density fiberboard (MDF) to create a box that encompass the propeller mold design. The MDF particle board can easily be milled using a 3-axis CNC router table to produce a rough propeller mold. The mold will need hand finishing as the milling tool path will typically leave tooling marks along the length of the mold. Two methods that have been repeatedly used by Oklahoma State University's Mechanical and Aerospace Engineering Department are to coat the MDF female mold in epoxy and graphite several times, sanding after each coat, or using the MDF male mold

to create a female mold from tooling gel coat and tooling fiber glass. The latter of the two methods makes for a longer lasting propeller mold.

Before the lay-up can begin the mold must be prepared with a releasing agent (Partall Film #10) that is applied to the surface where the wet composite material will come in contact. Depending on the orientation of the layers and the materials used, the layers of fiber or foam must be precut to ensure precision alignment within the mold part. In a RTM process the dry layers would all be placed in the mold at this step. A mixture of resin and hardener must be prepared and even spread across all the fibrous material that will be placed in the mold. Ensuring that all the dry fibrous material is coated with a layer of epoxy is critical to preventing dry spots. After applying epoxy to the precut layers, each layer is placed in the mold based on the predetermined location of the material. The entire mold is placed in a vacuum bag and sealed. Getting the mold and the wet propeller material under vacuum before the epoxy starts to harden is important to ensuring that a smooth surface results from the lay-up.
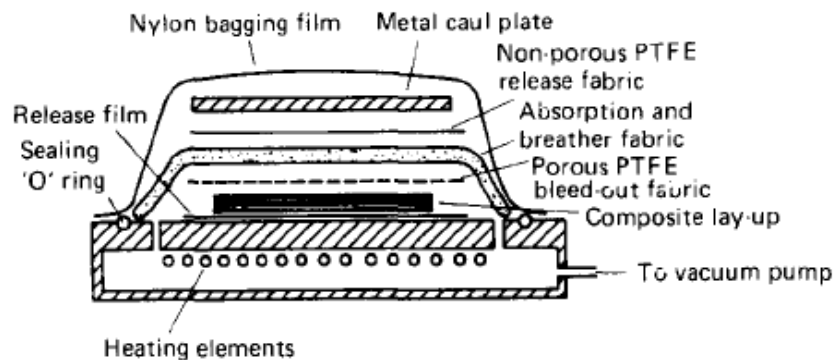
Figure 14 –Method for wet lay-up of composites (Stringer 1989)

Using wet lay-up techniques for construction of propellers is usually limited to low production runs and an increase in man hours when compared to RTM processes.

Resin Transfer Molding (RTM) Process – Dry Lay-up Propellers

Resin transfer molding is one of many liquid composite molding (LCM) techniques by which dry fibrous material can be layered in a mold to form the internal structure of a part before being injected with resin to combine and stabilize the fibrous structure (Potter 1997:2). The dry fibrous material is typically fiber glass or carbon fiber weave with layers of uni-directional carbon fiber for axial stiffness along the blade length. Common resin transfer molded propeller blades have an internal core that is high density foam or some type of carbon fiber spar that acts as both a filler material and axial load reinforcement. Along with the lay-up material and orientation there are several other considerations that need to be taken into account when performing a resin transfer molding process.
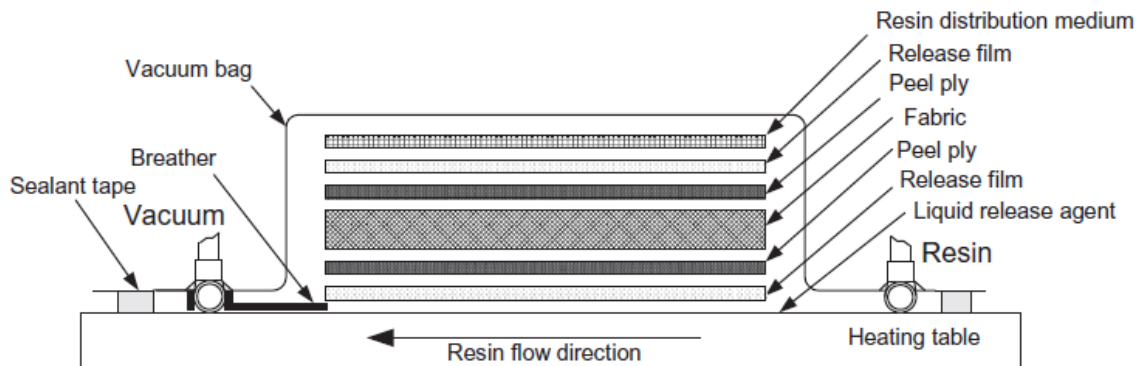
Figure 15 – Resin transfer molding process (Atas et al 2010)

One of the most important considerations during an RTM process is the injection points along the mold (Potter 1997:6). If the injection points are not chosen correctly then the flow of the resin may result in the resin not being dispersed uniformly, a phenomenon also known as race-tracking (Bickerton and Advani 1998). Race-tracking leaves dry spots in the lay-up that can ruin the entire part. Considerations such as cure time of the resin, viscosity of the resin, vacuum pressure applied to the mold, and

material wetting rates are additionally crucial to the success of a completely and uniformly cured part (Potter 1997:6). Most RTM processes make use of a heating system that allows the resin and fibrous material to reach a higher temperature in order to allow the resin to flow through the material easier (Potter 1997:22).
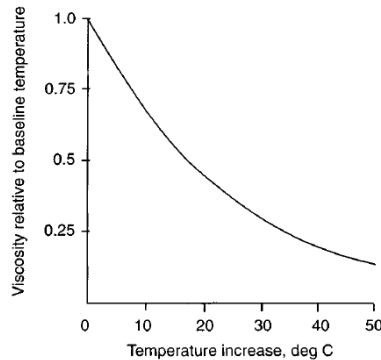
Figure 16 – Viscosity versus temperature profile (Potter 1997:21)

Once the mold material has absorbed all the resin allowable, the excess resin is collected in one of several vent ports that allow excess resin to escape the mold. Curing time is then dependent on the resin chosen; be sure to allow for enough time for the part to completely cure or the resulting part may be still tacky or flimsy. After removing the part from the mold, minimal trimming of the edges is required before the part is complete. For propellers, after the RTM process has been completed the blades get a protective coating over the composite lay-up and are finished off by hand polishing. Figure 17 shows the typical layers that are incorporated into a composite propeller blade.

26
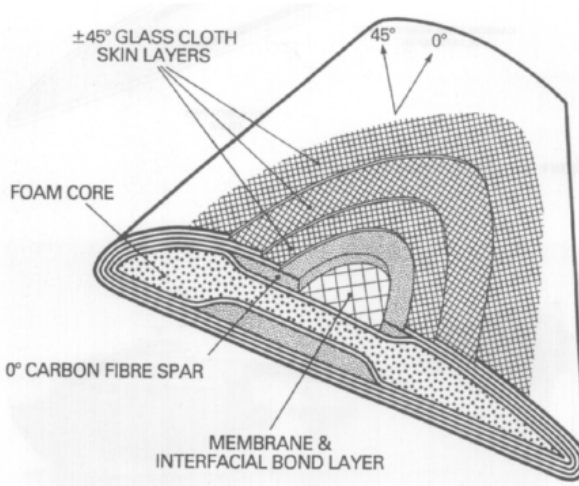
Figure 17 –Layers in a composite propeller blade (McCarthy et al 1994)

This method for manufacturing of composite propeller blades is the result of decades of experimental testing with composites and over a hundred years of propeller manufacturing. RTM processes have become the predominant method for construction of complex geometry propellers by composite propeller manufacturers and for the construction of many automotive panels due to their ease and repeatability of manufacturing.

However, each of the methods for manufacturing of propeller blades have their advantages and disadvantages when used. Table 1 highlights key advantages and disadvantages associated with each of the manufacturing methods for producing propellers.

Hand Carved Wooden Propellers	
Advantages	**Disadvantages**
• Ability to naturally damp out vibrations	• Strength to weight ratio is low, due to low strength
• Low Cost of Materials	• High cost of manufacturing due to labor intensive process (days)
• Good fatigue resistance	• Lengthy Manufacturing Process
• Light Weight	• Deformation and warping due to moisture
• Aesthetically pleasing	

CNC milled Aluminum and Steel Propellers	
Advantages	**Disadvantages**
• High strength to weight ratio • High precision blade geometry • For aluminum, easier to machine than steel	• Machining time is lengthy (hours) • High cost of materials • High cost of manufacturing tools • Fatigue limitation from engine vibration

Casted Aluminum Propellers	
Advantages	**Disadvantages**
• High strength to weight ratio • Better surface finish than direct CNC milling • Quicker Manufacturing time than direct CNC milling • Low cost of manufacturing	• Heavy blades only used for maritime applications • High cost of materials • Fatigue limitation from engine vibration

Injection Molded Propellers	
Advantages	**Disadvantages**
• Cheap material cost • Mass production of consistent propellers capable • Light weight • Man-hours required is minimal	• High initial cost of injection molding machinery • Low strength for most injection material

RTM (Dry lay-up) Composite Propellers	
Advantages	**Disadvantages**
• Complex blades can be created with different materials • Higher strength to weight ratio than metal or wood • No time limit to get material in correct orientation • Set-up for manufacturing larger quantities than wet lay-up	• High cost of material • High cost of manufacturing tools • Dry spots in internal structure may not be visible • Limited control of epoxy distribution

Wet lay-up Composite Propellers	
Advantages	**Disadvantages**
• Set-up not as complex as RTM process	• Limited to cure rate of epoxy to get material oriented correctly
• Higher strength to weight ratio than metal or wood	• High cost of material
• Lower manufacturing cost than RTM process	• Craftsmanship plays a critical role in the outcome of the lay-up
• Set-up for manufacturing small quantities	

Table 1 –Advantages and Disadvantages of Propeller Construction Techniques

The manufacturing techniques for multi-bladed propellers significantly vary based on the material used for construction. Propellers constructed of wood offer advantages such as good vibration damping and fatigue resisitance but do not offer the same strength to weight characteristics as carbon fiber composite propellers (Brahney 1986). Propellers built from metal offer higher strength properties but lack fatigue resistance and low weight (McCarthy 1985). Depending upon the specific aircraft size and power required each of these manufacturing techniques has their advantages over the other. Selection of a manufacturing method ultimately comes down to vehicle size, environmental operating conditions, project budgets and time available.

Tensile Testing

Material properties for most composites are readily available either online or in a library database. However, for better accuracy and uncertainty calculations it is necessary to indepedently verify the material properties of the composites that are being used. According to ASTM D 3039, a suggested tensile specimen of the material should be 10" long by 1" wide and 0.1" thick. The tensile specimen may require gripping tabs at both ends to prevent gripping damage that may cause premature failure in the test

coupon. Table 2 illlustrates recommendations for material testing geometries for polymer matrix composites.

Tensile Specimen Geometry Recommendations						
Fiber Orientation	Width, mm [in.]	Overall Length, mm [in.]	Thickness, mm [in.]	Tab Length, mm [in.]	Tab Thickness, mm [in.]	Tab Bevel Angle,°
0° unidirectional	15 [0.5]	250 [10.0]	1.0 [0.040]	56 [2.25]	1.5 [0.062]	7 or 90
90° unidirectional	25 [1.0]	175 [7.0]	2.0 [0.080]	25 [1.0]	1.5 [0.062]	90
balanced and symmetric	25 [1.0]	250 [10.0]	2.5 [0.100]	emery cloth	—	—
random-discontinuous	25 [1.0]	250 [10.0]	2.5 [0.100]	emery cloth	—	—

Table 2 –Tensile Specimen Geometry Recommendations (ASTM D3039/D3039M - 08)

Strain gages should be attached with minimal adhesive so that the material properties are measured and not the adhesive properties. Strain gages attached in both the longitudinal and lateral directions will allow for Poisson's ratio to be measured. The modulus of elasticity will be measured by the strain gage in the longitudinal direction. The method for testing material coupons has been applied to composite propeller blade and spar material testing numerous times to characterize the strength of the composites (Smith and Lattavi 2000).

Material testing using this ASTM standard provides a baseline measurement when comparing the experimental data for the material that will be used in this thesis to manufacture propeller blades. Similar carbon fiber weave at 0/90° orientation has produced elastic modulus' in the range of 57.8 to 71.5 GPa (Paiva, 2006). These values can be compared to the elastic modulus' that are experimentally tested in a later chapter.

Experimental Deflection Testing of Advanced Beams

Deflection testing of an advanced composite beam can be accomplished through the use of cantilever beam theory. There are many different test methods dependent on the equipment at hand, however most methods result in the same desired outcome. ASTM Standard B223-08 describes a simple process for measuring the deflection of a cantilever beam using a micrometer depth gage. The equipment setup is simply the test

specimen securely clamped to the mechanism and a loading rod used to deliver the
desired point load. Figure 18 shows a general equipment setup for measuring deflection
according to ASTM Standard B223-08.
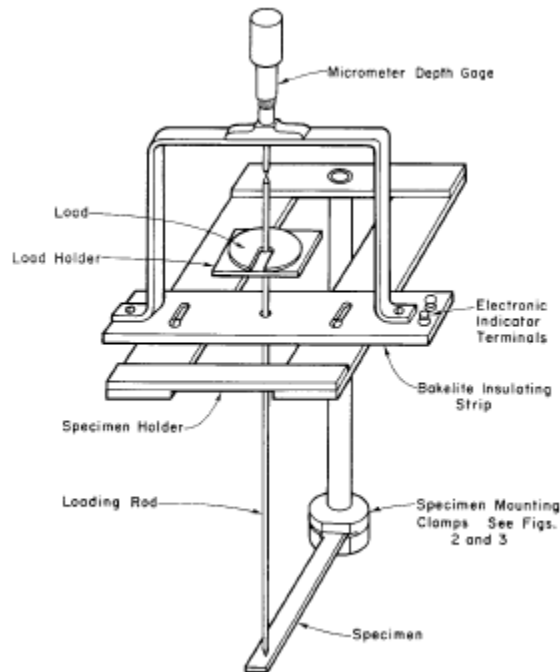
Figure 18 – Testing Machine for Determine Modulus of Elasticity (ASTM B223 – 08)

Applying the ASTM Standard to advanced beam deflection allows for the
calculation of the modulus of elasticity at a point, development of the force versus strain
curve and the maximum force allowable by the test specimen. Another approach for
measuring deflection in a cantilever beam is to measure the angle of deflection from the
unloaded reference point. A build up can be created based on different loading scenarios
to produce stress versus strain plots to show elastic and plastic regions of the cantilever
beam. ASTM Standard D747-10 outlines a procedure for measuring the apparent
bending modulus of a test specimen using the deflection angle and the force applied to
the cantilever beam. These methods allow for standards to be implemented during

deflection testing to ensure proper calculation of material properties when experimentally tested.

Airborne Composites of the Netherlands developed a composite propeller for the Dutch Royal Navy in 2010 which they performed ultimate load testing on (Brødsjø and Putting 2010). The basic propeller geometry was 5 blades with a 2.5 m diameter. Each propeller blade contained a total of 180 plies consisting of fiberglass and carbon fiber offset at angles of 0/90 and +/-45 degrees. Each layer is individually cut using a numerically controlled cutting machine and labeled for proper placement in the lay-up.
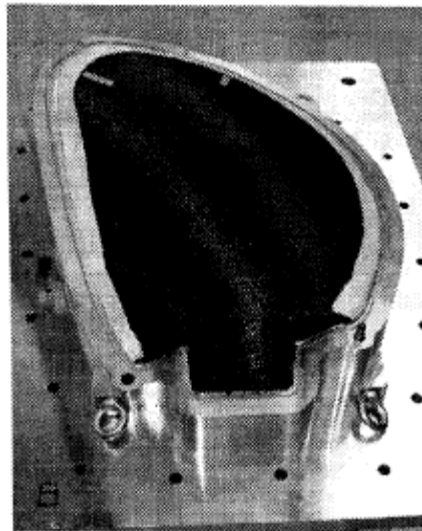
Figure 19 – Preform in RTM Mold (Brødsjø and Putting 2010)

A RTM process was used to combine the materials that were placed within the metal heated molds. Resin injection locations and resin selection were examined to produce the greatest reliability in the manufacturing process. Once the blades were finished with a protective coating of polyurethane, the blades were individually tested to 120% of the operational loading (Brødsjø and Putting 2010). The graph in Figure 20 shows the tip deflection results when the operational loads are applied.
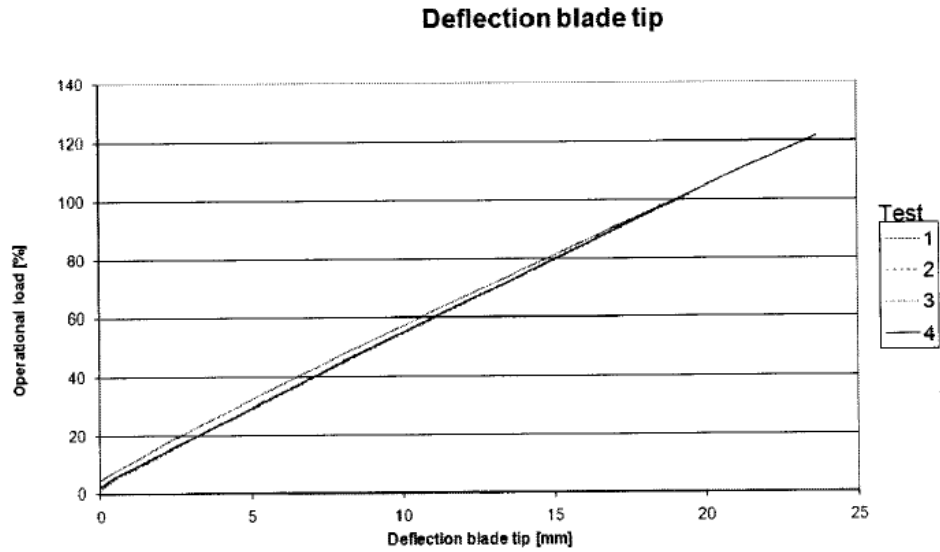
Figure 20 – Deflection Testing of Airborne Composite Propeller Blade (Brødsjø and Putting 2010)

In order to fully understand the experimental deflection testing results, the dynamic forces exerted on a propeller blade during operational conditions need to be understood. There are five main forces that are exerted on the blades during dynamic conditions which are the centrifugal force, the bending moment, the twisting moment, the torque and the thrust. These five forces can be seen acting on the blade in Figure 21.
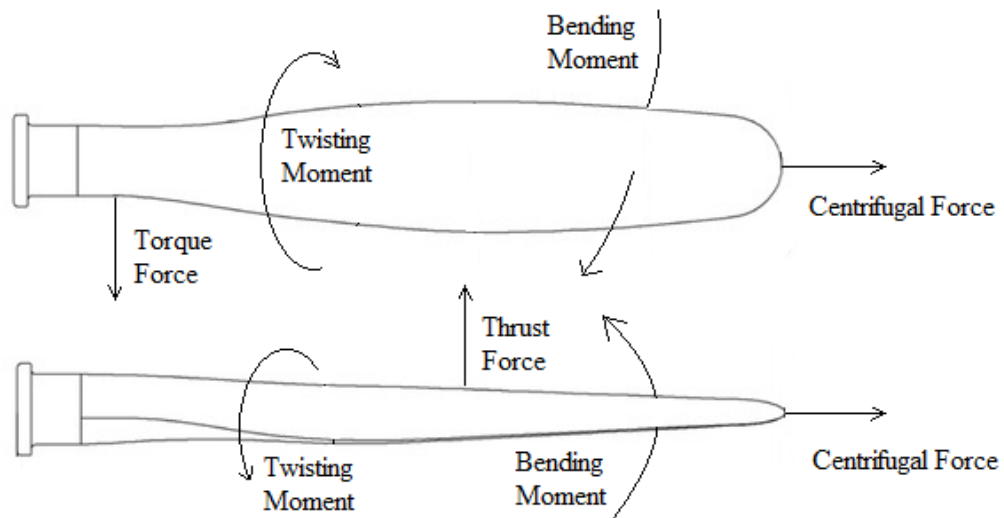
Figure 21 – Dynamic Forces Exerted on Propeller Blade

For this thesis the static and dynamic bending moment will be experimentally tested and verified to show that the strength of the manufactured blades is within an acceptable tolerance. The theoretical and experimental testing will be discussed more in the next chapter.

CHAPTER III

EXPERIMENTAL ARRANGEMENT

This chapter will examine how to theoretically predict the stress, strain and deflection associated with propeller blades as well as the experiment used to validate thesse numbers. The theoretical prediction is based on advanced cantilever beam bending analysis incorporating different material properties at the same cross-section. The comparison curves generated will be discussed as to the reason for their selection. Finally, the equipment used to perform all deflection tests will be descirbed.

Theoretical Background

A propeller blade can be broadly defined as a rotating aircraft wing with an associated twist. This definition makes it fitting that an analysis of an advanced cantilever beam be examined along the length of the blade. Using the Euler-Bernoulli theory of beams, the modulus weighted section properties can be calculated based on the materials used and the geometry of the airfoil cross-section. When using this theory two assumptions for simplification of the advanced beam can be made: "(1) the tranverse components of normal stress σ_{yy} and σ_{zz} are assumed to be negligible compared to the axial stress σ_{xx}; and (2) cross sections are assumed to remain planar and normal to the centroidal axis of deformation" (Allen and Haisler 1985:164). The modulus weighted

section properties allow for the stress and strain at different locations on the blade to be

calculated based on the load applied to the cantilever beam. Figure 22 shows the

reference axes and cross section of a composite beam for this discussion.

y" and z' are arbitrary coordinate axes

⊕ = modulus weighted centroid of the composite cross section

⊕_i = geometric centroid of the ith portion

Cross-section of a composite beam.
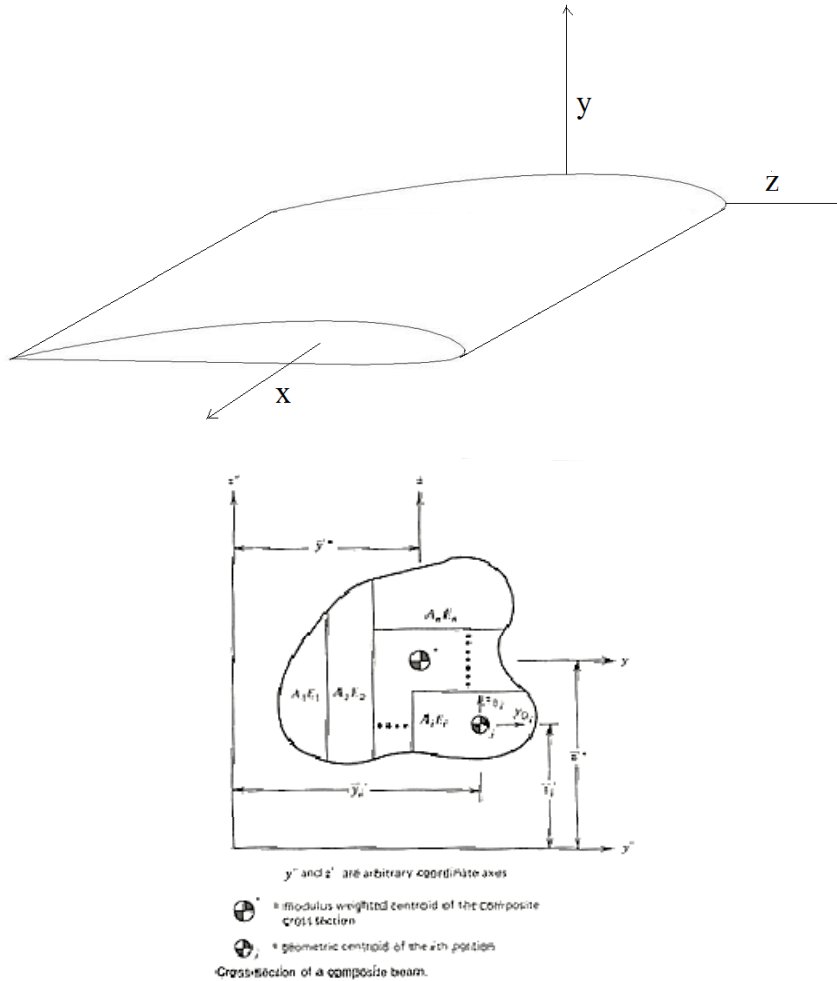
Figure 22 – Reference Axes and Cross Section of a Composite Beam (Allen and Haisler 1985:175)

For a composite beam that is compiled of numerous sections of homogeneous

segments, the cross sectional properties can be calculated as a summation of all the

discrete portions. The summation of properties is weighted based on elastic modulus to

account for stronger and weaker materials in the composites structure. The first three

equations give the modulus weighted area and centroid coordinates for the composite cross section.

$$A^* = \sum_{i=1}^{n} \frac{E_i}{E_1} A_i$$

$$\bar{y}'^* = \frac{1}{A^*} \sum_{i=1}^{n} \frac{E_i}{E_1} \bar{y}'_i A_i$$

$$\bar{z}'^* = \frac{1}{A^*} \sum_{i=1}^{n} \frac{E_i}{E_1} \bar{z}'_i A_i$$

$$I^*_{y'y'} = \sum_{i=1}^{n} \frac{E_i}{E_1} (I_{y_0 y_{0i}} + \bar{z}'^2_i A_i)$$

$$I^*_{y'z'} = \sum_{i=1}^{n} \frac{E_i}{E_1} (I_{y_0 z_{0i}} + \bar{y}'_i \bar{z}'_i A_i)$$

$$I^*_{z'z'} = \sum_{i=1}^{n} \frac{E_i}{E_1} (I_{z_0 z_{0i}} + \bar{y}'^2_i A_i)$$

$$I^*_{yy} = I^*_{y'y'} - (\bar{z}'^*)^2 A^*$$

$$I^*_{yz} = I^*_{y'z'} - (\bar{z}'^*)(\bar{y}'^*) A^*$$

$$I^*_{zz} = I^*_{z'z'} - (\bar{y}'^*)^2 A^*$$

The last six equations here are the second moments of inertia which characterize the cross sections deflection under loading. $I^*_{y'y'}$, $I^*_{y'z'}$, and $I^*_{z'z'}$ are the seond moments of inertia about an arbitrary axis. I^*_{yy}, I^*_{yz}, and I^*_{zz} are the seond moments of inertia about the modulus weighted centroid.These modulus weighted section properties allow us to calculate the stress and strain associated with a point along the length of the blade.

The following equations for a heterogeneous advanced beam with no thermal loads can then be used to calculate the stress and strain.

$$\varepsilon_{xx} = \frac{P}{E_1 A^*} - \frac{1}{E_1}\left[\frac{M_z I_{yy}^* + M_y I_{yz}^*}{I_{yy}^* I_{zz}^* - I_{yz}^{*^2}}\right]y + \frac{1}{E_1}\left[\frac{M_y I_{zz}^* + M_z I_{yz}^*}{I_{yy}^* I_{zz}^* - I_{yz}^{*^2}}\right]z$$

$$\sigma_{xx} = \frac{EP}{E_1 A^*} - \frac{E}{E_1}\left[\frac{M_z I_{yy}^* + M_y I_{yz}^*}{I_{yy}^* I_{zz}^* - I_{yz}^{*^2}}\right]y + \frac{E}{E_1}\left[\frac{M_y I_{zz}^* + M_z I_{yz}^*}{I_{yy}^* I_{zz}^* - I_{yz}^{*^2}}\right]z$$

The stress and strain equations become a repetitive process that must be recalculated for different cross sections along the length of the cantilever beam to determine the location of maximum stress and strain. Based on the equations for modulus weighted properties the theoretical deflection at a known point on the propeller blade can be calculated by integrateing the slope at the free end of the beam using the equation below.

$$\theta_x = \int_0^x \frac{M_y}{EI_{yy}}$$

$$\delta_x = \int_0^x \theta_x$$

The double integral of slope at the known load point gives the theoretical deflection that is anticipated when the known load is applied at the point x. E is the modulus weighted elasticity and I_{yy} is the second moment of inertia about the z-axis.

Load versus Displacement

For a propeller one comparison parameter between blade material strengths is the stiffness of the blade. The stiffness of a material can be defined as the force applied at a location divided by the deflection induced on the material from the applied force. SI

38

units for stiffness are in Newtons per meter. For each type of propeller that will be experimentally tested, a stiffness value for the propeller can be found using the force versus displacement curves. Stiffness can also be related to the elastic modulus for the propeller. Stiffness is equal to the cross-sectional area of the material multiplied by the elastic modulus and divided by the length to the cross-sectional area measured from the fixed end.

For composite materials the load versus displacement curve increases linearly until a ply fails. At the point where the ply fails, the curve shifts horizontally increasing the displacement without increasing the force until it reaches the linear portion of the new elastic modulus curve for the composite. After ply failure, the elastic modulus decreases to a certain percentage of the initial modulus. This phenomenon makes composites very attractive due to their ability to resist brittle failure. Figure 23 shows the change in elastic modulus of a composite after the failure of multiple or a single ply.
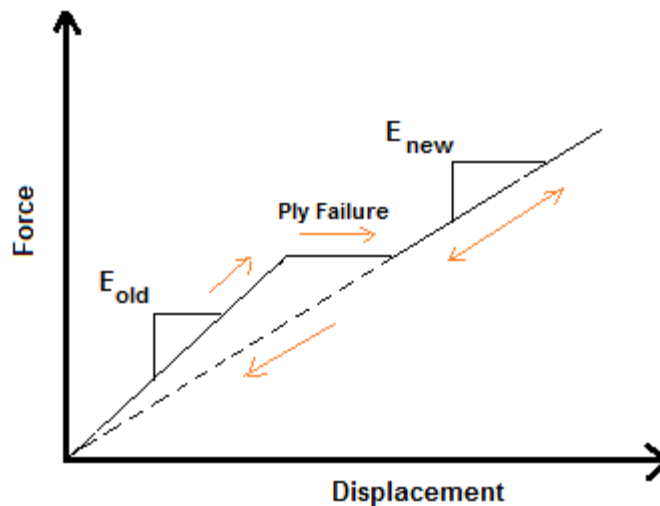
Figure 23 – Force versus Displacement for ply failure

Experimental Set-up

In order to verfiy the theoretical analysis on a propeller blade, an experimental

apparatus must be created for blade deflection testing. The apparatus used is a modified

version of the load-deflection test arrangement for inflated beams created by Jeremy Hill

for use in Dr. Jamey Jacob's Hydrodynamics and Aerodynmaics Laboratory at Oklahoma

State University. Hill's paper, "Load-Deflection Test Arrangement for Inflated Beams,"

highlights the set-up of the testing apparatus as well as a process for running deflection

tests. The modified test apparatus uses many of the same testing components that are

described in the following paragraphs. Figure 24 shows the modified test appartus used

for single blade deflection testing.
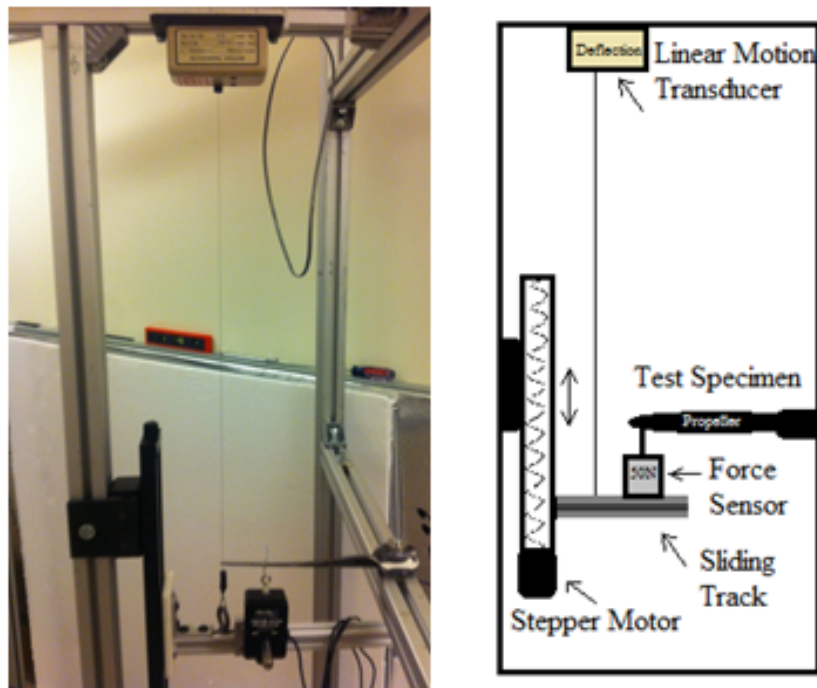
Figure 24 – Modified Load Deflection Test Apparatus

There are several components critical to the load deflection test apparatus which

are the force sensor, the stepper motor and controller, the motion transducer and the

Vernier LabPro interface. These components interact with a computer to control and record the deflection test data.

The force sensor that was used is the Vernier Dual-Range Force Sensor that can be used to measuring both pushing and pulling forces. The sensor uses strain gages to measure a resistance change which corresponds to a change in force. The sensor has the capability to switch between low and high force measurement settings. The low end setting can measure +/- 10 N with a 0.01 N resolution and the high end setting can measure +/- 50 N with a 0.05N resolution. The force sensor has a track attachment that allows the sensor to slide along a track to maintain a perpendicular alignment with the direction of pull on the propeller blade. Figure 25 shows the dual range force sensor mounted on the sliding track.

Figure 25 – Vernier Dual-Range Force Sensor

The stepper motor and controller are used in the test apparatus to deflect the perpendicular attached track that the force sensor is mounted to. The stepper motor and controller allows for the test specimen to be deflected vertically in both directions. The

stepper motor is controlled using software known as SI Programmer. SI Programmer allows users to pre-program commands that are outputted to servo or stepper motors. This allows the stepper motor to deflect the test specimen an exact distance. SI Programmer also allows the user to control motor parameters like direction of rotation and rate of rotation. Figure 26 shows the stepper motor controller and the stepper motor.
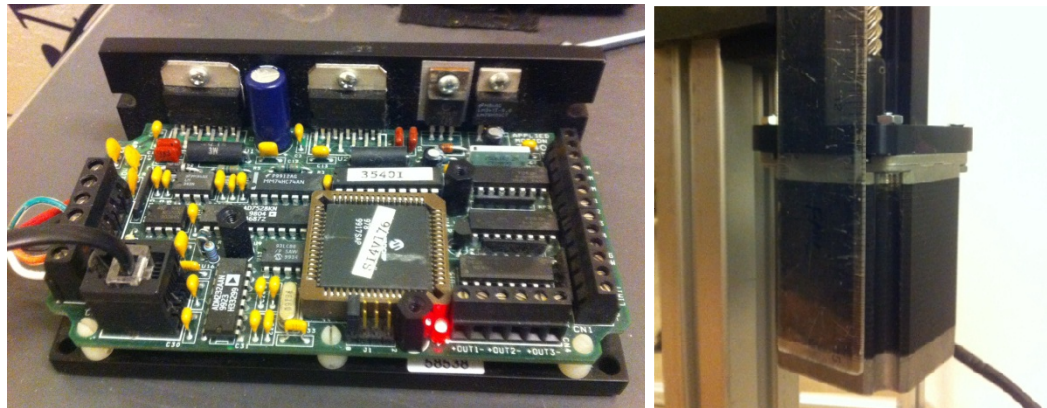
Figure 26 – Stepper Motor Controller and Stepper Motor

The stepper motor used is manufactured by Applied Motion Products with a high torque intended design. The model number is HT23-399 and the motor is roughly 3 inches long. The two phase stepper motor has a unipolar holding torque of 187 oz.-in. and a bipolar holding torque of 267 oz.-in. The unipolar current and resistance of the hybrid motor are 1.0A/phase and 8.2 Ohms/phase, respectively. The bipolar current and resistance of the hybrid motor are 0.71A/phase and 16.4 Ohms/phase, respectively.

The motion transducer that is used is an Ametek Linear Motion Transducer that measures position displacement based on the change created from a cable connected to the sliding track. The cable connects to a potentiometer which measures and outputs the resistance change to voltage through the Vernier LabPro interface. In order to convert the voltage to actual displacement, a calibration run must be done at known

displacements to be able to calculate the displacement from the voltage. Figure 27 shows the linear motion transducer connected to the top of the testing apparatus.

Figure 27 – Ametek Linear Motion Transducer

The last critical component to the testing apparatus is the Vernier LabPro interface that brings all of the component's data together so that it can be output to a usable format. The Vernier LabPro is a data collection interface that allows users to collect data through a computer, graphing calculator, or through the device itself and download it at a later time. Each Vernier LabPro comes with 4 analog channels and 2 digital channels for data collection. Figure 28 shows the Data Acquisition Schematic that connects the monitoring sensors with the computer for data collection.
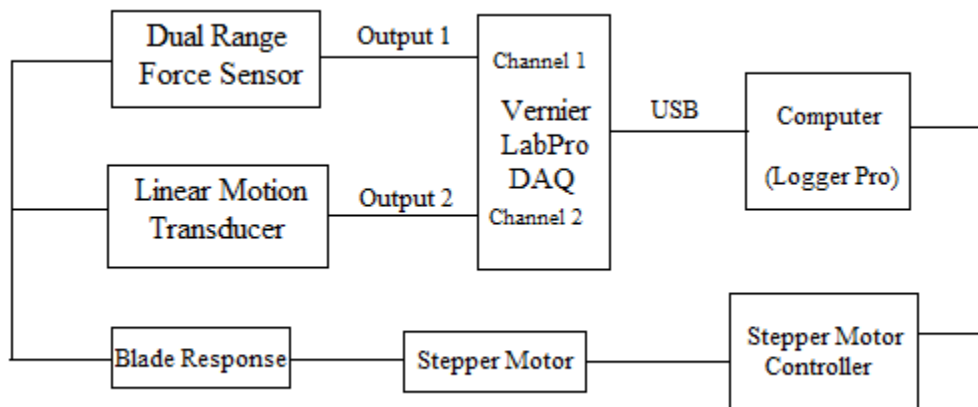
Figure 28 – Data Acquisition Schematic

The software used in conjunction with the Vernier LabPro is Logger Pro which allows the user to record specific test runs and view live data collection. Logger Pro allows the user to collection multiple data sets simultaneously and export the data to be further analyzed. Logger Pro will show the graphical representation of the data as well as the numerical representation of the data. The sampling rate used was 50 samples per second with a sampling length of 60 seconds. These inputs can be adjusted as needed. The data collected can then be export as a text file or CSV file for use with Microsoft Excel for further data analysis. Figure 29 shows a screenshot of the Logger Pro software after a data collection run.
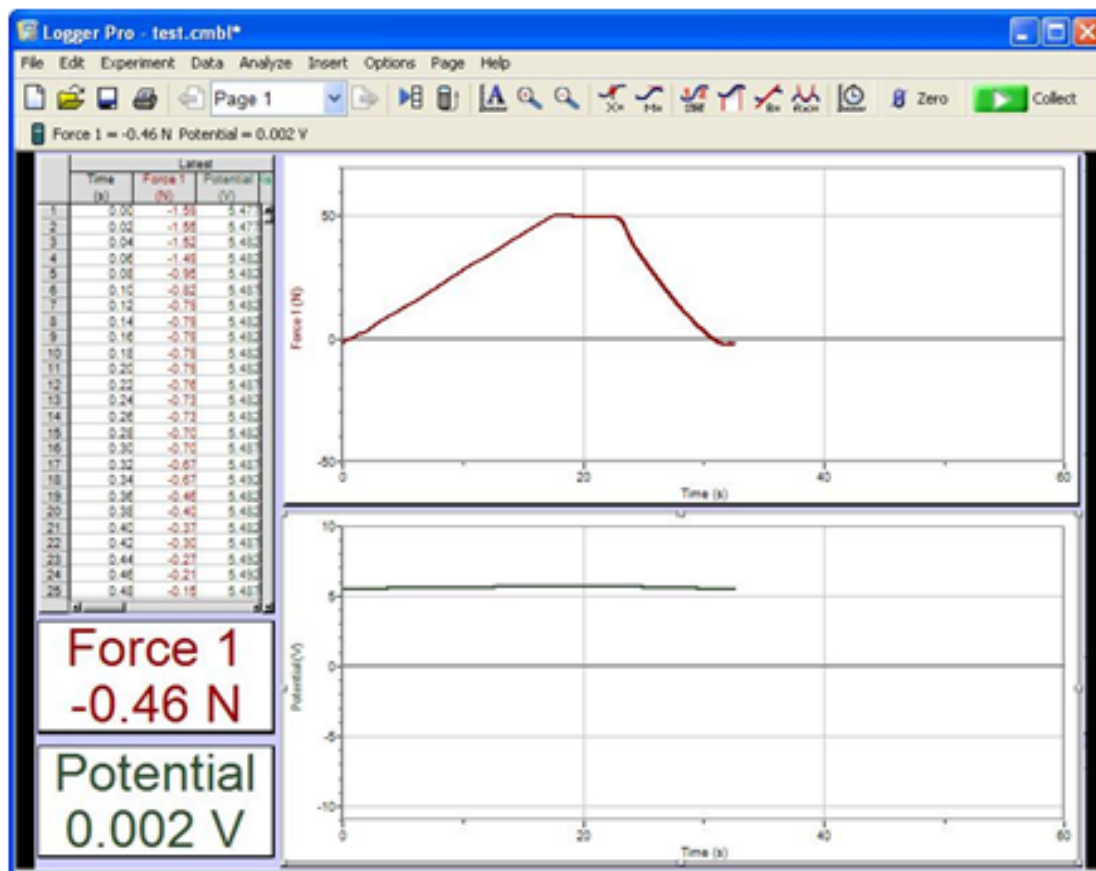
Figure 29 – Logger Pro Software Screenshot of force and displacement

Once these components have been securely fastened together, the deflection associated with the entire testing apparatus needs to be measured in order to account for the variation in deflection in the final results. By measuring the deflection of an aluminum beam with known uniform elastic modulus at the exact same locations as the propeller blades, the deflection of the entire apparatus plus the beam can be recorded. Subtracting the theoretical deflection of the beam from the measured deflection gives the deflection associated with the testing apparatus. The deflection associated with the testing apparatus can be used as a correction factor for the propeller blades when comparing the true theoretical deflection associated with the blades with the experimentally measured deflection. Details of this process are discussed in the results section of this thesis. Figure 30 shows the measured and theoretical deflection of a 12"x 1"x 0.2" 6061-T6 Aluminum beam when deflected at 75% of the blade length distance while Figure 31 shows the measured and theoretical deflection of the 6061-T6 Aluminum beam when deflected at 100% of the blade length distance.
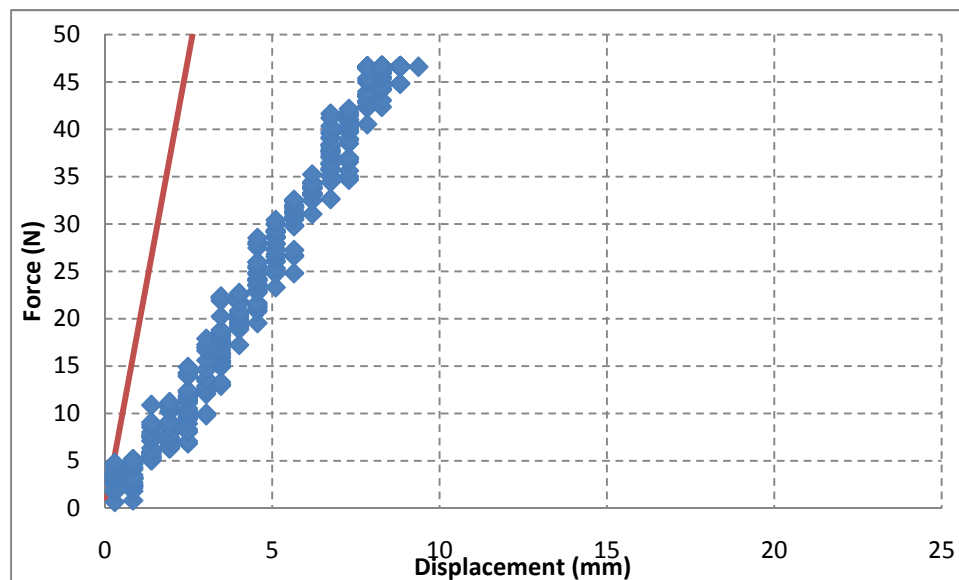
Figure 30 – 6061-T6 Aluminum Beam deflected at 75% of blade length distance
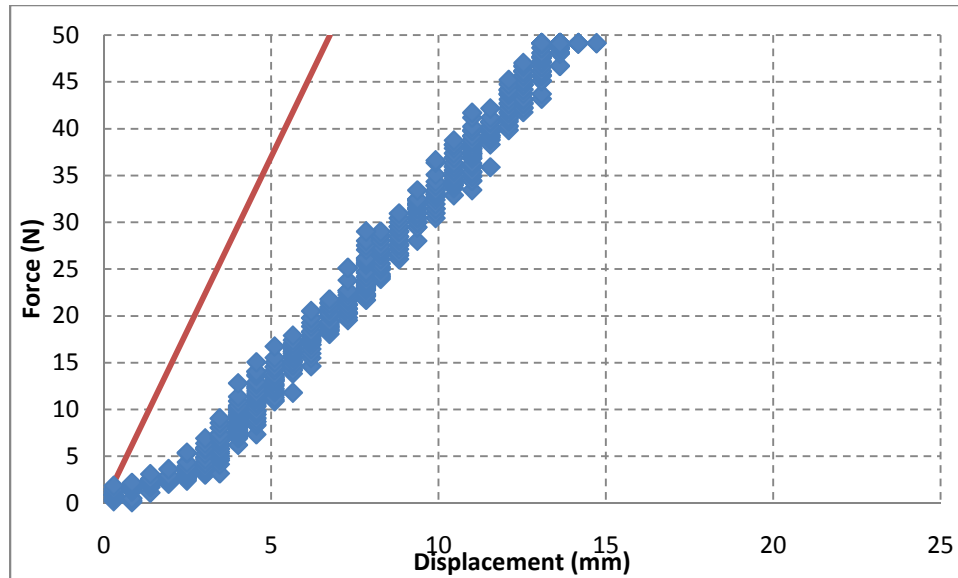
Figure 31 – 6061-T6 Aluminum Beam deflected at 100% of blade length distance

After the deflection associated with the testing apparatus has been quantified the deflection testing is ready to begin. The first step in running the deflection testing is to securely mount the propeller blade to the testing apparatus and make sure it is connected perpendicular to the Vernier Dual-Range Force Sensor. Make sure the live force read out on the Logger Pro software is within a few tenths of zero. Download the SI Programmer file to the stepper motor controller and run through an initial set of low deflection tests to slowly step up to the maximum capacity that the force sensor can handle. Once the maximum blade deflection has been found for the force sensor, download another SI Programmer file to the stepper motor controller that runs through an entire sequence of deflections while the Logger Pro software collects the incoming data. Output the data collected to either a text file or a CSV file compatible with Excel. Repeat this sequence for multiple blade deflection locations and different blade composition cores. Figure 32 shows an example of force versus displacement data that was collected using the data acquisition system.

46
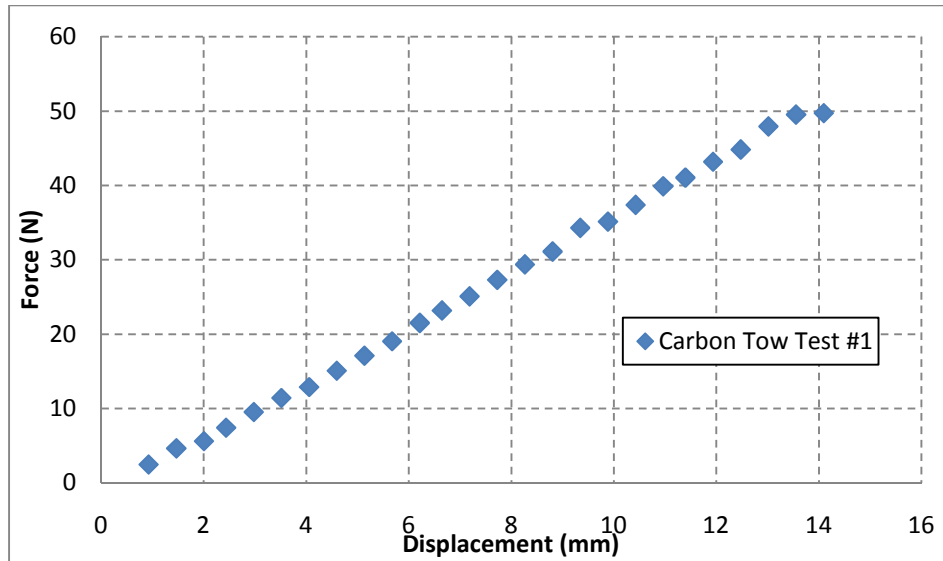
Figure 32 – Sample Data of force versus displacement for Carbon Tow blade

The next validation of the stiffness of the propeller blades is the load versus strain

curves that are generated by using the same testing apparatus as previously described

with strain gages attached to the top and bottom surfaces of the propeller blades. The

strain gages are attached at 50% of the blade length on the quarter-chord. Once attached

and mounted to the testing apparatus load and strain measurements are taken for both

compression and tension on the blade skin. The strain gages used are Omega single axis

pre-wired strain gages, Model number KFG-5-120-C1-11L1M2R. Figure 33 shows the

strain gage attached to the blade surface.

Figure 33 – Strain gage attached to the blade surface

In order to validate performance data of the propeller, the propeller must be run under operational conditions in a wind tunnel. Located in the basement of the Advanced Technology and Research Center (ATRC), Oklahoma State University's wind tunnel is approximately 50 ft in length with a contraction ratio of 15:1 (Gamble, 2009). The test section that was used for testing all the manufactured propellers has dimensions of 6 ft by 3 ft by 3 ft. The wind tunnel is capable of generating dynamic pressures of up to 26 lb_f/in^2 with its 125 horsepower electric motor (Gamble, 2009). The dynamometer that is used in conjunction with the wind tunnel is a custom built small scale dynamometer for testing propellers less than 30 inches in diameter on electric motors. The dynamometer outputs RPM, thrust and torque measurements with its RPM sensor and two independent load cells that are interchangeable for varying capacities of thrust and torque. Schematics for both the wind tunnel and dynamometer can be seen in Figure 34.
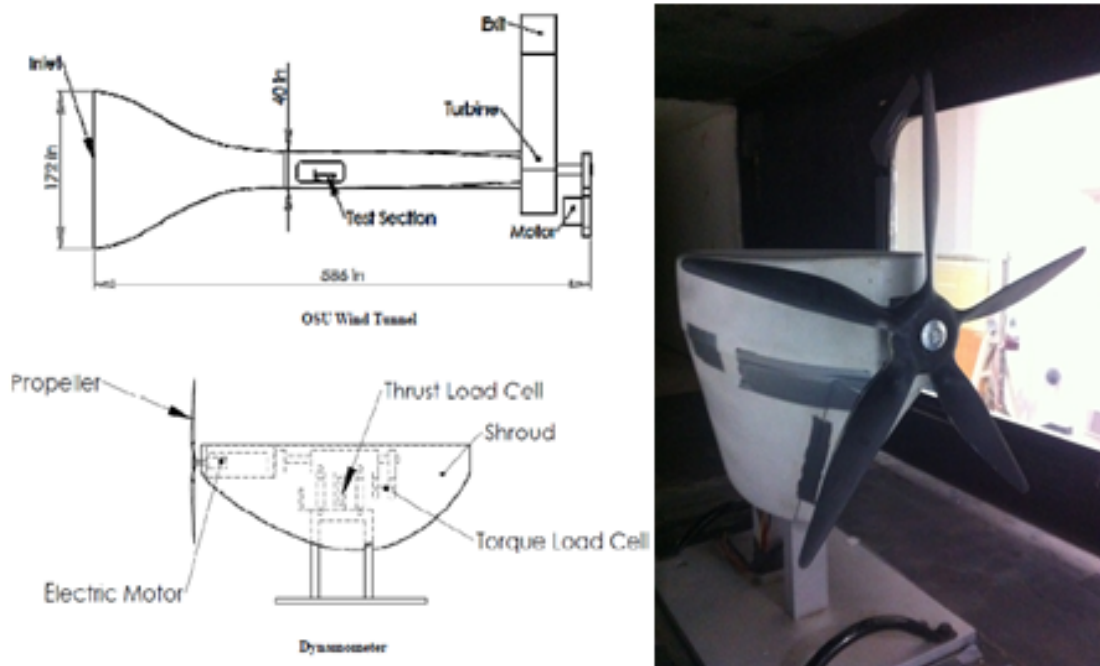
Figure 34 – OSU Wind Tunnel, Dynamometer and 5-blade propeller (Gamble, 2009)

Another dynamometer that was used for validation of static performance parameters was the Propeller Test Module (PTM) designed by a group of undergraduate mechanical engineers at Oklahoma State University (McGovney, 2010). The Propeller Test Module, or dynamic dynamometer, fits in the bed of a pick-up truck and is used for simulating dynamic conditions experienced by the propeller in flight. The truck dynamometer can also be used statically for propeller validation. The truck dynamometer powers an electric motor with four 12 V car batteries wired in series. The electric motor is a Hacker A200-6 that is capable of handling up to 230 A at 42 V continuously. The electric motor can also handle burst of 350 A for 15 seconds at the same voltage. Figure 35 shows the dynamic dynamometer and the 5-blade carbon fiber propeller mounted to the A200-6 electric motor.
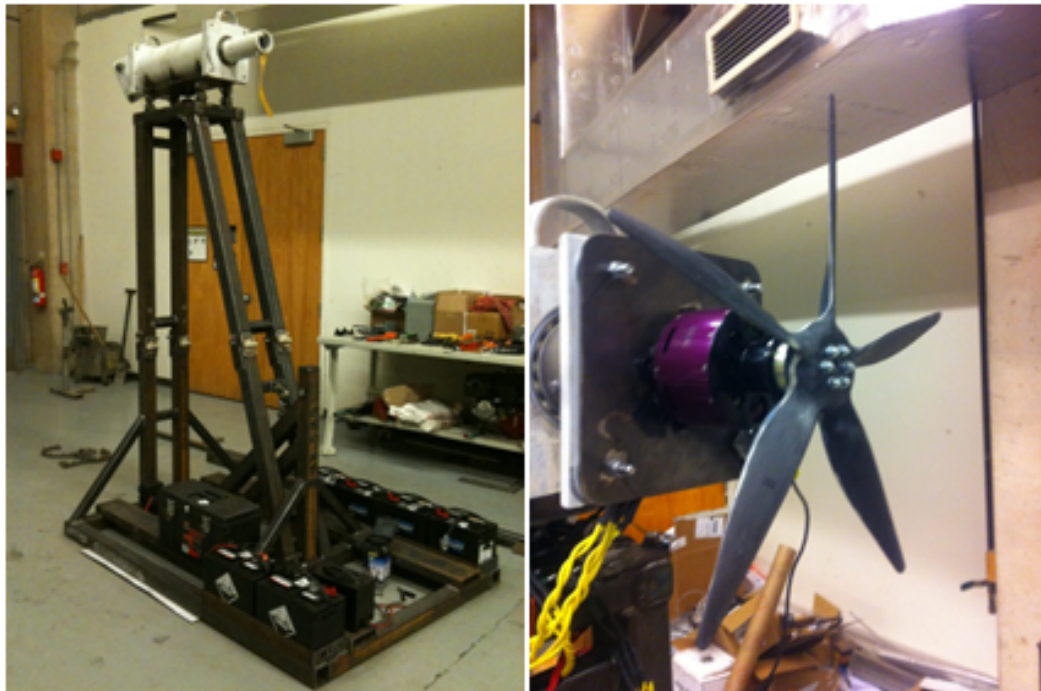
Figure 35 – Propeller Test Module with 5-blade propeller (McGovney, 2010)

The last testing apparatus used in this thesis was a gas engine statically mounted to a test stand and placed against a grid pattern to measure the propeller tip deflection at a range of RPMs. The engine that will be used in this experiment is a two-cylinder 2-stroke internal combustion engine by Desert Aircraft, the DA-100. The DA-100 has manufacturer's specs of 9.8 horsepower with a 2.5 oz/min fuel consumption rate. The maximum RPM for this engine is 8500 RPM, which is well above the RPM range that needs to be tested. Figure 36 shows the DA-100 gas engine with the 5-blade carbon fiber propeller mounted on the static test stand.

Figure 36 – DA-100 gas engine with 5-blade propeller

The deflection at the propeller tip due to the vibrations of the gas engine had to be captured with a high-speed camera in order to pick up any deflection. The camera used

for the high-speed deflection data collection is a Casio Exilim EX-FH20 Digital Camera.

The capture rate of the camera was set to 1000 frames per second. The high-speed

camera was mounted to a tripod and positioned in line with the axis of rotation of the

propeller.

CHAPTER IV

GEOMETRY GENERATION

This chapter will outline the procedure using SolidWorks of how to generate

known propeller geometries as well as create molds from these geometries. The first

section will describe how to generate a 3-blade propeller with a blended hub to include

importing different airfoils, blending contours and using guide curves. The second

section will build on the first by taking the propeller generation and creating using mold

halves. This section will be highlighted with demonstrations of several molding tools in

SolidWorks such as the parting line command and the parting surface command.

SolidWorks Propeller CAD

For a known propeller geometry, the chord wise distribution can be visualized

graphically using a CAD package. An individual blade distribution should be created

first by importing the desired blade airfoils. To do this in SolidWorks, airfoil data

coordinates need to be saved to a text file with x, y, and z coordinates. Since airfoils are

2-D objects, a third column will need to be created in the text file for the z coordinates.

The z coordinate for all points should be input as zero. To bring the airfoils into

SolidWorks use the *Curve through XYZ points* command under the *Curves* dropdown in

the Features tab.
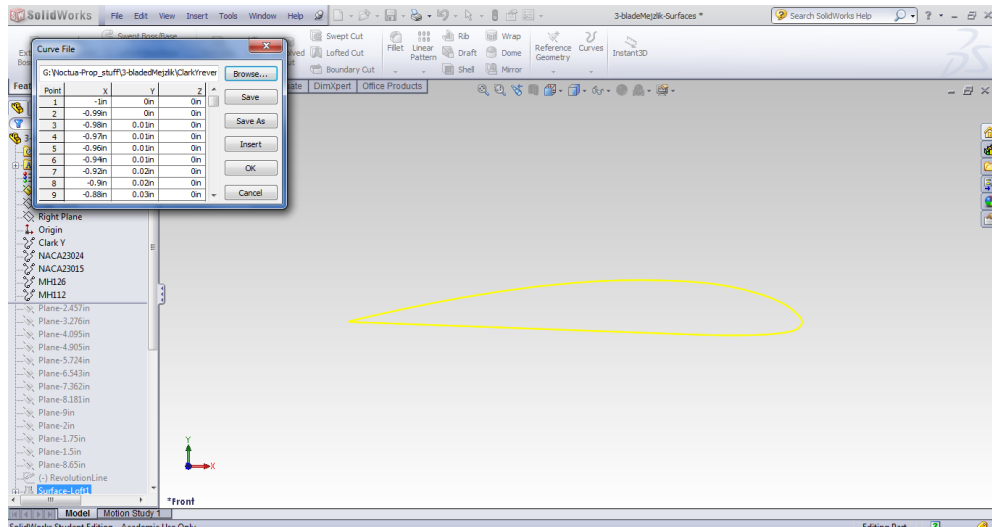
Figure 37 – Importing Airfoils into SolidWorks

Next, offset the plane that the airfoil was imported onto to create planes along each section that coordinates are available for. This does not transfer the airfoil onto those planes. To transfer airfoils onto a desired plane, select the plane and sketch on that plane. Select the imported airfoil curve and *convert entities* to that sketch. Rotate and scale those same entities as needed about the quarter-chord to match the desired chord and pitch. Figure 38 shows the airfoils projected onto each of the planes that coordinates are available.
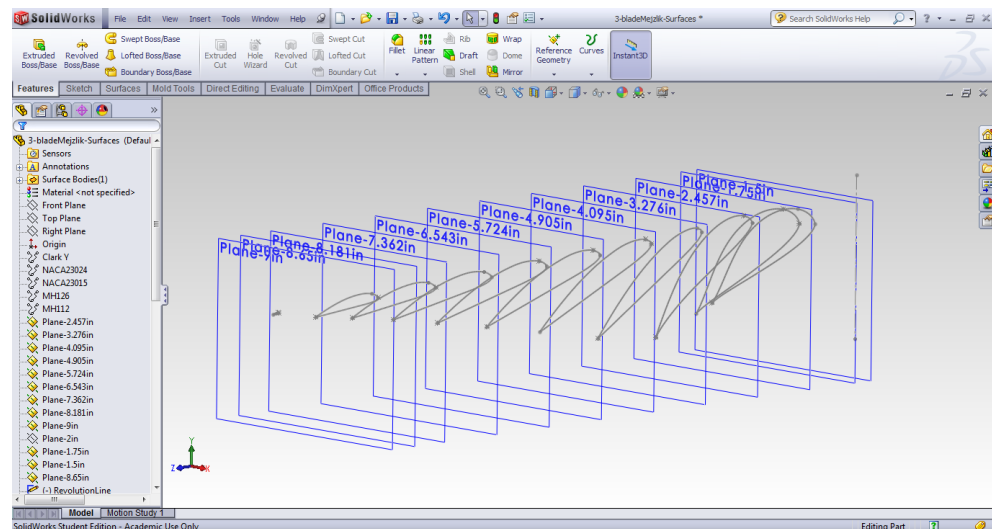
Figure 38 – Converting Airfoils into Entities in SolidWorks

The airfoil cross sections can be used with the loft feature to create a solid or hollow blade. Use guide curves on the leading and trailing edges of the blades to avoid uneven lofts. Guide curves can be created using the *projected curve command*. A sketch must be created in both the top and right planes of the blade that connects the leading or trailing edges together using a spline. The *projected curve command* combines these two spline sketches to form a guide curve along the leading or trailing edge of the blade. Figure 39 shows the guide curves along the leading and trailing edge of the blade.
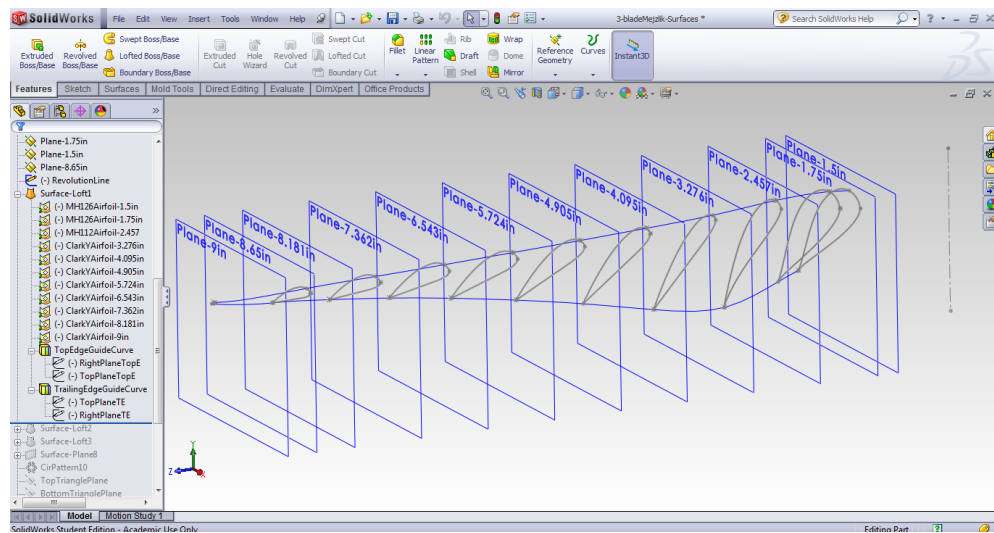
Figure 39 – Blade guide curves in SolidWorks

Using these guide curves and the airfoil cross-sections, a lofted surface or solid can be created for better visualization and complete propeller creation. Under the *lofted surface command*, select the airfoil cross-sections as the profiles and the guide curves as the paths which the lofted surface will follow. Depending on the blade geometry, more than one lofted surface may need to be created to create the entire blade surface.
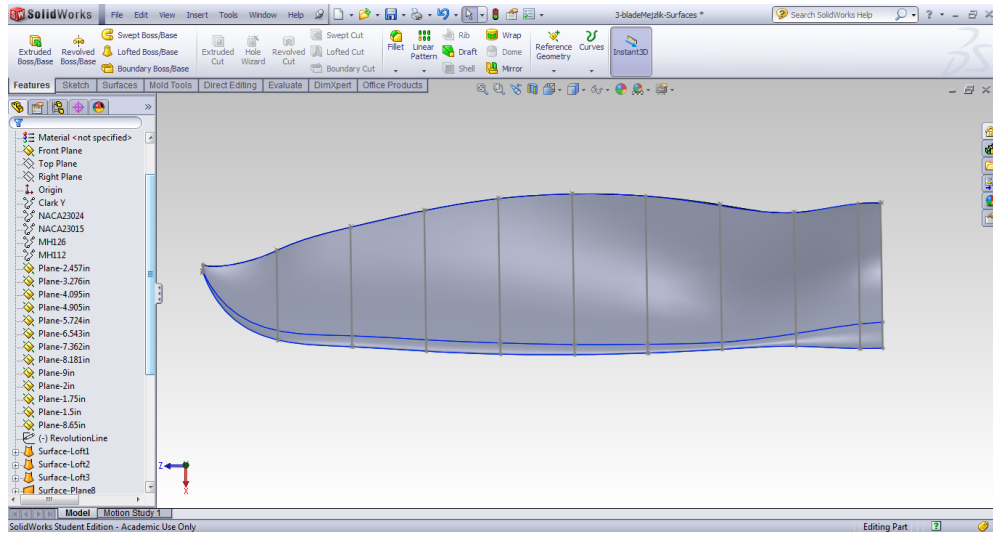
Figure 40 – Top Plane of Single Blade Surface Loft in SolidWorks

Figure 40 shows the airfoil cross sections generated in SolidWorks as well as the

leading and trailing edge guide curves. Creating only one blade allows for the entire

propeller to be created easier than drafting each individual blade. Use the *circular*

pattern feature and simply input the desired number of blades to pattern for the entire

propeller. After selecting the number of blades and finishing the circular pattern, a hub

needs to be integrated into the design that flows smoothly between blades.

Guide curves and boundary surfaces are just one example of how the hub could be

created. Another is with a circular extruded boss and fillets to blend the blades to the

hub. The method for creating the hub is solely up to the user and can be created

numerous ways. The method that will be described is the method with guide curves and

boundary surfaces. The first step to creating the hub is to create splines in the top and

right plane that connect the leading edge of one blade with the trailing edge of the next

blade. These curves are combined using the *projected curve command* and made tangent

to the leading and trailing edge guide curves. Figure 41 shows the guide curve that

55

connects the leading edge of one blade to the trailing edge of the next using a projected curve.
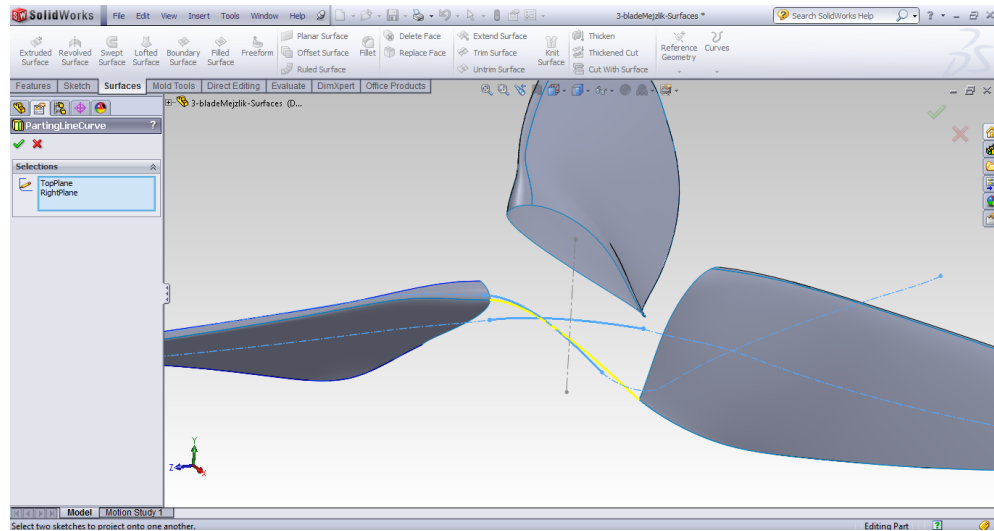
Figure 41 –Hub guide curve in SolidWorks

After the guide curve between the leading edge and trailing edge has been created, the top and bottom surfaces of the hub need to be created so the boundary surfaces can be generated. For a 3-blade propeller, a triangular shape can be used for the top and bottom surfaces. The region between the hub guide curve and the top and bottom hub surfaces can now be generated using the *boundary surfaces command*. Figure 42 shows the boundary surfaces at the hub of the propeller that combine the patterned blades.
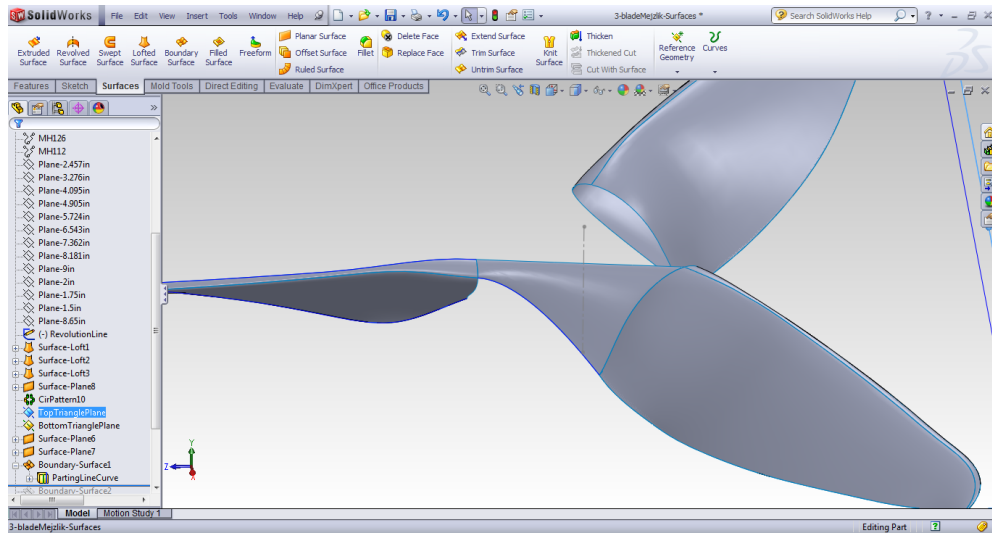
Figure 42 – Boundary Surface of hub in SolidWorks

The boundary surface is generated all the way around the hub and the final propeller is now complete. Figure 43 shows the completed propeller in SolidWorks that is ready for mold creation. After the propeller has been designed, it is time to create the propeller molds in SolidWorks that will be CNC machined out.
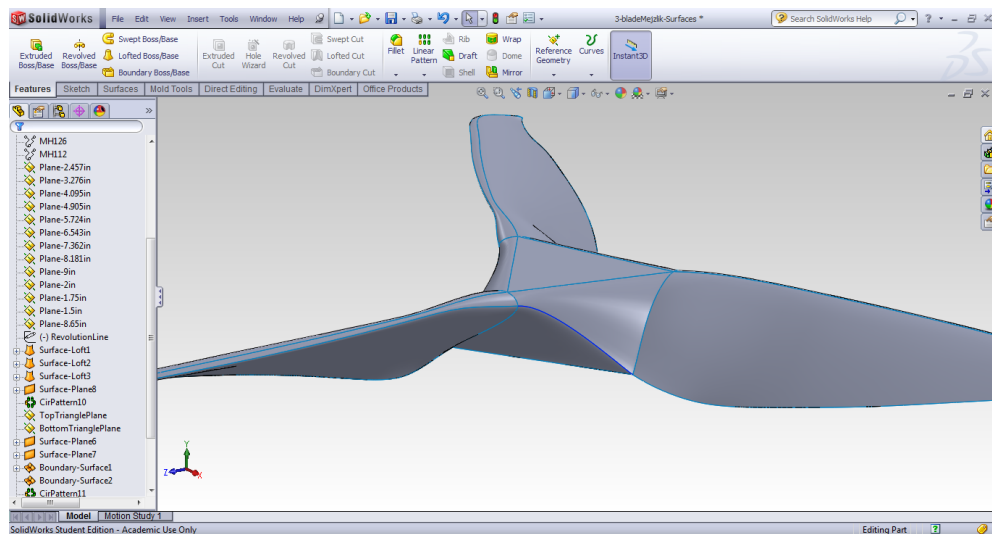
Figure 43 – Hub created with guide curves in SolidWorks

SolidWorks Mold Design

There are several steps that need to be taken to transform the propeller design to two usable mold halves in SolidWorks. The steps are creating a parting line, creating a parting surface, creating a base for the mold and trimming any unwanted surfaces on the mold. Choosing whether to make male or female molds is a step that can be done at a later time in SolidWorks and only requires that one surface be hidden and the other surface is unconcealed. For this walkthrough, female mold halves have been chosen for use. Figure 44 shows the 5-blade propeller that will be used to create molds in SolidWorks.
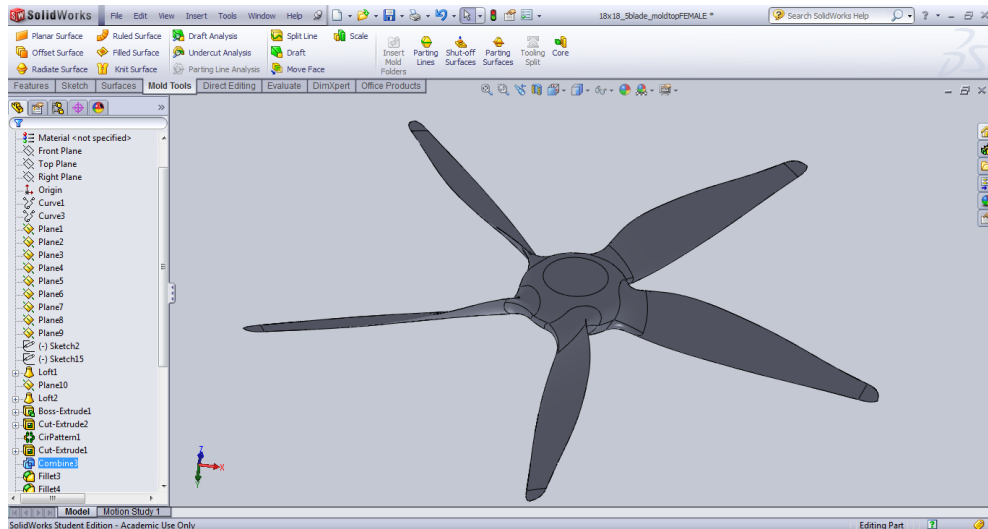
Figure 44 – 5-bladed propeller design in SolidWorks

The first step is to create a parting line along the entire circumference of the propeller. This will allow the propeller to be split into two halves that can be used to create mold halves. Using the *parting line feature* in SolidWorks, run a draft analysis of the propeller making sure to select *Use for Core/Cavity Split* and *Split faces*. This will create a shell for each of the halves of the propeller. Draft analysis angle should be less than 3 degrees; preferably lower. Draft analysis will make sure that the part does not

have any negative angles on the mold halves.   Figure 45 shows the draft analysis

performed on the 5-blade propeller.
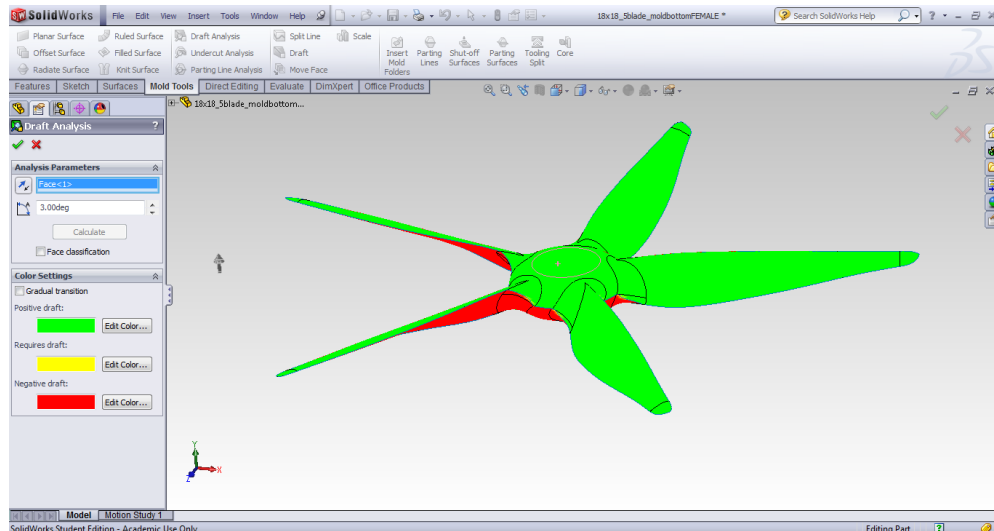
Figure 45 – Draft Analysis of 5-bladed propeller in SolidWorks

The second step to create one of the molds is to hide one of the shell surfaces that

have been created by the parting line. Use the *parting surface command* to create a

surface that extends around the entire propeller a certain distance. Depending on how

complex the geometry of the propeller is will determine if surface knits are required for

the parting surface. Figure 46 shows the parting surface created on one-half of the 5-

blade propeller.
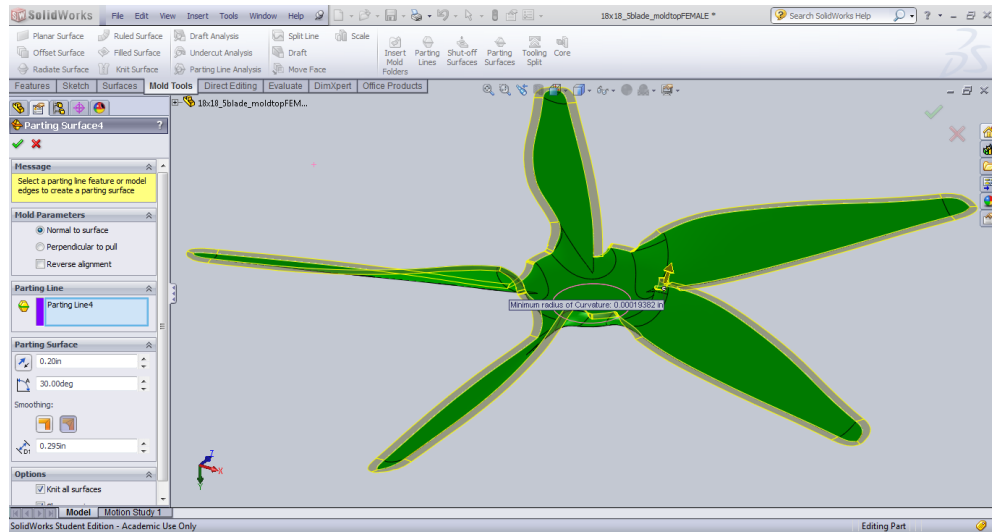
Figure 46 – Parting Surface of 5-bladed propeller in SolidWorks

After the parting surface has been created there are typically gaps between the parting surface and the mold half that need to be knitted together. Use the *surface knit command* to knit the parting surface with the propeller mold half. There are several ways that the remaining area between the propeller blades can be filled. One method is to use a surface loft between the edge of the parting surface and a sketch that extends past the boundaries of the mold. Another method is to use a boundary surface that extends outward from the propeller to a sketch. Both methods result in similar surfaces being created, but more control of the surface is given in the boundary surface command. Figure 47 shows the method of using a surface loft to connect the propeller blades.
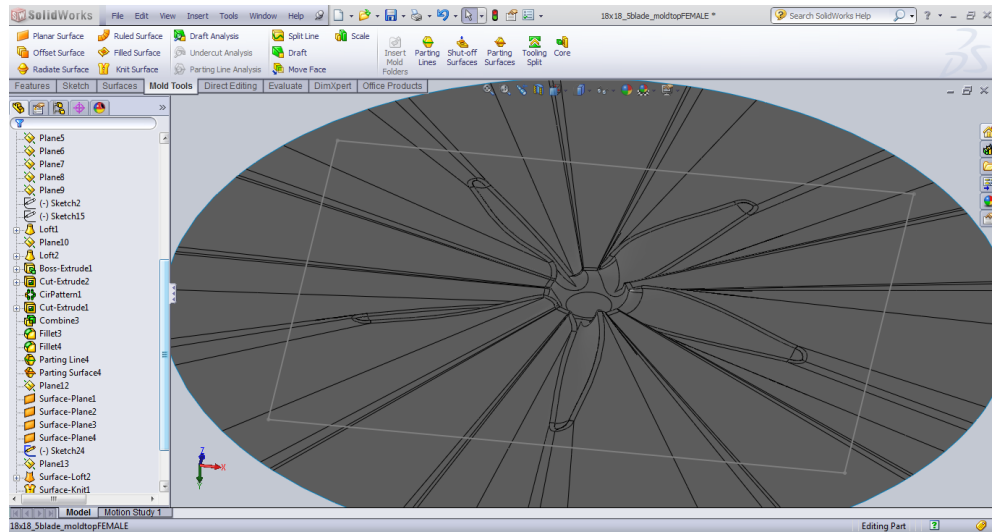
Figure 47 – Surface Loft between propeller blades in SolidWorks

The third step is to create a base for the propeller mold half. This is done by creating a mold outline in a sketch and extruding that outline up to the mold surface. Make sure that the mold base is short enough to accommodate any z-axis restrictions that could be faced when using a CNC router. Also note the overall height of the mold base for future reference when gluing multiple layers of MDF board. Figure 48 shows the mold base that is about to be created for one-half of the 5-blade propeller.
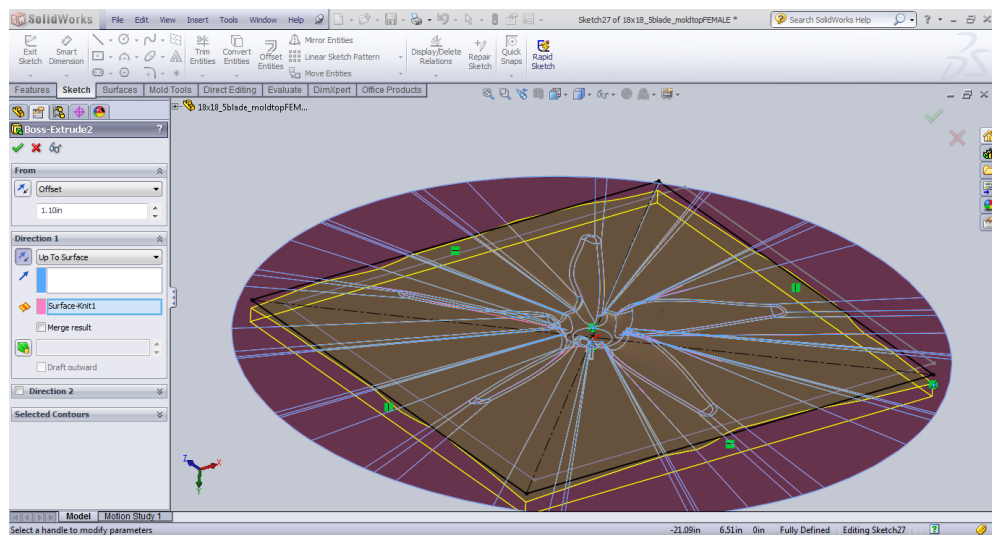
Figure 48 – Mold base for 5-bladed propeller in SolidWorks

The final step in SolidWorks is to trim any unwanted surfaces around the edges of the mold base. The mold base can also be trimmed down to a certain dimension based on the MDF board used or the dimension restrictions of the CNC router being used. Figure 49 shows the mold base after the unwanted edges have been trimmed. The step between SolidWorks and actually machining the part out on a CNC router is to generate the G-code used by the CNC. This step will not be examined in the context of this thesis and will be left to the user to decide which method is best for G-code generation.
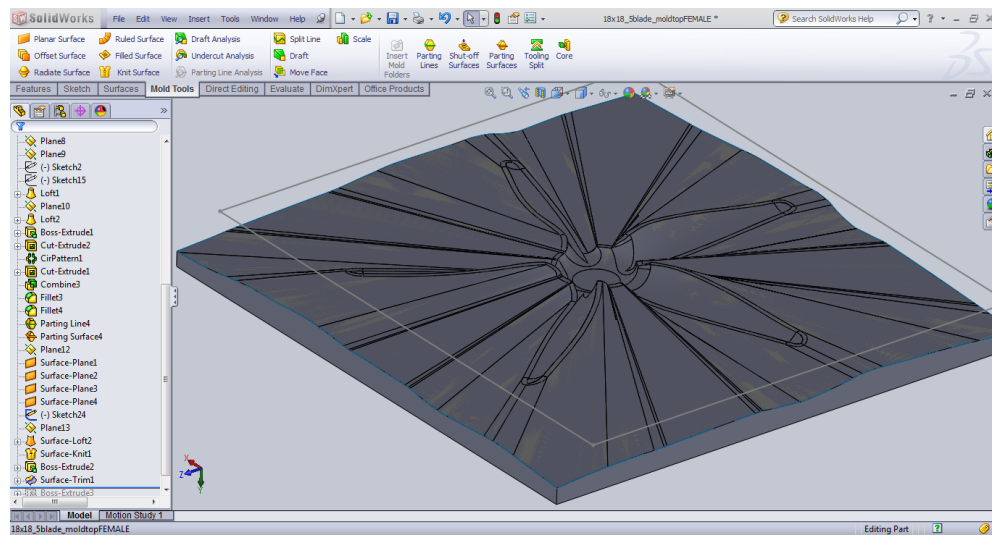
Figure 49 – One mold half of 5-bladed propeller in SolidWorks

Depending on the CAD software package being used, some of the commands outline in this section will not be available to users. Many other CAD packages require that the user manually generate one of these steps with several individual commands. For the user friendliness and availability, SolidWorks was chosen to design and generate the propeller and mold CAD.

CHAPTER V

PROPELLER MANUFACTURING

This chapter will outline the steps taken to construct a multi-bladed propeller from mold making to final prototype. The first part will explain the process for creating tool coat propeller molds, which will be followed by the actual building of the final propeller. The final propeller will go through several iterations of sanding and coats of epoxy to make sure that the propeller is balanced and structurally sound. Each of these stages is critical to the next one so utmost care should be taken at all times in the process. Corners should not be cut when creating a propeller due to the high centrifugal forces that it will be experiencing.

Mold Creation

The first step to creating male mold plugs using medium density fiberboard (MDF) is to cut the MDF down to the appropriate outer dimensions of the mold that will be created. Be sure to include additional material around the edges that will be trimmed later (1-2 inches). Typically MDF is ¾" thick therefore if the part has a depth of more than ¾" multiple pieces will need to be stacked together. A method for combining layers of MDF is to first rough both bonding surfaces in lateral and longitudinal directions with 120 grit or lower sandpaper. The MDF bonding surface needs to be cleaned with a moist rag and dried immediately to avoid warping of the board. Apply an even coating of wood

glue to both sides. Applying wood glue to both bonding surfaces ensures that the entirety

of the surfaces will be coated with adhesive. After stacking the desired layers of MDF,

be sure to clamp the layers together or to a level surface. Drying time of the wood glue is

dependent on manufacturer, but is typically 24 hours. Once the wood glue has dried, the

edges should be trimmed or sanded to remove spillover glue. The MDF is now ready to

be machined out with a CNC.

Figure 50 – Stacked and glued MDF board

Now that the MDF has been prepared for milling, the mold plugs can start taking

shape on the CNC router. Depending on the CNC milling equipment available and the

mold size, milling the MDF plug can take a significant amount of time; on the order of 5-

10 hours. Make sure to align the x and y axes on the router table with the correct x and y

directions along the MDF board. The first pass that removes the bulk of the material

from the MDF part is a roughing pass. The roughing pass cuts out a general shape of the

part that is being created. A tooling change will be required between the roughing pass

and the next pass. The second pass that creates the final geometry of the mold part is the

finishing pass. After the finishing pass is complete, the mold surface of the newly

created part must be sanding to remove tooling marks left by the router bit.
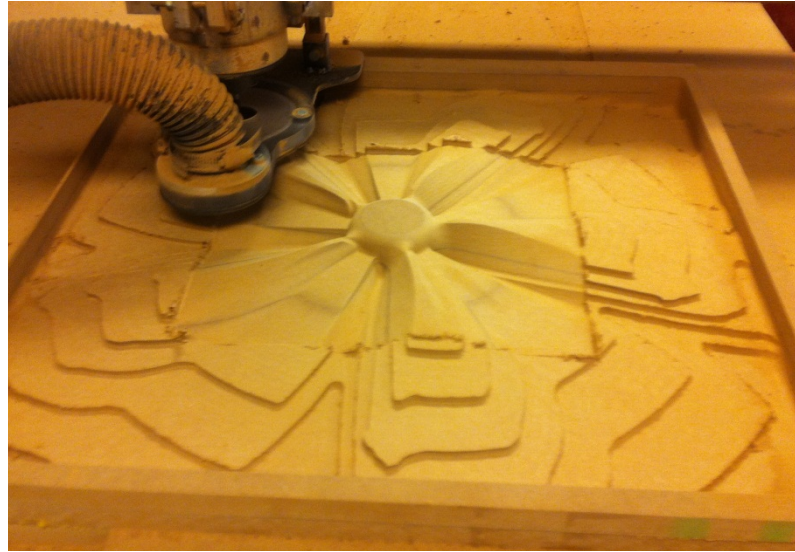
Figure 51 – Finishing pass on 5-bladed propeller male mold plug

Preparing the plug surface for creating the female mold that will be used to create

parts takes time and patience. The MDF surface will be fuzzy after milling and will need

to be smoothed out. Coat the entire plug with a layer of painting primer and allow the

primer to dry for a minimum of 2 hours before sanding. Lightly sand the plug to avoid

changing the geometry of the part. Reapply the primer and sand until the surface finish is

extremely smooth and all tooling marks have been removed. If the tooling marks are not

removed, they will show up in the female mold later in the process. The male plug

should be waxed and buffed a minimum of 3 times to fill any micro-voids in the surface

that still remain. A releasing film should be painted on the surface and dried quickly

using a heat source. A common releasing film used is Partall #10. Using a heat source to

dry the releasing film decreases the chances that bubbles will form in the releasing film.

Similar to waxing, apply a minimum of 2 layers of releasing film to the surface. The MDF male mold plug can now be used to create the final female mold.

Figure 52 – Primer coating on 5-bladed propeller male mold plug

In preparation for producing the final female mold, tooling fiberglass should be cut to the size of the required part. Approximately 13 layers of 9 oz. fiberglass should be cut making sure that each layer has the fiber alignment offset by 45° from the previous layer. This helps to prevent unwanted warping in the final mold. Mix a combination of tooling gel coat and hardener with a 5 to 1 ratio to lightly coat the surface of the male plug with. Apply the mixture to the surface and allow the coat to harden to the touch or kick. While waiting for the tooling gel coat mixture's working time to expire, it is good practice to take an X-acto knife or razor blade and pop any air bubbles that can be seen coming to the surface of the tooling gel. Removing these unwanted air bubbles will make the surface of the female mold have a smoother finish. Once the tooling gel coat mixture has kicked apply the layers of tooling fiberglass with a mixture of resin and hardener. Make sure to offset each successive layer of tooling glass by 45°. One epoxy mixture that can be used is WB-400 resin with SC-150-N hardener in a 2 to 1 ratio. The drying

time required when using this epoxy mixture is approximately 12 hours with a working time of 30 minutes to an hour.

Figure 53 – Tooling fiberglass layers on 5-bladed propeller male mold plug

After the required drying time the female mold can be removed from the male plug. The final product is a quality female mold that can be used numerous times to produce the desired part.
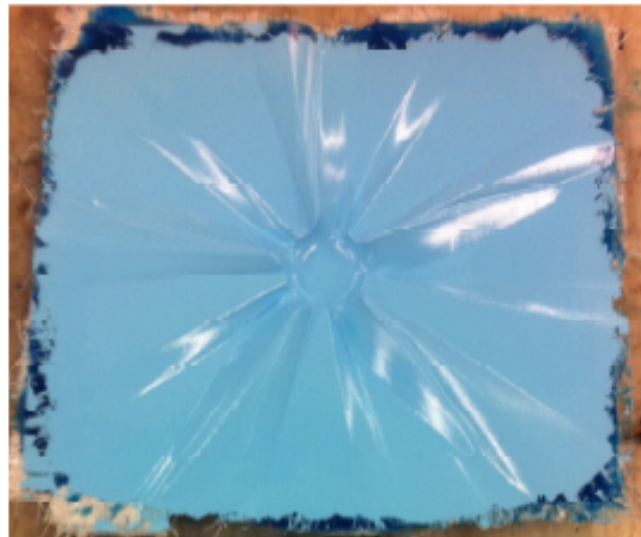
Figure 54 – One side of final female 5-bladed propeller mold

Propeller Creation

The process for creating a usable propeller consists of four major stages; preparing the molds and material, laying-up the material, trimming the material, and sanding and balancing the propeller. Each of these stages is critical to the next one so utmost care should be taken at all times in the process. Corners should not be cut when creating a propeller due to the high centrifugal forces that it will be experiencing. After all the hard work put into this method, the results will be highly reliable carbon fiber propellers that are specific to the user's vehicle. The process for creating a propeller in this section will detail the material and procedures for a 3-blade propeller that has one layer of outer skin and a solid core.

Before any lay-ups can take place using the molds, the molds need to be waxed and released. Each mold half should be waxed and buffed a minimum of 3 times to fill any micro-voids in the surface that still remain. A releasing film should be painted on the surface and dried quickly using a heat source. Using a heat source to dry the releasing film decreases the chances that bubbles will form in the releasing film. Similar to waxing, apply a minimum of 2 layers of releasing film to the surface.

The key decision in how much material to cut for the propeller mold is dependent on the propeller geometry and thickness. Thicker propellers require less material for the same propeller stiffness as thinner ones. However, the user should pre-determine the amount of composite plies they will use based on the type of engine the propeller will be operating on. The carbon fiber weave that will be used is from Fibre Glast Developments Corporation, Part #530 3K, 5.7oz/sq. yd. Plain Weave Carbon Fiber Fabric. Using the molds as a reference cut out 6 pieces of carbon fiber that is at a 45° offset with the axial direction of the blades. There will be 3 pieces for each side of the

mold halves. Each piece should be roughly 1" bigger than the mold parting lines for the propeller blade. For the 3-blade hub, 4 triangular pieces should be cut. There will be 2 pieces for each side of the hub.   Figure 55shows an example of the carbon fiber material that needs to be cut for the 3-blade propeller.
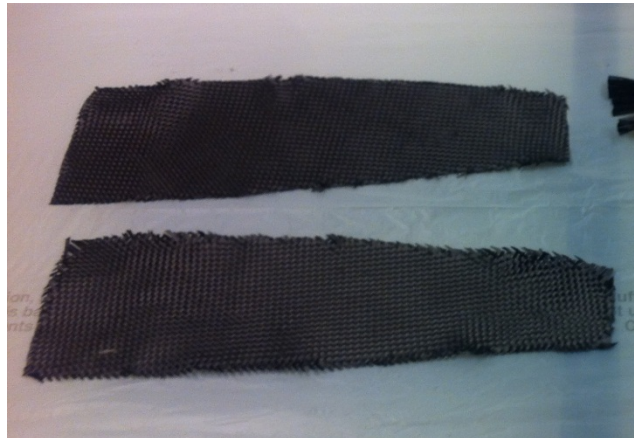
Figure 55 – Carbon Fiber Material cut at 45° offset

The next stage of the process is the wet lay-up of the propeller.   Mix enough WB-400 resin and SC-150-N hardener to be able to generously coat both sides of the carbon fiber pieces. First place one of the hub pieces in each side of the mold halves. Next, carefully place the individual blade pieces in the mold halves, making sure to go over the entire piece with a plastic squeegee or your finger. Doing this will help to ensure that air bubbles do not get trapped on the outer surface of your propeller blades. Place the last 2 hub pieces in each mold half to overlap the blade pieces. Next mix a combination of WB-400 resin and SC-150-N hardener with chopped fiber pieces. A suitably amount of chopped fiber to add to the mixture of epoxy is 10 grams of chopped fiber for every 75 grams of epoxy. More of this mixture may need to be made depending on the thickness of your propeller blades and hub. Place enough of the chopped fiber and epoxy mixture in each of the individual blade halves to fill each half. The chopped fiber and epoxy

mixture should fill both the propeller blades and the center hub. Excess chopped fiber

and epoxy in each mold half is a good thing. This will be your validation that the

propeller blades are solid on the inside. Next, carefully align the alignment pins on the

two molds halves so that the two sides of the mold fit together. Firmly press the two

mold halves together and wrap the edges of the molds with release paper and breather

material. Place the molds, release paper, breather material, and one-half of the thru-bag

vacuum connector in a vacuum bag. Seal the edges of the vacuum bag and connect the

other half of the thru-bag vacuum connector. Connect the 25 psi vacuum to the thru-bag

vacuum connector and make sure that there are no leaks in the vacuum bagging. If

needed, use extra chromate tape to seal any unwanted holes in the vacuum bag. The

drying time for the WB-400 resin with SC-150-N hardener is approximately 12 hours

under vacuum. If the WB-400 resin with SC-250 hardener were used the drying time

would increase to 24 hours under vacuum.

After the appropriate drying time the propeller is ready to come out of the molds.

Release the vacuum connected hose and open the vacuum bag. Most of the vacuum

bagging material can be re-used so be careful when pulling out the molds. The mold

halves will be tightly epoxied together. Use either a plastic wedge and mallet or

compressed air to split the two mold halves apart. Once the propeller molds are split and

propeller has been removed from the molds, the result will look similar to Figure 56. The

black splotches that circle around the entire mold serve as a validation that there was

enough chopped fiber and epoxy to fill the core of the propeller.
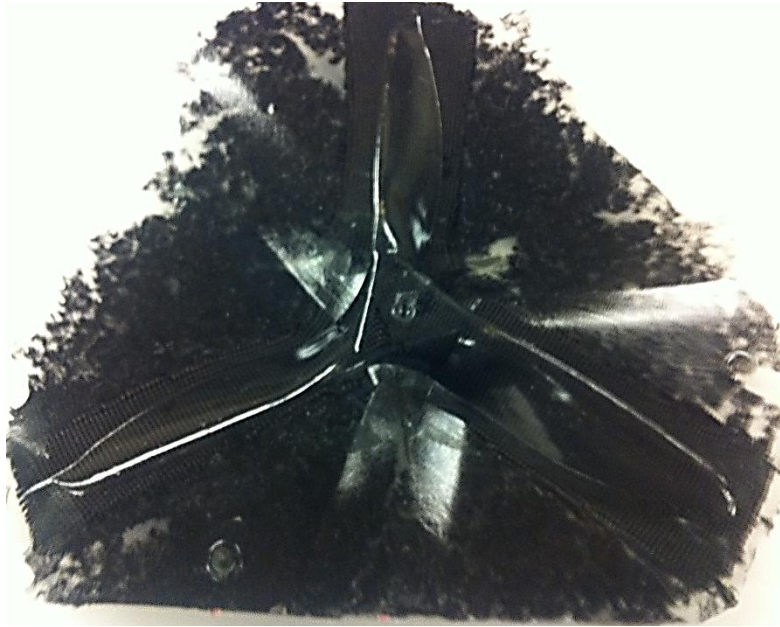
Figure 56 – 3-blade Propeller immediately after being pulled from mold

The next stage is the trimming stage of the propeller. Trimming of carbon fiber should be done in a well-ventilated area and with proper breathing equipment. Using a Dremel equipped with the rotating cutting wheel, trim off the excess material from the propeller up to a ¼" to ½" away from the parting line on the propeller. Next, change out the Dremel head to the sanding bit and carefully sand up to the parting line. Be sure to not sand off any extra material from the propeller blades as this could cause the propeller to be more out of balance than it already will be. Using sanding blocks the parting line edge can be rounded at the leading edge and tapered at the trailing edge to blend the top and bottom surfaces together. After the propeller parting line has been smoothed to acceptable tolerances, the top and bottom surfaces of the propeller blades need to be checked for voids in the epoxy and carbon fiber. These voids must be filled with epoxy before balancing of the propeller can begin. Figure 57 shows the parting line after being

sanding down with the Dremel and by hand and some small voids in the epoxy that need

to be filled before balancing the propeller.

Figure 57 – Propeller parting line and voids in the epoxy

While filling the voids with epoxy it is good practice to go over the parting line of

the propeller with a light coat of epoxy to fill any other voids that have resulted from

sanding the parting line. Depending on the type of epoxy used, allow sufficient drying

time before sanding any extra epoxy off. Try to avoid sanding the top and bottom

surfaces of the propeller to avoid changing the geometry of the propeller and risk creating

unsymmetrical propeller blades.

The next and final stage of the process is to balance the propeller. At this point

the propeller will be unbalanced and require some amount of balancing. However, before

balancing can begin the shaft hole must be drilled out of the center of the propeller hub.

For the 3-blade propeller, drill alignment guides have been incorporated into the molds

for precision drilling alignment. For the 5-blade propeller, an alignment jig was created

to drill out the center hole. Once the center hole is drilled, the propeller can be placed on

the propeller balancing shaft and checked to see how out of balance the propeller is.

Figure 58 shows the 3-blade propeller being balanced with a simple propeller balancer.

Figure 58 – Balancing 3-blade propeller

The proper technique for balancing a 3-blade propeller is to first spin the propeller

on the balancer and let it come to a stop by itself. The blade closest to the 12 o'clock

position is your lightest blade and should be marked with a one. The next blade that is

closest to 12 o'clock is the second lightest blade and should be marked with a two. The

last blade that will be farthest away from the 12 o'clock position or closest to the 6

o'clock position is the heaviest blade and should be mark with a three. Lightly sand the

heaviest blade on the leading edge and the bottom surface until blades two and three are

balanced or blade one sits perfectly at 12 o'clock. Next, position blade two at 12 o'clock

and sand blades one and three until blade two sits perfectly at 12 o'clock. Now, place

blade three at 12 o'clock and sand blades one and two until blade three sits perfectly at 12

o'clock. The propeller should now be returned to blade one at the 12 o'clock position

and blades two and three re-checked for balance. It is good practice to re-check the

balance of each blade at the 12 o'clock position several times to confirm proper balance.

This process is similar for propellers with odd numbers of blades. For propellers with

even numbers of blades the process becomes much simpler. Even number of blades

allows the propeller to be balanced symmetrically along one of its axes.
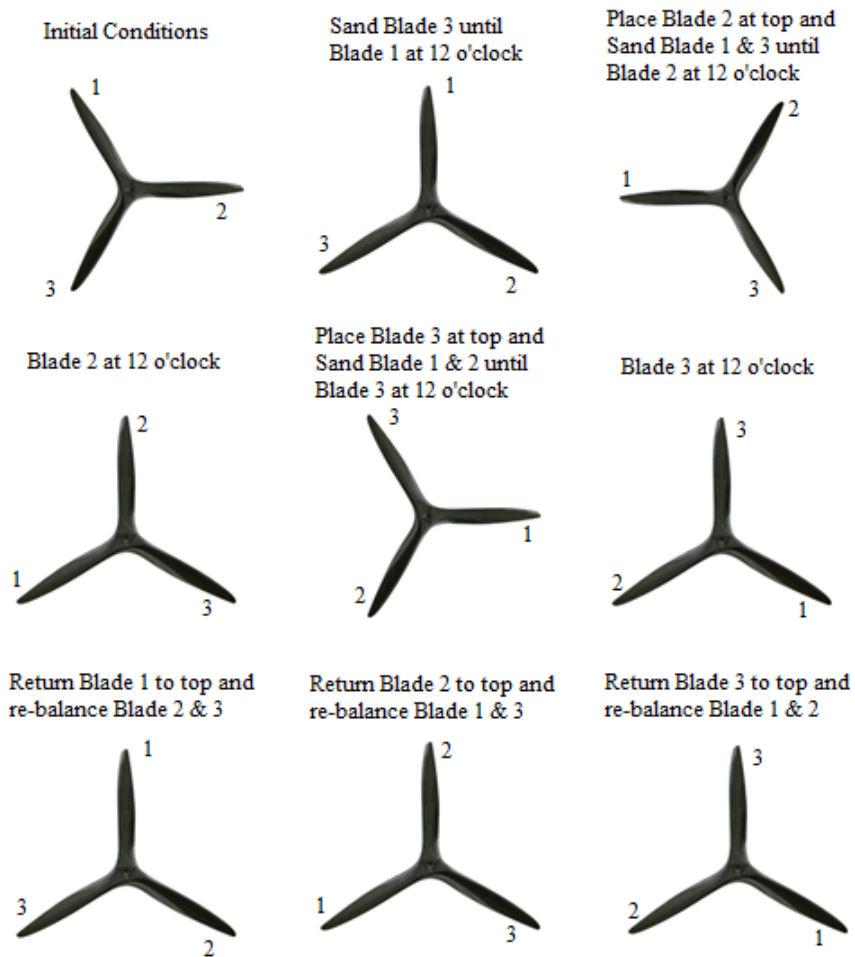
Figure 59 –3-blade balancing schematic

The last step described here is an optional procedure that is primarily for looks of

the propeller. At this stage the propeller has been sanding quite a bit and will not be

aesthetically pleasing to avid aircraft enthusiasts or potential customers. However, a light

coat of epoxy brushed on with a foam brush will restore the carbon fiber look and

produce an aesthetically pleasing propeller. The only drawback of this additional step is

that the propeller must be re-balanced before it can be used operationally. To retain the

glossy look, when re-balancing the propeller only lightly sand on the bottom or back

surface of the propeller blades. After this step the propeller is ready to be put into use on

a dynamometer to verify the performance parameters and that the propeller has been

properly balanced.

Figure 60 – Finished propeller blade after epoxy coating

CHAPTER VI

RESULTS AND DISCUSSION

This chapter will be highlighted by the results from the different propeller

manufacturing techniques that were attempted and the deflection testing that was

associated with the different constructed propellers. The different propeller

manufacturing techniques include rapid proto-typing of propellers, CNC milling of

wooden propellers, and wet lay-up of composite propellers. Load versus deflection

curves are measured for three different 5-blade propeller blades. High-speed deflection

data of the 5-blade propeller is recorded and can be compared with the load versus

displacement curves to predict the induced load at a measured deflection.

Rapid Prototyping
The first attempt at creating a custom propeller was using the technology of rapid

prototyping. A 3-blade propeller was designed and then modeled using Rhino3D CAD

software by McNeel and Vehicle Sketch Pad (VSP) by NASA. The 3-blade propeller

was 14" in diameter and had a 12" pitch. The chord distribution was similar to that of the

YO-3A propeller blades. The hub of the propeller was simply a ring that connected the

individual propeller blades. The hub looked similar to an oversized washer. The design

of this propeller was very different at the hub than any of the rest of the propellers

developed in this thesis. The propeller file was exported as an STL file for the rapid

prototyping machine. The material used for rapid prototyping the propeller was ABS

plastic. The rapid prototyped propeller turned out to be extremely porous and had to be

filled to maintain the propeller geometry. A mixture of epoxy and filler was used to fill

in the voids left from rapid proto-typing. After sanding the filler to the correct propeller

geometry the blades had to be balanced. Initial runs on a dynamometer under static

conditions looked promising; however, dynamically running the propeller caused the

propeller to fail under stress. The ABS plastic and the thin root section combined with

the high centrifugal forces being experienced by the propeller was not nearly strong

enough. Figure 61 shows the rapid prototyped propeller on a dynamometer and the

propeller after the failure. After the failure of the propeller it was determined that a

different approach needed to be undertaken.
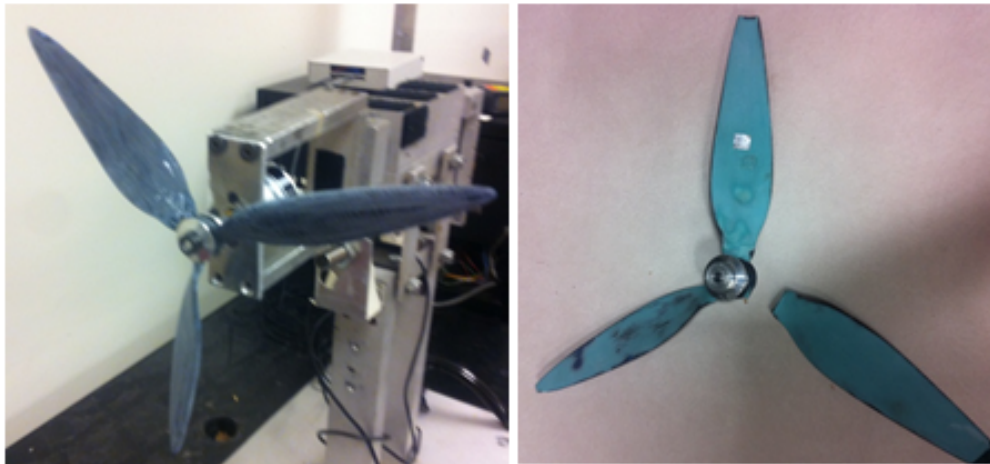
Figure 61 – Rapid Prototyped Propeller

CNC machining of wooden propeller blades

The next attempt at producing a propeller was direct CNC machining of

individual propeller blades. This attempt was simultaneously evaluated with producing

propellers from carbon fiber composites which will be discussed later. The wood that

was used was poplar sheets selected for their lack of knots in the wood and their grain

orientation. The sheets had to be layered and epoxied together to form a block of poplar from which the blades could be created. Aligning the wood block on the CNC table was a critical step that required an alignment jig be manufactured for CNC machining the individual blades. The wood block was secured into the jig with screws and the top surface of the propeller blade was machined out. The wood block was then removed from the jig and flipped over for the bottom surface of the propeller blade to be machined out. The feed rate of the CNC had to be slowed to roughly 20-30 lines per minute in order not to split the wood. Even with the slower feed rates, the trailing edge of all the machined blades ended up splitting or chipping off. Figure 62 shows a wooden propeller blade that has been machined out. It was determined that the manufacturability of this process was not feasible for the propellers that needed to be produced.

Figure 62 – CNC machining of wooden propeller blades

Carbon Fiber Composite Propellers

The next attempt at manufacturing an operational propeller was with molds and carbon fiber composites. After several iterations of working the flaws out, this is the method that was chosen to be most suitably for our manufacturing application. Two different propeller designs were produced using the technique described in the Propeller

Manufacturing chapter; a 5-bladed propeller and a 3-bladed propeller. Various 5-bladed propellers were created with different core materials such as micro-balloon filler, chopped fiber, and uni-directional carbon tow. The 3-blade propeller design was used to create a propeller with a solid chopped fiber core and a hollow propeller. This method provided enough customization that it allowed for various strength propellers to be easily produced when compared to the previous two methods. Once propellers had been produced through this technique, there were several tests that were performed on each of the propellers.

Experimental Propeller Testing

The first test to validate performance parameters was to simply run the propeller with an electric motor on the truck dynamometer as discussed in the Experimental Set-up section. These tests were performed to match theoretical data with experimental data collected from the propellers. The second test that was performed on individual propeller blades was deflection testing with an applied load at two different locations. This test method is further described in the experimental arrangement chapter. The last test that was performed on the propellers was a high-speed video deflection capture on a gas engine. This test was performed on a small 2-cylinder, 100cc gas engine, the DA-100, by Desert Aircraft. The high-speed video was used to capture the tip deflection of the blades due to the centrifugal, thrust and vibrational forces exert on the propeller. The propeller had to withstand all of these forces created by the gas engine to ensure the safety of the vehicle in flight.

Deflection Testing

Using the testing apparatus described in the experimental arrangement chapter, three different types of propeller blades were tested at two different locations on the

blade. The three different blades that were tested are a single layer of 5.7 oz/sq. yd. carbon fiber weave shell filled with a mixture of micro-balloons and epoxy, a single layer of 5.7 oz/sq. yd. carbon fiber weave shell filled with a mixture of chopped carbon fiber and epoxy and a single layer of 5.7 oz/sq. yd. carbon fiber weave shell filled with uni-directional carbon tow and epoxy. Each one of these three different types of propellers had three test specimens for deflection data validation. A total of nine single propeller blades were used in the deflection testing. The propeller blades were tested at two different locations along the length of the blade; at 75% of the radius and at the tip. The results aim to show the increase in stiffness from the micro-balloon filled samples to the chopped fiber filled samples to the uni-directional carbon tow filled samples.

During testing with the load deflection test apparatus it was discovered that the entire testing apparatus had some level of deflection associated with the configuration. Using an aluminum beam with known uniform elastic modulus, the deflection was measured at the exact same locations as the propeller blades to get the deflection of the entire apparatus plus the beam. Taking the theoretical deflection of the beam and subtracting this from the measured deflection gives the deflection associated with the testing apparatus. Using this as a correction factor for the propeller blades, the true theoretical deflection associated with the blades can be compared with the experimentally measured deflection. Figure 63 shows the stiffness analysis schematic for the deflection associated with the entire testing apparatus.
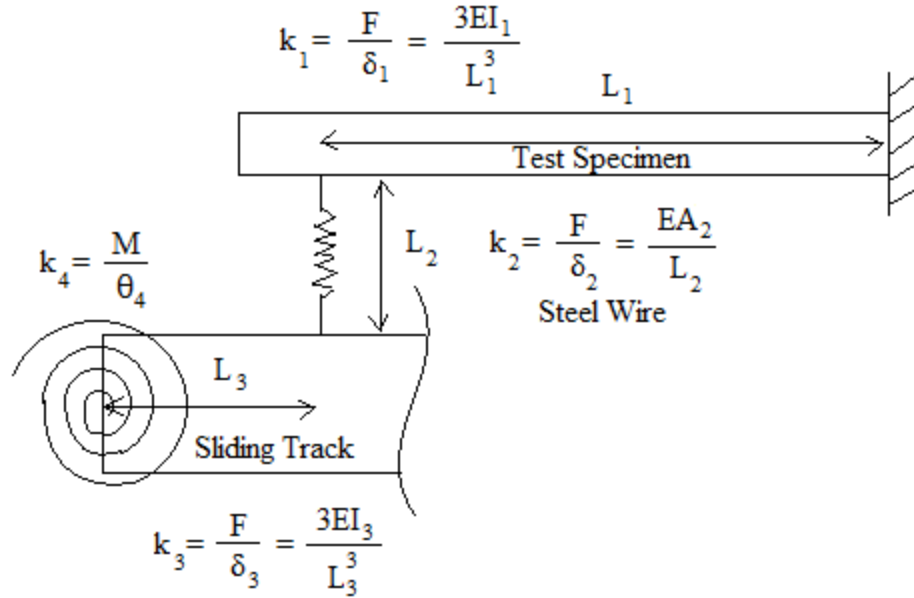
Figure 63 – Stiffness analysis schematic for load deflection testing apparatus

Based on the schematic in Figure 63, the following equations can be developed to relate the stiffness of the entire testing apparatus to the deflection of the entire testing apparatus.

$$\delta = \delta_1 + \delta_2 + \delta_3 + \delta_4$$

$$\frac{F}{k} = \frac{F}{k_1} + \frac{F}{k_2} + \frac{F}{k_3} + \frac{FL_3^2}{k_4}$$

Since the force is the same throughout the entire test for all points, the force can be factored out of the equation. Next, the stiffness term for the testing apparatus can be summed together (k_{234}).

$$\frac{1}{k} = \frac{1}{k_1} + \frac{1}{k_2} + \frac{1}{k_3} + \frac{1}{k_4} = \frac{1}{k_1} + \frac{1}{k_{234}}$$

Solving for the correction factor (k_{234}), an equation is obtained that is purely a function of L_3 and known constants.

$$k_{234}(L_3) = \cfrac{1}{\cfrac{L_2}{EA_2} + \cfrac{L_3^3}{3EI_3} + \cfrac{L_3^2}{k_4}}$$

Finally, using a transfer function to scale the theoretical results based on the correction factor associated with the deflection of the testing apparatus the true theoretical deflection associated with the test specimen can be found.

$$\frac{\delta}{\delta_1} = 1 + \frac{k_1}{k_{234}}$$

After scaling the theoretical deflection curve, the results can be compared with the experimentally tested blade deflection. Figure 64 shows the force versus deflection curve for the micro-balloon filled samples at the tip of the blade.
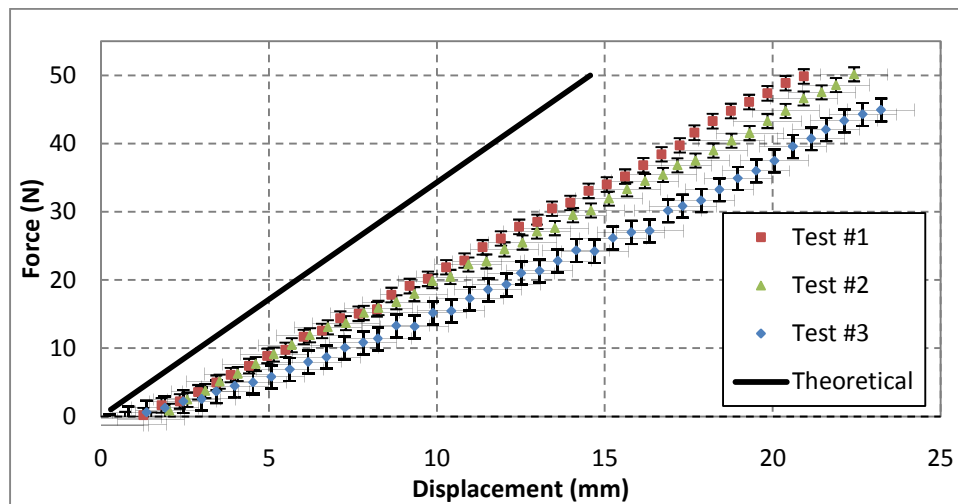
Figure 64 – Force vs. Displacement of the Micro-balloon samples at the blade tip

The force of each of the test samples is an average of two deflection test runs at the tip of the propeller blades. Each test was then analyzed for the average error experienced at each particular displacement location. The error bars on each test sample indicate the average error per displacement location and the force at each displacement

location is an average of the forces seen at that displacement location. This set of data

shows that at the maximum force of 50 N, the blades experienced between 21 mm and 25

mm of deflection at the tip of the micro-balloon propeller blades. These results yield an

average displacement at 50 N of 23 mm. The error between samples starts to propagate

as the load applied to the tip is increased. This propagation results in a percent difference

in displacement between samples at similar forces of 50 N to be 17% at the extreme case.

The difference between the theoretical data and the experimental average is a factor of

1.5 for the deflection at the tip. This error could be a result of a number of factors that

include error in the elasticity modulus of the tensile samples and error in manufacturing a

blade whose geometry perfectly matches the CAD model.
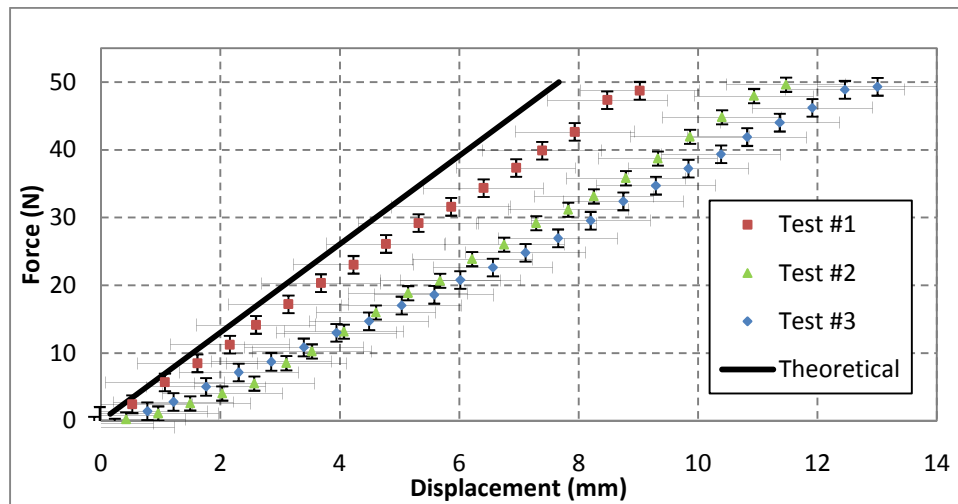
Figure 65 – Force vs. Displacement of the Micro-balloon samples at 75% of the blade length

Figure 65 shows the force versus deflection curve for the micro-balloon filled

samples at 75% of the blade length. This set of data shows that at the maximum force of

50 N, the blades experienced between 9 mm and 13 mm of deflection at 75% of the

micro-balloon propeller blade length. These results yield an average displacement at 50 N

of 11 mm. The first test in this figure seems to be off a significant amount when

compared to the other test samples. This could be due to a number of uncertainty errors for the testing apparatus or from a defective propeller blade. The error between samples propagates significantly as the load applied at 75% of the blade length is increased. The percent difference in displacement between samples at similar forces of 50 N is 36% at the extreme case. The difference between the theoretical data and the experimental average is a factor of 1.5 for the deflection at 75 % of the blade length.
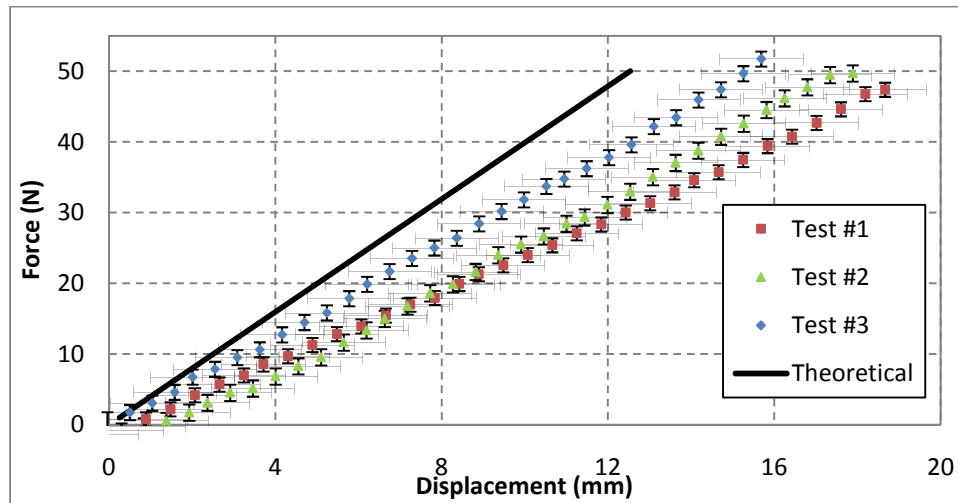
Figure 66 – Force vs. Displacement of the Chopped Fiber samples at the blade tip

Figure 66 shows the force versus deflection curve for the chopped fiber filled samples at the tip of the blade. This set of data shows that at the maximum force of 50 N, the blades experienced between 15 mm and 19 mm of deflection at the tip of the chopped fiber propeller blade. These results yield an average displacement at 50 N of 17 mm, which is 6 mm less than the micro-balloon filled samples. The error between samples only slightly propagates as the load applied to the tip is increased. The percent difference in displacement between samples at similar forces of 50 N is 23% at the extreme case. The difference between the theoretical data and the experimental average is a factor of 1.4 for the deflection at the tip.

Figure 67 – Force vs. Displacement of the Chopped Fiber samples at 75% of the blade length

Figure 67 shows the force versus deflection curve for the chopped fiber filled samples at 75% of the blade length. This set of data shows that at the maximum force of 50 N, the blades experienced between 9 mm and 10 mm of deflection at 75% of the chopped fiber propeller blade length. These results yield an average displacement at 50 N of 9.5 mm, which is 1.5 mm less than the micro-balloon filled samples. The error between samples does not propagate as the load applied at 75% of the blade length is increased. The percent difference in displacement between samples at similar forces of 50 N is 10% at the extreme case. The difference between the theoretical data and the experimental average is a factor of 1.3 for the deflection at 75% of the blade length.

Figure 68 – Force vs. Displacement of the Carbon Tow samples at the blade tip

Figure 68 shows the force versus deflection curve for the carbon tow filled samples at the tip of the blade. This set of data shows that at the maximum force of 50 N, the blades experienced between 12 mm and 14 mm of deflection at the tip of the carbon tow propeller blade. These results yield an average displacement at 50 N of 13 mm, which is 10 mm less than the micro-balloon filled samples and 4 mm less than the chopped fiber filled samples. The error between samples only slightly propagates as the load applied to the tip is increased. The percent difference in displacement between samples at similar forces of 50 N is 15% at the extreme case. The difference between the theoretical data and the experimental average is a factor of 1.35 for the deflection at the tip.
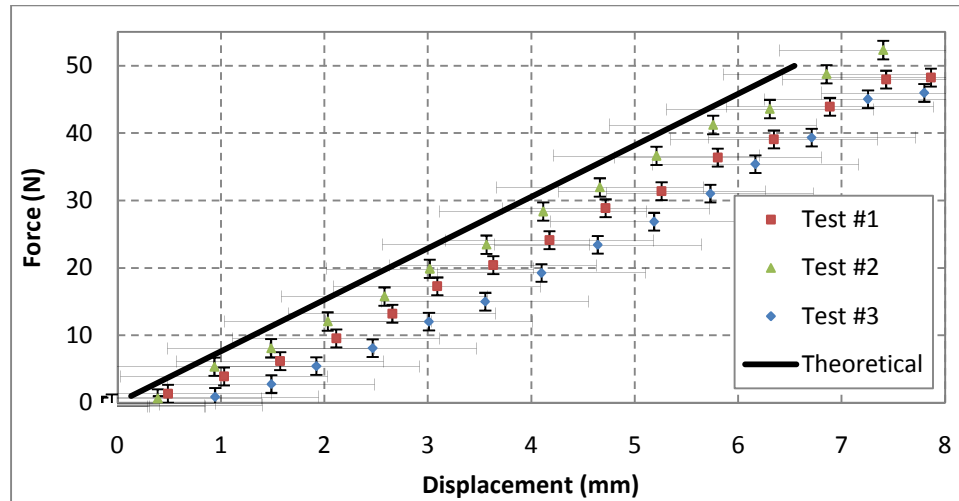
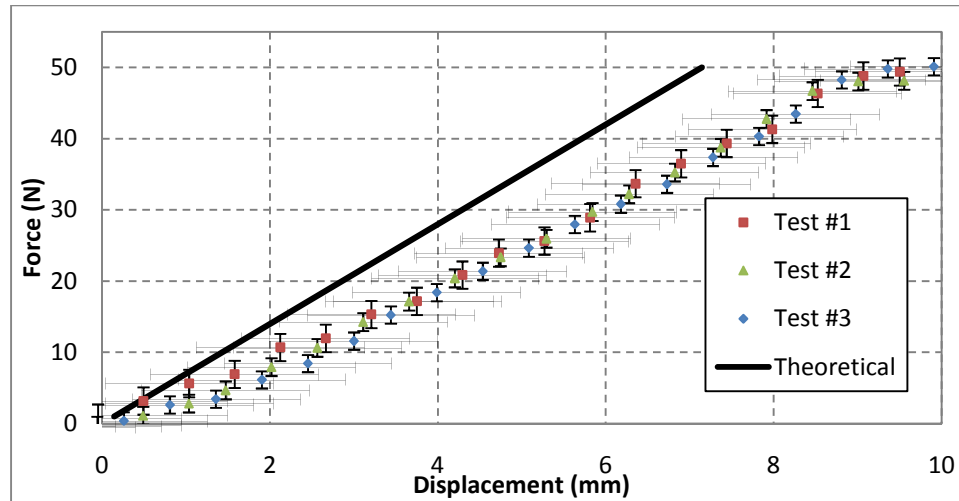**Figure 69 – Force vs. Displacement of the Carbon Tow samples at 75% of the blade length**

Figure 69 shows the force versus deflection curve for the carbon tow filled samples at 75% of the blade length. This set of data shows that at the maximum force of 50 N, the blades experienced between 7 mm and 8 mm of deflection at 75% of the carbon tow propeller blade length. These results yield an average displacement at 50 N of 7.5 mm, which is 3.5 mm less than the micro-balloon filled samples and 2 mm less than the chopped fiber filled samples. The error between samples propagates slightly, but then comes back together as the load applied at 75% of the blade length is increased. The percent difference in displacement between samples at similar forces of 50 N is 13% at the extreme case. However, these numbers are better visualized when compared graphically with one another.   The difference between the theoretical data and the experimental average is a factor of 1.1 for the deflection at 75% of the blade length.

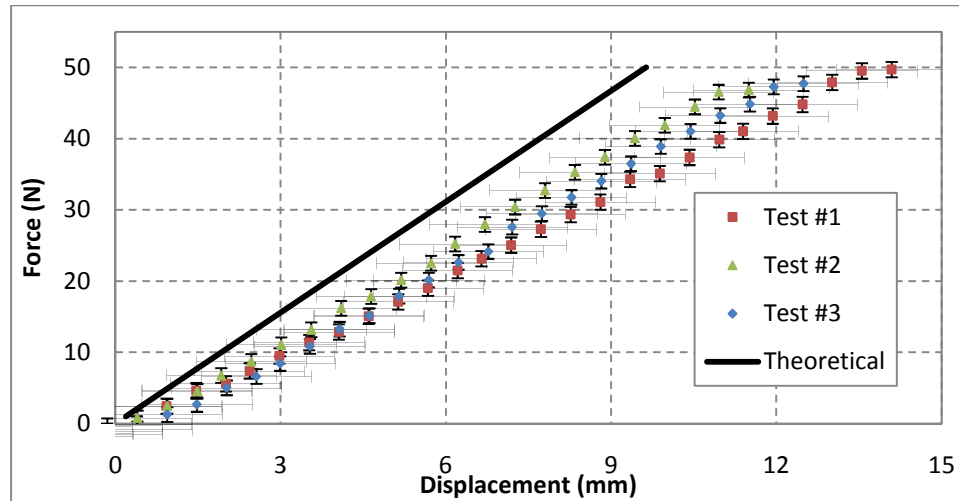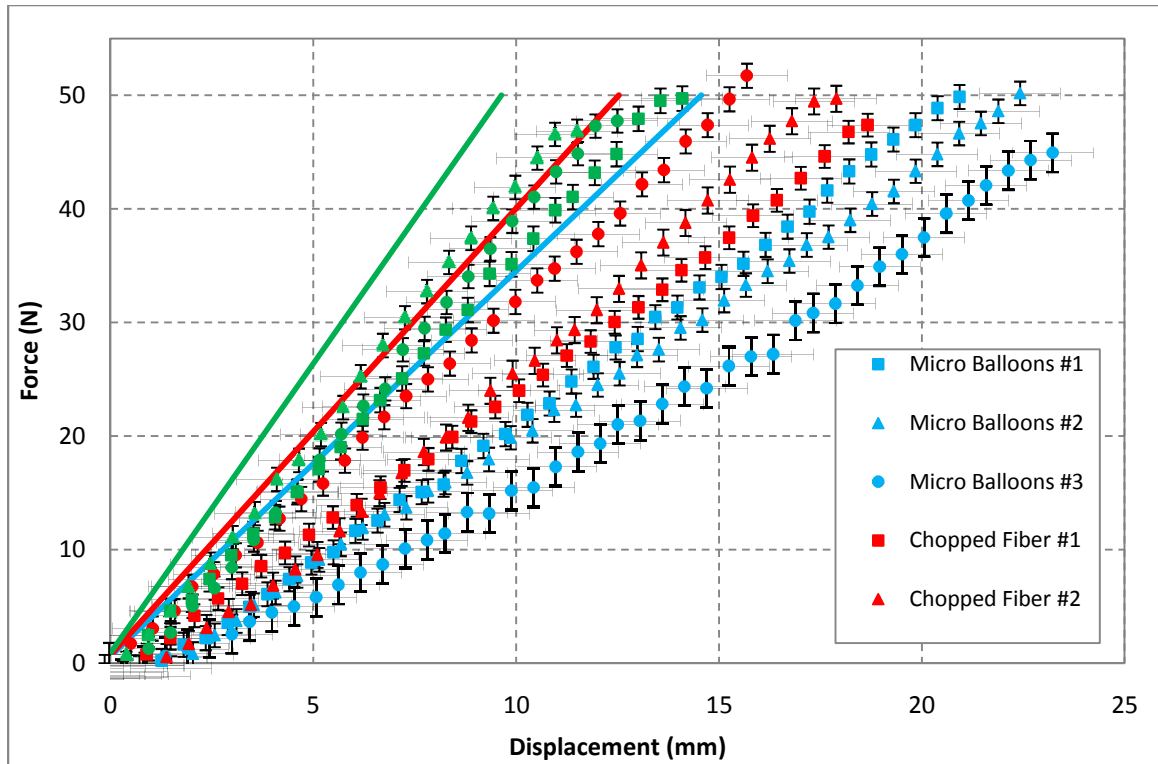**Figure 70 – Force vs. Displacement of all the samples at the blade tip**

Figure 70 shows the force versus deflection curve for all of the test samples at the blade tip. This graphical representation of the data demonstrates the major differences in strength of each type of propeller blade. For equally applied forces Figure 70 shows that the carbon tow filled samples are the strongest and the micro-balloon filled samples are the weakest of the different propeller types.
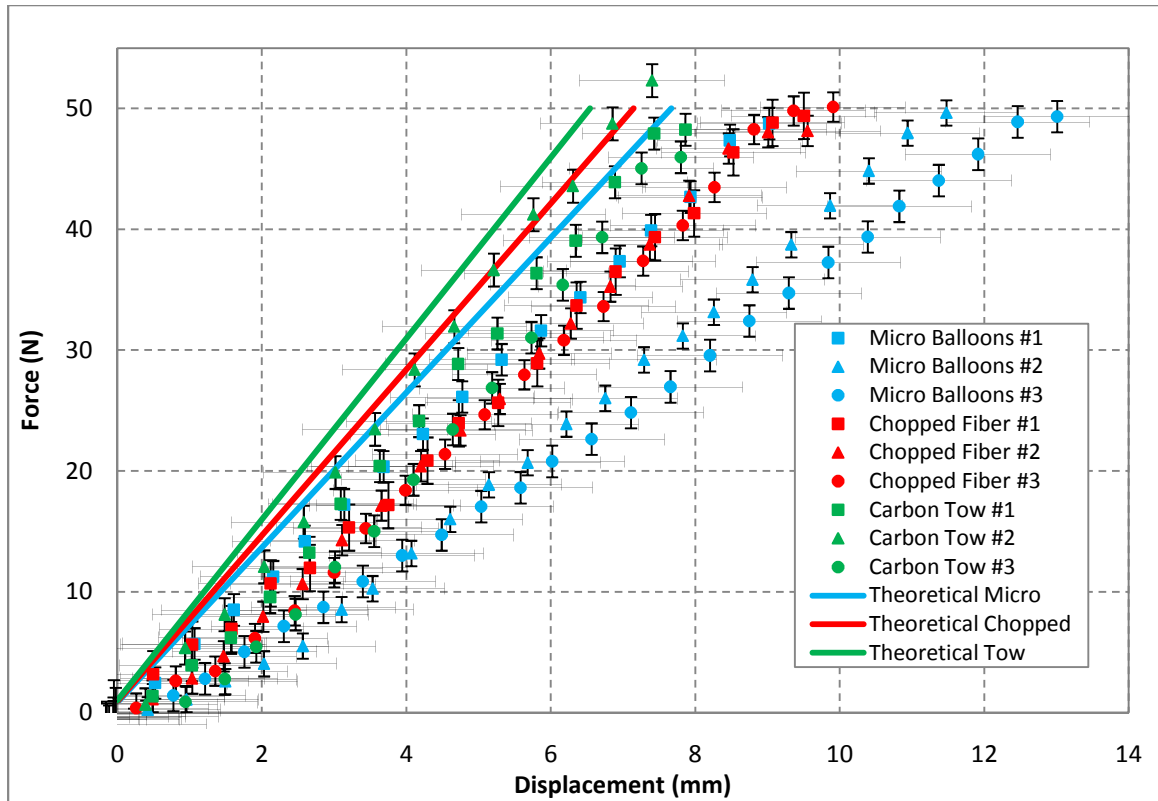
Figure 71 – Force vs. Displacement of all the samples at 75% of the blade length

Figure 71 shows the force versus deflection curve for all of the test samples at 75% of the blade length. This graphical representation of the data demonstrates the major differences in strength of each type of propeller blade at the given location. The comparison shows how far off the micro balloon test #1 is compared to the rest of the micro balloon tests. The strength of the micro balloon test #1 is equal to that of a chopped fiber test sample, which cannot be true. This outlier should be disregarded and possibly re-tested multiple times to verify that the error is in the propeller blade and not the testing apparatus. However, this graph reiterates Figure 70 by showing that the carbon tow filled samples are the strongest and the micro-balloon filled samples are the weakest of the different propeller types.
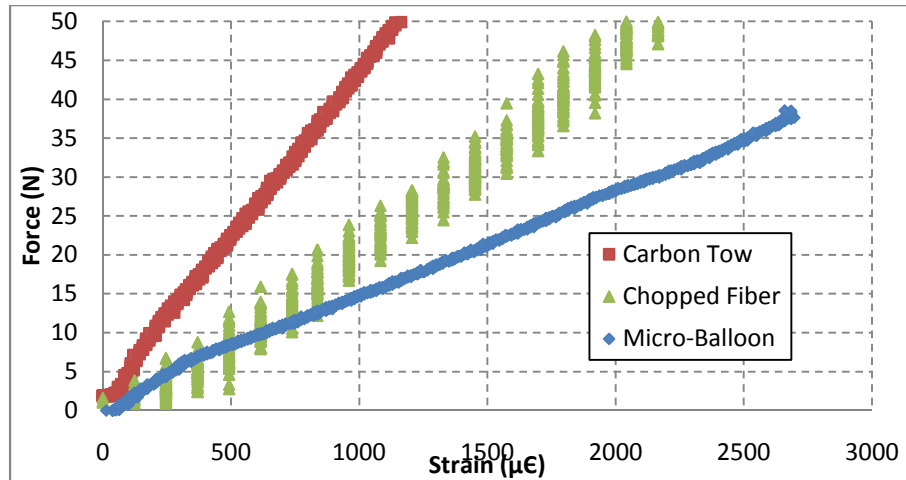
Figure 72 – Force vs. Strain at 50% of the blade length for the tension gage

Figure 72 shows the force versus strain curves for the three different types of propeller blade core materials in tension. The strain gage is measuring the strain at 50% of the blade length with the load applied at the tip of the blade. The graph re-iterates that the micro-balloon core blades are the weakest and the carbon tow core blades are the strongest. The results show that less of the load has to be carried by the skin material due to the increased strength of the core material.
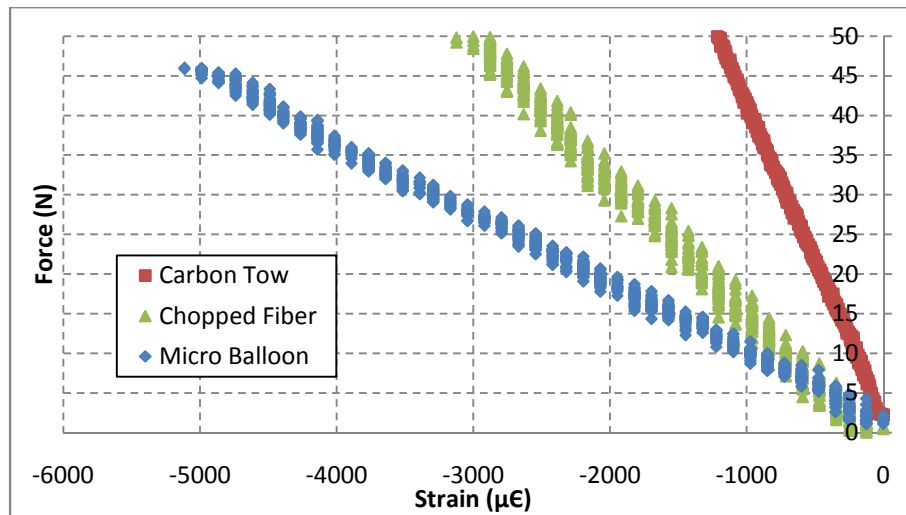
Figure 73 – Force vs. Strain at 50% of the blade length for the compression gage

Figure 73 shows the force versus strain curves for the three different types of propeller blade core materials in compression. The strain gage is measuring the strain at 50% of the blade length with the load applied at the tip of the blade. The graph re-iterates the results of the load versus deflection testing for the different core materials. The compression results show that more of the load is carried by the skin material on the top surface of the blade. These results help to validate the results from the load versus deflection testing.

High-Speed Deflection Testing

For a more realistic approximation of the deflection that will be experienced by the propeller blades during operational conditions a high-speed camera was set-up to capture the deflection seen at various RPM ranges and through propeller transition phases. The camera used for the high-speed deflection data collection is a Casio Exilim EX-FH20 Digital Camera. The capture rate of the camera used was 1000 frames per second. After deflection testing with the three different types of propeller cores, it was determined that the propeller blades filled with carbon tow and epoxy were the strongest in bending stiffness. For high-speed deflection capture it is only necessary to test the 5-bladed custom built propeller filled with carbon tow and epoxy of the three different types of internal cores. The other propellers tested are a 3-bladed 22x12 Mejzlik hollow carbon fiber propeller and a 3-bladed 18x18 custom built propeller using the method described in the previous chapter. For each of the 3 different propellers being tested, the DA-100 2 cylinder gas engine was used with the high speed camera. The camera was positioned in line with the direction of rotation of the blades to capture the tip deflection at a range of different RPMs. The first deflection data captured is for the 5-blade 18x18 custom built propeller.
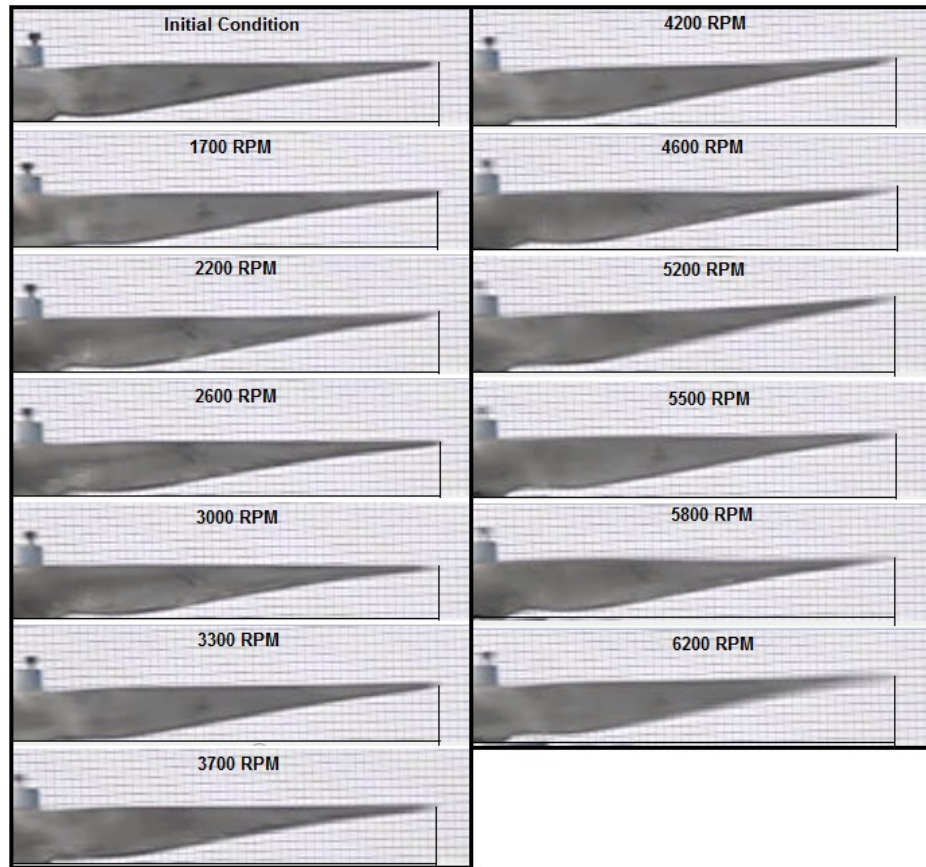
Figure 74 – 5-blade 18x18 custom built propeller high speed camera deflections

Figure 74 shows the deflection at the tip of the 5-bladed 18x18 custom built propeller for a range of different RPMs. As the RPM increases the deflection at the tip also increases. This trend can be seen in Figure 75, which shows a comparison between the three different types of propellers. At each RPM capture the deflection is measured from a reference point on the blade. Measuring the deflection relative to the propeller hub allows the propeller to move forward in the camera view due to thrust generated. The maximum deflection at the tip seen in one direction of the 5-bladed 18x18 custom built propeller is 12.7 mm. Throughout the high speed video, manufacturing imperfections in the blades can be seen as well as an asymmetry in the propeller. The

pulses from the gas engine cylinders can also be seen as vibrations in the individual

blades that causes the blades to resonant back and forth. Between 4000 and 5000 RPM,

there seems to be a wobble in one of the blades on the high speed video. Later it was

discovered that the root of one of the blades had cracked and this seems to be the cause of

the wobble. However, composites do not fail all at once as discussed in the section on

Load versus Displacement. Multiple or even a single ply could have failed and only

would reduce the elastic modulus at that point by a certain percentage. Typically brittle

failure is not seen in composites, which allowed the test to be continued even at the

higher RPMs.
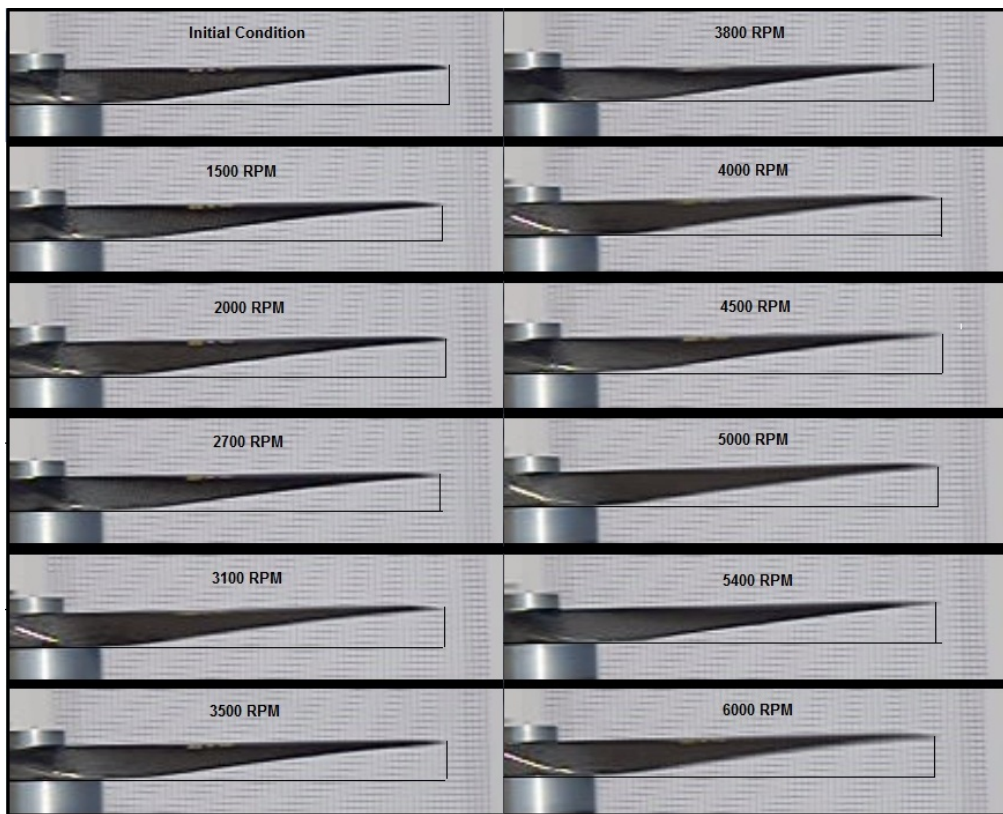
Figure 75 – 3-blade 22x12 Mejzlik propeller high speed camera deflections

Figure 75 shows the deflection at the tip of the 3-bladed 22x12 Mejzlik propeller for a range of different RPMs. At each RPM capture the deflection is measured from a reference point relative to the blade. Measuring the deflection relative to the aluminum alternator substitute allows the propeller to move forward in the camera view due to thrust generated. The maximum deflection at the tip seen in one direction of the 3-bladed 22x12 Mejzlik propeller is 6.35 mm. An interesting phenomenon that the 5-blade custom built propeller experiences that the 3-blade Mejzlik propeller does not is a transition phase in the RPM run through. The 5-blade custom built propeller experiences a transition phase between 4500 and 5500 RPM where the deflection worsens before stabilizing at the higher RPMs.
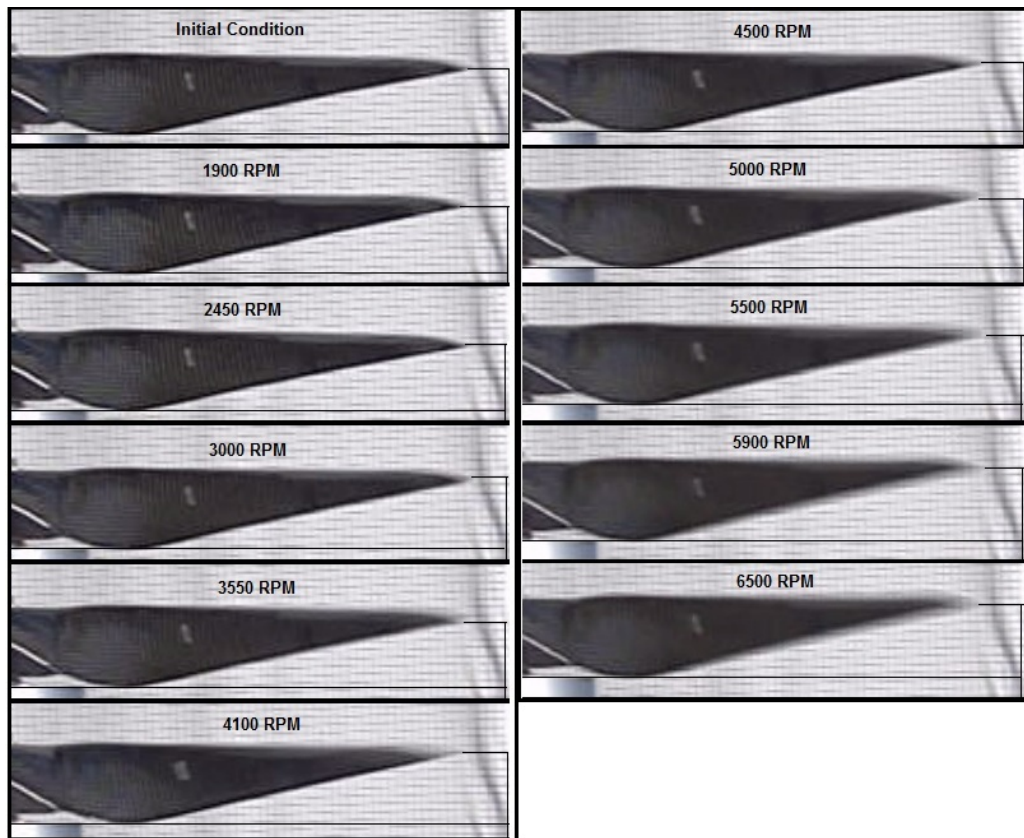
Figure 76 – 3-blade 18x18 custom built propeller high speed camera deflections

Figure 76 shows the deflection at the tip of the 3-bladed 18x18 custom built propeller for a range of different RPMs. At each RPM capture the deflection is measured from a reference point relative to the blade. Measuring the deflection relative to the aluminum alternator substitute allows the propeller to move forward in the camera view due to thrust generated. The maximum deflection at the tip seen in one direction of the 3-bladed 18x18 custom built propeller is 6.35 mm same as the 3-blade Mejzlik propeller. However the differences lie in the fact that the 3-blade 18x18 custom built propeller does not experience its maximum deflection until 1000 RPM higher than the 3-blade Mejzlik propeller.
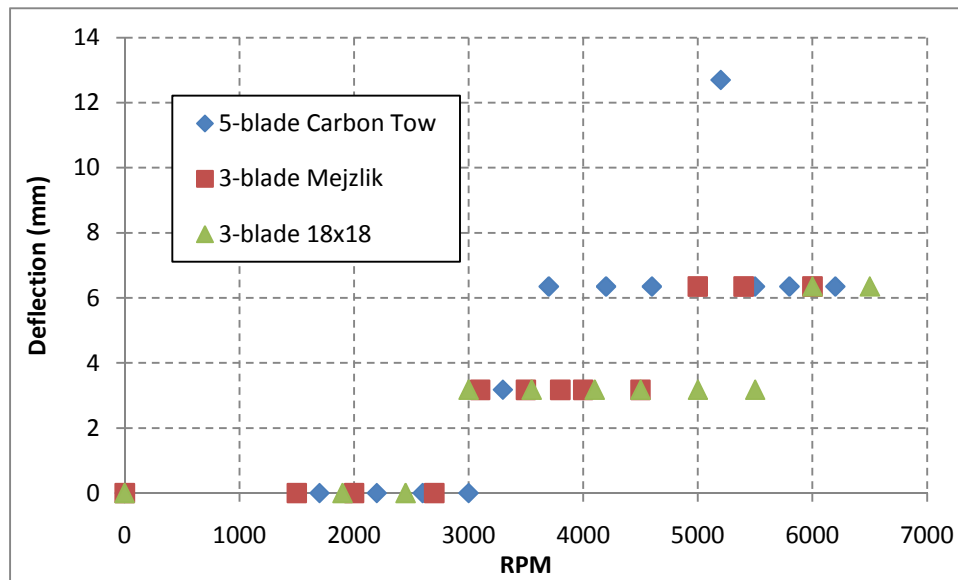
Figure 77 – Comparison between propellers of high speed camera deflections

Figure 77 shows a comparison between the three different types of propeller blades tested with the high speed camera for deflection at the tip. All three of the propellers appear to be stable with no deflection up to 2500 RPM. At this point the three different propellers start to experience tip deflection at varying rates. The 5-blade 18x18 custom built propeller experiences a sharp rise in tip deflection between 3000 and 5000

RPM from 0 to 12.7 mm of deflection. The 3-blade Mejzlik starts to see its maximum

deflection for this RPM range at 5000 RPM whereas the 3-blade custom built propeller

doesn't see its maximum deflection for this RPM range until 6000 RPM.

Using the data collected from the high-speed deflection tests, the loads

experienced by the propeller blades at the tip can be estimated from the experimental data

collected from the load versus displacement tests. Since the 5-blade carbon tow filled

propeller is the only propeller that was tested with both experimental procedures, we will

only be able to predict the loads for this propeller. This analysis will tie the data from

both experimental procedures together. The predicted tip loads for the 5-blade propeller

during the high-speed data captured can be seen in Table 3. The outlier in the data at

5200 RPM is due to transitions in the flow over the propeller blade and the vibrations

from the gas engine at the high speeds.

RPM (rev/min)	δ (mm)	Tip Load (N)	Measured Static Thrust (N)
0	0	0	0
1700	0	0	-
2200	0	0	-
2600	0	0	-
3000	0	0	15.6
3300	3.2	21.3	23.1
3700	6.4	42.5	-
4200	6.4	42.5	33.8
4600	6.4	42.5	47.1
5200	12.7	85.1	67.6
5500	6.4	42.5	-
5800	6.4	42.5	-
6200	6.4	42.5	-

Table 3 – Tip Load Prediction based on experimental deflection testing

With this knowledge, the 5-blade 18x18 custom built propeller with the carbon

tow core is determined not to be a feasible option to run on the 2-cylinder gas engine.

However, this propeller could be used with an electric motor due to the lack of vibrations

produced by electric motors. With the data gathered between the two 3-blade propellers,

either propeller is a feasible option for operation on the 2-cylinder gas engine. The

determining factor will now remain in the hands of the acoustic signature of each

propeller.

CHAPTER VII

CONCLUSION AND FUTURE WORK

The final chapter in this thesis will attempt to bring together all the testing and knowledge that has been gained throughout this paper. The propeller manufacturing technique that was initally set out to develop was successfully achieved and implemented. The objectives for using current techniques and new techniques for propeller manufacturing have all been completed. Test and analysis of the propeller blades have been compared with commercially available ones and found to be comparable in both strength and performance.

Conclusion

After applying several lessons learned through multiple iterations of the propeller manufacturing process, a unique technique was developed to manufacture custom designed propellers. Using carbon fiber weave and various core materials, composite propellers were manufactured. The technique harnesses the use of wet lay-up composites and molds to create beautifully crafted propellers that are comparable with those commercially produced in industry. Only after rigorous testing and inspection of the propellers are they allowed to run under operational conditions. Deflection testing at static and dynamic conditions help to verify the operational performance of each of the propellers manufactured. The error between the theoretical prediction of deflection and

the experimentally tested deflection is due to several factors that affect the calculation of deflection for the blade geometry.

The ASTM regulated tensile testing of the materials used in the propellers was far from exact. The tensile testing encountered significant set-backs such as incompatible equipment and human error in making the tensile test specimens. Another source of error in the theoretical data prediction is that the manufactured propeller blades were not perfectly the same as the modeled propeller blades. The modeled propeller blades account for a perfect shell of the carbon fiber weave at 45° to encompass the core material without any breaks or mixing of material in the weave layers. It was found that in manufacturing the propeller blades the core material typically had air pockets that were trapped inside the blade. These air pockets reduced the stiffness of the propeller blades due to the decrease in cross sectional area which affects the second moment of inertia. This would explain why the theoretical deflection prediction is slightly higher than the experimental deflection data. Figure 78 shows an example of the air pockets that formed in the chopped fiber core.

Figure 78 – Air pockets in chopped fiber core material

Even with these errors in manufacturing and testing, the propeller blades performed their required task with no catastrophic failures. Aside from a few manufacturing and human errors the overarching goal of this thesis, to develop and

implement a unique and innovative manufacturing process for constructing multi-bladed

SUAS propellers, has been achieved along with the objectives set forth at the beginning

of this thesis. Table 4 highlights each of the propellers that were constructed during the

duration of this thesis.

Picture	Blades	Diameter	Pitch	Skin	Internal Core	Manufacturing Method	Comments:
	3	14"	12"	Epoxy with West System 410 Microlight Filler	ABS Plastic	Rapid Proto-type	Material not strong enough to withstand dyanmic loads, poor blending with the hub at the root
	1	18"	18"	Poplar Wood	Poplar Wood	CNC milled	Wood splinters and flakes off during milling, time required to mill individual blades lengthy
	5	18"	18"	1 layer 5.7 oz/sq. yd. Plain Weave Carbon Fiber ±45°	Micro-ballon filler	Wet Lay-up	Micro-balloon filler stiffness not high enough for gas engine
	5	18"	18"	1 layer 5.7 oz/sq. yd. Plain Weave Carbon Fiber ±45°	Chopped Fiber filler	Wet Lay-up	Porous core with air pockets in chopped fiber
	5	18"	18"	1 layer 5.7 oz/sq. yd. Plain Weave Carbon Fiber ±45°	Uni-directional carbon tow filler	Wet Lay-up	Strongest of the 5-bladed propellers , still too much tip deflection on gas engine though
	3	18"	18"	1 layer 5.7 oz/sq. yd. Plain Weave Carbon Fiber ±45°	Chopped Fiber filler	Wet Lay-up	Best propeller made to date, stiffness is excellent and minimal deflection on gas engine
	3	18"	18"	2 layers 5.7 oz/sq. yd. Plain Weave Carbon Fiber ±45° with Uni-directional carbon tow in between	Hollow	Wet Lay-up	Hollow core is extremely difficult to balance with current technique, good stiffness

Table 4 – Summary of all propellers manufactured

Future Work

There are several areas in which the manufacturing process could be improved, but were limited by resources and time. The first area that could benefit from better resources is the propeller molds. Higher axis CNC machines would allow for better precision and accuracy when creating the plugs for the fiberglass molds. Use of aluminum molds that have been directly CNC machined out would increase the accuracy of the molds, but the cost and time required for this application would not be worth the effort due to the small number of propellers created.

Another key area that could use further research in is the composite lay-up schedule of the propeller blades. Combinations of carbon fiber with other materials such as uni-directional carbon tow in a multi-layered laminate would increase the stiffness of the individual blades and reduce the deflection seen in the 5-blade 18x18 custom built propeller. Geometry optimization due to composite strength and dynamic loads could increase the feasibility of using the 5-blade 18x18 custom built propeller. The use of the 5-blade 18x18 custom built propeller over the 3-blade 18x18 custom built propeller could potential further reduce the noise associated with the propeller.

To further reduce the noise associated with the propeller, the blade geometry could be optimized using several software packages that keep the desired Mach number at the tip below a specified threshold. This approach would only optimize the propeller at a given RPM value. However, a variable pitch propeller would optimize the propeller performance over a range of RPMs which would further reduce the noise and increase the engine performance. The possibilities for SUAS propeller manufacturing are nearly

endless and the unique technique discussed in this thesis is only the tip of the iceberg in

manufacturing vehicle specific custom propellers.

REFERENCES

Aeroproducts Division General Motors Corporation. *Blades for Victory: The Story of the Aeroproducts Propeller & the Men & Women Who Build It*. Vandalia (Ohio): General Motors Corporation, 1944. Print.

"ASTM B223 - 08." *Standard Test Method for Modulus of Elasticity of Thermostat Metals (Cantilever Beam Method)*. 2008. Web. 6 Feb. 2012. <http://www.astm.org/Standards/B223.htm>.

"ASTM D3039 / D3039M - 08." *Standard Test Method for Tensile Properties of Polymer Matrix Composite Materials*. 2008. Web. 1 Feb. 2012. <http://www.astm.org/Standards/D3039.htm>.

"ASTM D747 - 10." *Standard Test Method for Apparent Bending Modulus of Plastics by Means of a Cantilever Beam*. 2010. Web. 5 Feb. 2012. <http://www.astm.org/Standards/D747.htm>.

Atas, Cesim, Yalın Akgun, Olgay Dagdelen, Bulent M. Icten, and Mehmet Sarikanat. "An Experimental Investigation on the Low Velocity Impact Response of Composite Plates Repaired by VARIM and Hand Lay-up Processes." *Composite Structures* 93 (2010): 1178-186. Print.

Bahnson, Dave. "Basic Propeller Construction." *Wooden Propellers*. 2003. Web. 10 Jan. 2012. <http://www.woodenpropeller.com/Basic_Propeller_Construction_-_Techniques.html>.

Bass, R. M. "Techniques of Model Propeller Testing." *Business Aircraft Meeting and Exposition*. Wichita (Kansas). SAE Technical Paper Series, 1983. Print.

Bickerton, Simon, and Suresh G. Advani. "Characterization and Modeling of Race-tracking in Liquid Composite Molding Processes." *Composites Science and Technology* 59 (1999): 2215-229. Print.

Brahney, James. "Composite Propellers: Some Pros and Cons." *Aerospace Engineering* 6.5 (1986): 12-17. Print.

Bralla, James G. *Handbook of Manufacturing Processes: How Products, Components and Materials Are Made*. 1st ed. New York: Industrial, 2007. Print.

Breteau, T., T. Damay, E. Duc, and J. Y. Hascoët. "Design for Manufacturing with Tool Paths Adapted to Marine Propeller." *Int J Interact Des Manuf* 5 (2011): 271-75. Print.

Brødsjø, A., and P. Putting. "The Design and Manufacturing of a RTM Composite Propeller for a Navy Vessel." *10th International Conference on Textile Composites*. Lille Grand Palais, Lille (France). Lancaster: DEStech Publications, 2010. 118-24. Print.

"Composites Offer Advantages for Propellers." *Reinforced Plastics* 37.12 (1993): 24-26. Print.

Daniels, R. W. "DURALUMIN1." *SAE Technical Papers* 11.6 (1922): 477-80. Print.

Foley, Hamilton. "Manufacture and Magnetic Testing of Hollow Steel Propellers." *STEEL* (1933): 23-26. Print.

Gamble, Dustin E., and Andrew S. Arena. "Automated Dynamic Propeller Testing at Low Reynolds Numbers." *48th AIAA Aerospace Sciences Meeting Including the New Horizons Forum and Aerospace Exposition*. Orlando. Stillwater: Oklahoma State University, 2010. Print.

Gamble, Dustin E. *Automated Dynamic Propeller Testing at Low Reynolds Numbers*. Master's Thesis. Oklahoma State University, 2009. Print.

Gangler, J. P. "Naval Propellers From Design to Manufacture." *Naval Forces* 18.6 (1997): 112-17. Print.

Gospodnetić, Draško, and Slobodan Gospodnetić. "Computer Numerically Controlled Milling of Monoblock Propeller Models." *45th Annual Technical Conference of the Canadian Maritime Industries Association*. Ottawa. Ontario: Dominis Engineering, 1993. Print.

Harlamert, W. B., and R. Edinger. "Development of an Aircraft Composite Propeller." *Business Aircraft Meeting and Exposition*. Wichita (Kansas). SAE Technical Paper Series, 1979. Print.

Hsu, C. Y., C. K. Huang, and G. J. Tzou. "Using Metallic Resin and Aluminum Alloy Molds to Manufacture Propellers with RP/RT Technique." *Rapid Prototyping Journal* 14.2 (2008): 102-07. Print.

Kearns, Bryan. "Building a Propeller." *www.masshover.com*. 2009. Web. 23 Jan. 2012. <http://sites.google.com/site/kearnsbryan/propeller>.

Macfarlane, Robert. *History of Propellers and Steam Navigation: With Biographical Sketches of the Early Inventors.* New York: G.P. Putnam, 1851. Print.

McCarthy, R. F. J., G. H. Haines, and R. A. Newley. "Polymer Composite Applications to Aerospace Equipment." *Composites Manufacturing* 5.2 (1994): 83-93. Print.

McCarthy, R. "Manufacture of Composite Propellers Blades for Commuter Aircraft." *General Aviation Aircraft Meeting and Exposition.* Wichita (Kansas). SAE Technical Paper Series, 1985. Print.

McGovney, Grant, Justin Otto, and Brett Smith. "Propeller Test Module Final Report." Senior Capstone Design. Oklahoma State University, 2010.

Miracle, Daniel B., and Steven L. Donaldson. "Open Molding: Hand Lay-Up and Spray-Up." *ASM Handbook.* Vol. 21: Composites. Materials Park (Ohio): ASM International, 2001. 450-56. Print.

Moltrecht, Karl H. *Machine Shop Practice.* 2nd ed. Vol. 2. New York: Industrial, 1981. Print.

Paiva, Jane Maria Faulstich De, Sérgio Mayer, and Mirabel Cerqueira Rezende. "Comparison of Tensile Strength of Different Carbon Fabric Reinforced Epoxy Composites." *Materials Research* 9.1 (2006): 83-89. Print.

Potter, K. D. "The Early History of the Resin Transfer Moulding Process for Aerospace Applications." *Composites Part A: Applied Science and Manufacturing* 30.5 (1999): 619-21. Print.

Potter, Kevin. *Resin Transfer Moulding.* 1st ed. London: Chapman & Hall, 1997. Print.

Ravi, Ashwin, and Andrew S. Arena. "UAV Power Plant Performance Evaluation." *49th AIAA Aerospace Sciences Meeting including the New Horizons Forum and Aerospace Exposition.* Orlando. Stillwater: Oklahoma State University, 2011. Print.

Rosato, Dominick V., Donald V. Rosato, and Marlene G. Rosato. *Injection Molding Handbook.* 3rd ed. Boston: Kluwer Academic, 2000. Print.

Sihn, Sangwook, and Brian P. Rice. "Sandwich Construction with Carbon Foam Core Materials." *Journal of Composite Materials* 37.15 (2003): 1319-336. Print.

Smedresman, Adam, Derrick Yeo, and Wei Shyy. "Design, Fabrication, Analysis, and Testing of a Micro Air Vehicle Propeller." *29th AIAA Applied Aerodynamics Conference.* Honolulu. American Institute of Aeronautics and Astronautics, 2011. Print.

Smith, Stephen L., and Joseph L. Mattavi. "Structural Qualification of Composite Propeller Blades Fabricated by the Resin Transfer Molding Process." *Composite Structures: Theory and Practice* 1383 (2000): 210-28. Print.

Stringer, L. G. "Optimization of the Wet Lay-up/vacuum Bag Process for the Fabrication of Carbon Fibre Epoxy Composites with High Fibre Fraction and Low Void Content." *Composites* 20.5 (1989): 441-52. Print.

United States Army Air Corps. *The Airplane Propeller.* Washington: Govt. Print. Off., 1921. Print.

Weick, Fred E. "Composite Wood and Plastic Propeller Blades." *Society of Automotive Engineers (Transactions)* 44.6 (1939): 252-58. Print.

Youngren, Harold, and Ming Chang. "Test, Analysis and Design of Propeller Propulsion Systems for MAVs." *49th AIAA Aerospace Sciences Metting including the New Horizons Forum and Aerospace Exposition.* Orlando. American Institute of Aeronautics and Astronautics, 2011. Print.

5-blade Propeller Cross Sectional Geometries

Station (in)		A (in^2)	I$_{xx}$ (in^4)	I$_{yy}$ (in^4)	I$_{xy}$ (in^4)	X$_i$* (in)	Y$_i$* (in)
8.5	---	1.4E-02	5.3E-05	3.7E-04	1.2E-04	-0.13	-0.03
8.5	---	2.6E-02	5.0E-05	4.0E-04	1.3E-04	-0.10	-0.01
7.5	---	2.0E-02	1.6E-04	9.2E-04	3.4E-04	-0.18	-0.05
7.5	---	5.0E-02	2.3E-04	1.4E-03	5.3E-04	-0.13	-0.02
6.5	---	2.6E-02	4.8E-04	2.1E-03	9.2E-04	-0.24	-0.08
6.5	---	9.0E-02	9.5E-04	4.6E-03	2.0E-03	-0.18	-0.04
5.5	---	3.2E-02	1.2E-03	3.6E-03	1.9E-03	-0.29	-0.11
5.5	---	1.4E-01	2.7E-03	9.7E-03	4.9E-03	-0.21	-0.07
4.5	---	3.5E-02	2.0E-03	4.5E-03	2.8E-03	-0.31	-0.15
4.5	---	1.7E-01	5.6E-03	1.4E-02	8.3E-03	-0.23	-0.09
3.5	---	3.7E-02	3.1E-03	4.4E-03	3.5E-03	-0.31	-0.20
3.5	---	1.8E-01	9.3E-03	1.4E-02	1.1E-02	-0.23	-0.13
2.5	---	3.5E-02	3.7E-03	2.8E-03	3.0E-03	-0.25	-0.23
2.5	---	1.6E-01	1.0E-02	8.0E-03	8.8E-03	-0.19	-0.15
1.5	---	3.5E-02	3.3E-03	3.7E-03	1.6E-03	-0.11	-0.24
1.5	---	5.4E-01	2.6E-02	3.2E-02	1.7E-02	-0.11	-0.24
1.3	---	4.5E-02	5.8E-03	9.1E-03	7.1E-04	-0.08	-0.29
1.3	---	9.8E-01	5.8E-02	1.1E-01	1.1E-02	-0.08	-0.29
1.1	---	5.2E-02	9.7E-03	1.3E-02	9.7E-06	-0.10	-0.30
1.1	---	1.3E+00	1.1E-01	1.6E-01	3.1E-04	-0.11	-0.30
0.9	---	5.6E-02	1.2E-02	1.4E-02	0.0E+00	-0.12	-0.30
0.9	---	1.4E+00	1.5E-01	1.8E-01	-3.0E-06	-0.12	-0.30

Tensile Test Specimen Elastic Modulus

Elastic Modulus (Weave)	17516.738	(N/mm^2)	2540714.70	(psi)	17.5167	(GPa)
Elastic Modulus (Carbon Tow)	45677	(N/mm^2)	6625218.82	(psi)	45.677	(GPa)
Elastic Modulus (Chopped Fiber)	6350.3	(N/mm^2)	921079.04	(psi)	6.3503	(GPa)
Elastic Modulus (Micro-balloon)	1908.6	(N/mm^2)	276832.82	(psi)	1.9086	(GPa)

Theoretical Blade Deflection Calculation at the tip and 75% of the blade length

Carbon Tow 0.75R	x (mm)	x/R	Moment M(x) (N*mm)	$E*I_{yy}$ (N*mm^2)	$M(x)/E*I_{yy}$ (1/mm)	θ_z (1/rad)	δ_z (mm)
	22.86	0.1	-148.59	3E+09	-4.895E-08	0	0
	27.94	0.12222	-143.56079	2.2E+09	-6.523E-08	-2.9E-07	-7.37E-07
	33.02	0.14444	-138.5316	1.1E+09	-1.209E-07	-7.6E-07	-3.41E-06
	38.1	0.16667	-133.2738	5.2E+08	-2.547E-07	-1.7E-06	-9.71E-06
	63.5	0.27778	-107.8992	2.2E+08	-4.828E-07	-1.1E-05	-0.000172
	88.9	0.38889	-82.524597	2E+08	-4.098E-07	-2.2E-05	-0.000598
	114.3	0.5	-57.149994	1.2E+08	-4.727E-07	-3.4E-05	-0.00131
	139.7	0.61111	-31.775391	6.1E+07	-5.199E-07	-4.6E-05	-0.002324
	165.1	0.72222	-6.4007874	2.2E+07	-2.947E-07	-5.7E-05	-0.00363

Carbon Tow R	x (mm)	x/R	Moment M(x) (N*mm)	$E*I_{yy}$ (N*mm^2)	$M(x)/E*I_{yy}$ (1/mm)	θ_z (1/rad)	δ_z (mm)
	22.86	0.1	-205.74001	3E+09	-6.778E-08	0	0
	27.94	0.12222	-200.7108	2.2E+09	-9.12E-08	-4E-07	-1.03E-06
	33.02	0.14444	-195.68161	1.1E+09	-1.707E-07	-1.1E-06	-4.77E-06
	38.1	0.16667	-190.4238	5.2E+08	-3.64E-07	-2.4E-06	-1.36E-05
	63.5	0.27778	-165.04921	2.2E+08	-7.386E-07	-1.6E-05	-0.000253
	88.9	0.38889	-139.67461	2E+08	-6.936E-07	-3.5E-05	-0.000901
	114.3	0.5	-114.3	1.2E+08	-9.455E-07	-5.5E-05	-0.002045
	139.7	0.61111	-88.9254	6.1E+07	-1.455E-06	-8.6E-05	-0.00384
	165.1	0.72222	-63.550797	2.2E+07	-2.926E-06	-0.00014	-0.006729
	190.5	0.83333	-38.176208	5540821	-6.89E-06	-0.00027	-0.011908
	215.9	0.94444	-12.801605	1355392	-9.445E-06	-0.00047	-0.021304

Chopped Fiber 0.75R	x (mm)	x/R	Moment M(x) (N*mm)	$E*I_{yy}$ (N*mm^2)	$M(x)/E*I_{yy}$ (1/mm)	θ_z (1/rad)	δ_z (mm)
	22.86	0.1	-148.59	5E+08	-2.971E-07	0	0
	27.94	0.12222	-143.56079	3.7E+08	-3.916E-07	-1.7E-06	-4.44E-06
	33.02	0.14444	-138.5316	2E+08	-7.079E-07	-4.5E-06	-2.04E-05
	38.1	0.16667	-133.2738	9.4E+07	-1.424E-06	-1E-05	-5.72E-05
	63.5	0.27778	-107.8992	5.5E+07	-1.961E-06	-5.3E-05	-0.000856
	88.9	0.38889	-82.524597	4.8E+07	-1.712E-06	-1E-04	-0.002794
	114.3	0.5	-57.149994	3E+07	-1.925E-06	-0.00015	-0.00591
	139.7	0.61111	-31.775391	1.6E+07	-1.932E-06	-0.00019	-0.010236
	165.1	0.72222	-6.4007874	6120060	-1.046E-06	-0.00023	-0.015664

Chopped Fiber R	x (mm)	x/R	Moment M(x) (N*mm)	E*I_{yy} (N*mm^2)	M(x)/E*I_{yy} (1/mm)	θ_z (1/rad)	δ_z (mm)
	22.86	0.1	-205.74001	5E+08	-4.113E-07	0	0
	27.94	0.12222	-200.7108	3.7E+08	-5.475E-07	-2.4E-06	-6.19E-06
	33.02	0.14444	-195.68161	2E+08	-9.999E-07	-6.4E-06	-2.85E-05
	38.1	0.16667	-190.4238	9.4E+07	-2.035E-06	-1.4E-05	-8.05E-05
	63.5	0.27778	-165.04921	5.5E+07	-3E-06	-7.8E-05	-0.00125
	88.9	0.38889	-139.67461	4.8E+07	-2.898E-06	-0.00015	-0.004183
	114.3	0.5	-114.3	3E+07	-3.85E-06	-0.00024	-0.009155
	139.7	0.61111	-88.9254	1.6E+07	-5.407E-06	-0.00036	-0.01671
	165.1	0.72222	-63.550797	6120060	-1.038E-05	-0.00056	-0.028304
	190.5	0.83333	-38.176208	1808588	-2.111E-05	-0.00096	-0.047525
	215.9	0.94444	-12.801605	525411	-2.436E-05	-0.00153	-0.079159

Micro-Balloons 0.75R	x (mm)	x/R	Moment M(x) (N*mm)	E*I_{yy} (N*mm^2)	M(x)/E*I_{yy} (1/mm)	θ_z (1/rad)	δ_z (mm)
	22.86	0.1	-148.59	2.1E+08	-6.948E-07	0	0
	27.94	0.12222	-143.56079	1.6E+08	-9.004E-07	-4.1E-06	-1.03E-05
	33.02	0.14444	-138.5316	8.8E+07	-1.568E-06	-1E-05	-4.68E-05
	38.1	0.16667	-133.2738	4.5E+07	-2.958E-06	-2.2E-05	-0.000128
	63.5	0.27778	-107.8992	3.6E+07	-3.034E-06	-9.8E-05	-0.001649
	88.9	0.38889	-82.524597	3.1E+07	-2.705E-06	-0.00017	-0.005062
	114.3	0.5	-57.149994	1.9E+07	-2.986E-06	-0.00024	-0.010318
	139.7	0.61111	-31.775391	1.1E+07	-2.82E-06	-0.00032	-0.017428
	165.1	0.72222	-6.4007874	4298235	-1.489E-06	-0.00037	-0.02617

Micro-Balloons R	x (mm)	x/R	Moment M(x) (N*mm)	E*I_{yy} (N*mm^2)	M(x)/E*I_{yy} (1/mm)	θ_z (1/rad)	δ_z (mm)
	22.86	0.1	-205.74001	2.1E+08	-9.621E-07	0	0
	27.94	0.12222	-200.7108	1.6E+08	-1.259E-06	-5.6E-06	-1.43E-05
	33.02	0.14444	-195.68161	8.8E+07	-2.215E-06	-1.4E-05	-6.54E-05
	38.1	0.16667	-190.4238	4.5E+07	-4.226E-06	-3.1E-05	-0.00018
	63.5	0.27778	-165.04921	3.6E+07	-4.641E-06	-0.00014	-0.002393
	88.9	0.38889	-139.67461	3.1E+07	-4.579E-06	-0.00026	-0.007524
	114.3	0.5	-114.3	1.9E+07	-5.971E-06	-0.00039	-0.015843
	139.7	0.61111	-88.9254	1.1E+07	-7.893E-06	-0.00057	-0.028099
	165.1	0.72222	-63.550797	4298235	-1.479E-05	-0.00086	-0.04625
	190.5	0.83333	-38.176208	1369534	-2.788E-05	-0.0014	-0.074939
	215.9	0.94444	-12.801605	426890	-2.999E-05	-0.00214	-0.119841

Static RPM run through

3-blade 18x18 Propeller "Posada"		
RPM	Torque (lb$_f$*ft)	Thrust (lb$_f$)
6000	3.6	22.5
5500	3	19.3
5000	2.8	16.2
4230	1.8	11.5
4000	1.6	10.3
3500	1.2	7.8
3000	0.7	5.8
2500	0.6	4.4
2000	0.2	3
1500	0	1.9
6000	3.7	22.6
5500	3	19.2
5000	2.8	16.2
4240	1.7	11.5
3920	1.2	9.8
3540	1.2	8
3000	1	6
2500	0.4	4.4
2000	0.3	2.9
1500	0.2	1.7

3-blade 22x12 Mejzlik		
RPM	Torque (lb$_f$*ft)	Thrust (lb$_f$)
6000	3.5	29.8
5500	3.2	25.5
5000	2.3	21.7
4250	2.2	15.9
4000	1.9	14.3
3500	1.1	11.1
3000	0.9	8.3
2500	0.2	5.9
2000	0.2	4
1500	0.3	2.4
2000	0.5	3.9
2500	0.6	5.4
3000	0.7	7.8
3500	1.1	10.8
4000	1.7	13.7
4230	1.8	15.5
5000	2.4	21.2
5500	2.7	25.9
5930	3.3	29.5

VITA

Ben Thomas Bettinger

Candidate for the Degree of

Master of Science

Thesis: MANUFACTURING, ANALYSIS AND EXPERIMENTAL TESTING OF MULTI-BLADED PROPELLERS FOR SUAS

Major Field: Mechanical and Aerospace Engineering

Biographical:

Education:

Completed the requirements for the Bachelor of Science in Mechanical Engineering at Oklahoma State University, Stillwater, Oklahoma in December, 2010.

Completed the requirements for the Bachelor of Science in Aerospace Engineering at Oklahoma State University, Stillwater, Oklahoma in December, 2010.

Experience:

Graduate Research Assistant, Department of Mechanical and Aerospace Engineering, Oklahoma State University, Stillwater, Oklahoma from Spring 2011 to Spring 2012.

Graduate Teaching Assistant, Department of Mechanical and Aerospace Engineering, Oklahoma State University, Stillwater, Oklahoma from Fall 2011 to Spring 2012.

Summer Intern, US Government, Washington, D.C. from Summer 2008 to Summer 2011.

Professional Memberships:

AIAA
Tau Beta Pi

Name: Ben Thomas Bettinger   Date of Degree: May, 2012

Institution: Oklahoma State University   Location: Stillwater, Oklahoma

Title of Study: MANUFACTURING, ANALYSIS AND EXPERIMENTAL TESTING
         OF MULTI-BLADED PROPELLERS FOR SUAS

Pages in Study: 110   Candidate for the Degree of Master of Science

Major Field: Mechanical and Aerospace Engineering

Scope and Method of Study:

The emergence of small UAS with infinite applications has increased the demand for improved small aircraft components. For custom built UAS, optimized propellers are rarely available off the shelf. This paper presents a unique method for creating multi-bladed composite propellers that are optimized to a specific vehicle's thrust and noise requirements. The composite propellers are experimental tested to verify their performance parameters. This method produces high quality propellers that are comparable to commercially available ones with the advantage of better vehicle performance.

Findings and Conclusions:

After applying several lessons learned through multiple iterations of the propeller manufacturing process, a unique technique was developed to manufacture custom designed propellers. Using carbon fiber weave and various core materials, composite propellers were manufactured. The technique harnesses the use of wet lay-up composites and molds to create beautifully crafted propellers that are comparable with those commercially produced in industry. Only after rigorous testing and inspection of the propellers are they allowed to operate on live engines. Deflection testing at static and dynamic conditions help to verify the operational performance of each of the propellers manufactured. The error between the theoretical prediction of deflection and the experimentally tested deflection is due to several factors that affected the calculation of deflection for the blade geometry. This was concluded to be due to air pockets that form within the core material. Aside from a few manufacturing and human errors the overarching goal of this thesis, to develop and implement a unique and innovative manufacturing process for constructing multi-bladed SUAS propellers, has been achieved along with the objectives set forth at the beginning of this thesis.

ADVISER'S APPROVAL: Dr. Jamey Jacob